Yusuf OKUDUCU

METU 2005

DUAL BAND MICROSTRIP PATCH ANTENNA STRUCTURES

Yusuf OKUDUCU

DECEMBER 2005

DUAL BAND MICROSTRIP PATCH ANTENNA STRUCTURES

A THESIS SUBMITTED TO
THE GRADUATE SCHOOL OF NATURAL AND APPLIED SCIENCES
OF
MIDDLE EAST TECHNICAL UNIVERSITY

BY

YUSUF OKUDUCU

IN PARTIAL FULFILLMENT OF THE REQUIREMENTS
FOR
THE DEGREE OF MASTER OF SCIENCE
IN
ELECTRIC AND ELECTRONIC ENGINEERING

DECEMBER 2005

Approval of the Graduate School of Natural and Applied Science

Prof. Dr. Canan Özgen
Director

I certify that this thesis satisfies all the requirements as a thesis for the degree of Master of Science

Prof. Dr. İsmet Erkmen
Head of Department

This is to certify that we have read this thesis and that in our opinion it is fully adequate, in scope and quality, as a thesis for the degree of Master of Science

Assoc. Prof. Dr. Özlem Aydın Çivi
Supervisor

Examining Committee Members

Prof. Dr. Gülbin Dural	(METU, EE)	———
Assoc. Prof. Dr. Özlem Aydın Çivi	(METU, EE)	———
Assoc. Prof. Dr. Sencer Koç	(METU, EE)	———
Assoc. Prof. Dr. Şimşek Demir	(METU, EE)	———
Assoc. Prof. Dr. Vakur Ertürk	(Bilkent Unv, EE)	———

I hereby declare that all information in this document has been obtained and presented in accordance with academic rules and ethical conduct. I also declare that, as required by these rules and conduct, I have fully cited and referenced all material and results that are not original to this work.

Name, Last name :

Signature :

ABSTRACT

DUAL BAND MICROSTRIP PATCH ANTENNA STRUCTURES

Okuducu, Yusuf

M.S, Department of Electrical and Electronic Engineering

Supervisor : Assoc. Prof. Dr. Özlem (Aydın) Çivi

December 2005, 89 pages

Wideband and dual band stacked microstrip patch antennas are investigated for the new wideband and dual band applications in the area of telecommunications. In this thesis, aperture-coupled stacked patch antennas are used to increase the bandwidth of the microstrip patch antenna. By this technique, antennas with 51% bandwidth at 6.1 GHz and 43% bandwidth at 8 GHz satisfying S11<-15 dB are designed, manufactured and measured. A dual-band aperture coupled stacked microstrip patch antenna operating at 1.8 GHz with 3.8% bandwidth and at 2.4 GHz with 1.6% bandwidth is designed, produced and measured for mobile phone and WLAN applications. In addition, an aperture coupled stacked microstrip patch antenna which operates at PCS frequencies in 1.7-1.95 GHz band is designed. Dual and circularly polarized stacked aperture coupled microstrip patch antennas are also investigated. A triple band dual polarized aperture coupled stacked microstrip patch antenna is designed to operate at 900 MHz, at 1.21 GHZ and at 2.15 GHz. Mutual coupling between aperture coupled stacked microstrip patch antennas are examined and compared with the coupling of aperture coupled microstrip patch antennas.

Keywords: Stacked Patch Antennas, Dual Band Antennas, Aperture Coupled Microstrip Antennas, Wideband Antennas

ÖZ

ÇİFT BANT MİKRO ŞERİT YAMA ANTEN TASARIMI

Okuducu, Yusuf

Y.Lisans, Elektrik Elektronik Mühendisliği Bölümü

Tez Yöneticisi : Doç. Dr. Özlem (Aydın) Çivi

Aralık 2005, 89 sayfa

Bu tez kapsamında Telekomünikasyon alanındaki yeni geniş band ve çift band uygulamaların ihtiyaç duyduğu geniş band ve çift band mikroşerit yama antenler araştırılmıştır. Mikro şerit yama antenlerin band genişliğini artırmak amacıyla yarık bağlaşımlı ikiz mikro şerit yama yapılar kullanılmıştır. Bu teknik ile S11< -15 dB için 6.1 GHz `de %51 band genişliği olan ve 8 GHz`de ise %43 band genişliğine sahip antenler tasarlanmış, üretilmiş ve ölçülmüştür. S11<-15 dB`yi sağlayacak şekilde 1.8 GHz frekansta 3.8% band genişliğine ve 2.4 GHz frekansta 1.6% band genişliğine sahip çift band yarık bağlaşımlı ikiz bir mikro şerit yama anten gezgin telefon ve WLAN uygulamaları için tasarlanmış, üretilmiş ve ölçülmüştür. Bunlara ek olarak, PCS mobil haberleşme sistemlerinin 1.7-2 GHz bandlarında çalışan bir yarık bağlaşımlı ikiz mikro şerit yama anten tasarlanmıştır. Yarık bağlaşımlı antenlerin dairesel ve çift polarizasyonlu örnekleri araştırılmıştır. 900 MHz, 1.21 GHz ve 2.15 GHz frekanslarında çalışan üç bandlı çift polarizasyonlu yarık bağlaşımlı ikiz mikro şerit yama anten tasarlanmıştır. Ayrıca yarık bağlaşımlı ikiz mikro şerit yama antenler arasındaki etkileşim incelenmiştir ve yarık bağlaşımlı mikro şerit yama antenler arasındaki etkileşimler ile karşılaştırılmıştır.

Anahtar Kelimeler: İkiz Mikroşerit Yama Antenler, Çift Band Antenler, Yarık Bağlaşımlı Mikroşerit Antenler, Geniş Bandlı Antenler

To My Parents

ACKNOWLEDGMENTS

I wish to express my deepest gratitude to my supervisor Assoc. Prof. Dr. Özlem (Aydın) Çivi for her guidance, advice, criticism, encouragements and insight throughout the research.

I would like to express my special thanks and gratitude to Prof. Dr. Gülbin Dural, Assoc. Prof. Dr. Sencer Koç, Assoc. Prof. Dr. Şimşek Demir, Assoc. Prof. Dr. Vakur Ertürk for showing keen interest to the subject matter and accepting to read and review the thesis.

The technical assistance of Mr. Mustafa Seçmen is gratefully acknowledged.

TABLE OF CONTENTS

LIST OF TABLES

TABLES

LIST OF FIGURES

FIGURES

CHAPTER 1

INTRODUCTION

Microstrip patch antennas have been used in many areas like wireless telecommunication technology, satellites, remote sensing, aircraft and missile applications, because they have many advantages like being low profile, low size, low cost, light weight, ease of production and conformable to surfaces. Two most important application areas for microstrip antennas are mobile communication systems and internet based wireless applications (Global System Mobile (GSM) systems, Wireless Local Area Network (WLAN) systems, mobile phones etc). Recently, new mobile telecommunication technologies such as Code Division Multiple Access 2000 (CDMA 2000), Wideband Code Division Multiple Access (WCDMA), Wideband Interoperability for Microwave Access (WiMaX) mobile systems and other wireless networking technologies, which support both mobile voice and high data services, have been introduced. Wireless connection with high data rate requires higher bandwidth operation. Currently, even GSM phones require dual or triple band operation for different GSM operators. New mobile systems like WCDMA mobile systems need to work together with old generation GSM networks so that new mobile terminals need to support more frequency bands. In addition to this situation, new mobile terminals need to support new networking technologies like Bluetooth, WLAN access. Thus, new mobile terminals need to support not only wider bandwidth but also multi band operation. For example, one new WCDMA handset may need to support 900 MHz, 1800 MHz, 2000 or 1900 MHz and 2.4 GHz. Beyond these frequency requirements, these handsets also need to be small and low weight for marketing issues.

Microstrip antennas may provide different alternatives to satisfy these requirements. Currently, several dual band and wideband microstrip antenna structures are used in GSM handsets and WLAN devices, because in addition to

advantages mentioned above, microstrip antennas can easily be integrated with RF circuits in the device.

Techniques to obtain the dual-band operation for microstrip antennas can be divided into three groups namely: orthogonal mode, multi-patch and reactively loading techniques [1]. Probe fed, slot fed and proximity fed structures of orthogonal mode technique for dual frequency patch antennas are available in literature [2], [3], [4], [5]. Two orthogonal modes (0,1) and (1,0) modes of rectangular patch antenna can be excited by two separate feeds located perpendicular along center lines or feed at diagonal line. The frequencies of these modes are determined by the respective lengths of the patch.

Stubs, notches, shorting pins, capacitors and slots on patch are used to achieve dual-band operation [6], [7], [8]. Modal field distribution of the different modes of the antenna is perturbed by shorting pins or slots so that antenna operates at two different frequencies. Generally, the TM_{10} and TM_{30} modes of the rectangular patch antenna are used because these modes have broadside radiation pattern and same polarization. A spur line is embedded in the non-radiating edges of the patch to obtain dual band operation at two separate frequencies with good radiation characteristics [9]. A dual-band antenna operating at 2.38 GHz and 3.32 GHz is obtained with cross polarizations levels better than -18 dB for 2.38 GHz and -12 dB for 3.32 GHz.

A slotted patch structure is proposed to achieve dual band operation in [10]. The probe fed patch antenna has two slots on it. These two slots provide dual band operation of this antenna. Ratio of resonance frequencies that are proportional to width/length ratio of the antenna is important in the design. The second resonance frequency can be changed by slot parameters. These slots modify the TM_{30} mode so that antenna behaves like TM_{10} mode. Two different edges became radiating edges for each frequency.

Lastly, stacked patches with aperture coupled fed or probe fed structures and co-planar (dipoles, sub-arrays) radiators are used to achieve dual or wide band antennas [11], [12], [13], [14]. Two or more resonant elements with slightly different

resonance frequencies are stacked or located side by side to obtain multiband/wideband operation.

Aperture coupled feed technique is preferred in the design of many antennas due to its advantages such as, separation of feed network and radiator, low cross-polarization and wider bandwidth characteristics. In general, it is possible to obtain 10-15 % bandwidth by aperture coupled microstrip patch antenna, whereas probe fed or microstrip line fed patch antenna has 3-5% bandwidth [15]. Bandwidth can be increased by using a low permittivity dielectric and increasing dielectric material thickness. Increasing the thickness of the dielectric improves the bandwidth of the antenna but surface waves are strongly excited in thick dielectrics. Surface waves reduce radiated power and degrade radiation pattern and antenna polarization characteristics. Cavities under patch can be used to prevent this problem, however this increases the complexity of the design. Actually, these two techniques provide very limited improvement of the bandwidth. There is another technique to increase the bandwidth of the aperture coupled microstrip patch antenna, resonances of the aperture and patch can be selected close to each other to increase the bandwidth. Up to 35% bandwidth can be obtained with a single patch aperture coupled antenna with this technique. The drawback of this technique is high level of back radiation [16].

Using shorting pins and slots on a patch has some disadvantages for aperture-coupled structures. Position of shorting pins can intersect with the aperture position and shorting pins can disturb E- field distribution of the basic operation besides the higher order mode operation. Slots on patches can cause similar problems like disturbing the basic operation besides the higher order mode. As an orthogonal mode method, tilted aperture can be used for an aperture-coupled antenna structure. Aperture and patch will have low coupling for this structure. Performance of the antenna will be worse than the antenna with perpendicular centered aperture.

Unlike the methods mentioned above, stacking method can be employed easily with aperture coupled fed structures. Stacked microstrip patch antenna can provide high bandwidth, low cross-polarization and low back radiation characteristics [17], [18]. Stacked microstrip patch antennas are generally used for

wideband applications but also they can be used to obtain dual band antennas. Typical stacked microstrip path antenna consist of two patches, bottom patch can be excited by either aperture coupling or by a microstrip line or by a coaxial probe. The upper patch is proximity coupled to the bottom patch. Bottom and upper patch dimensions are slightly different from each other to have different resonant frequencies. Stacking method does not cause any extra space requirement so it provides a compact design possibility for arrays. Several examples of multi band and wideband aperture coupled stacked microstrip patch antennas can be seen in the literature. There are also probe fed stacked patch antenna structures in the literature, however aperture coupled antenna structures have better performance regarding to their wide bandwidth characteristics [16], [17], [19], [20].

Some examples for probe fed stacked antennas are following: triangular shape probe fed stacked patch antenna [21], dual-frequency stacked annular ring antenna [22], broadband stacked shorted patch with 30% bandwidth for S11< -10 dB [19], multi frequency probe fed microstrip patch antenna with four parasitic and one patch driven by the probe [20]. The last one have five resonance frequencies with low bandwidth (<5.5% for S11< -10 dB). However, by using stacked aperture-coupled structure, 30% to 70% bandwidth can be obtained [16], [17]. Aperture coupled stacked rectangular patch antenna with 67% (for voltage standing wave ratio (VSWR) <2) (5.2 to 10.4 GHz) bandwidth is reported in [17] and several stacked patch antennas are reported in the literature.

Another example of an aperture coupled stacked microstrip patch antenna with wideband, low cross polarization and low back radiation characteristics is given in [16]. Back to front radiation ratio of this antenna is about -18 dB with lower bandwidth. Higher bandwidth causes higher back to front ratio about -11 dB. There is a tradeoff between the bandwidth and the back to front radiation ratio. Also isotropic co-polarized component and low cross-polarized component for broadside are reported.

Different patch shapes like circular patch, triangular patch, and ring shaped patch stacked antenna examples have been reported in [11], [21], [22]. In [21],

triangular shaped stacked probe fed structure is used to have a broadband operation. A broadband model at 1.8 and 3.5 GHz is designed with 9% at 1.8 GHz (for VSWR<1.5) and 11% bandwidth at 3.5 GHz (for VSWR<1.5). Two circular stacked patches are used to achieve dual-band operation in [11]. Lower patch is driven by coaxial feed. This structure is useful only when narrowband characteristic for dual band operation is required. Feeding is very important to achieve dual-band operation in this model.

A probe fed dual-band circularly polarized antenna is obtained by inserting four T-shaped slits at the patch edges or four Y-shaped slits at the patch corners of a square microstrip antenna. Patch size is reduced up to 36% of a circular polarized design without slits [23].

A dual band circularly polarized aperture coupled stacked microstrip antenna for GPS applications is presented in [24]. Antenna operates at 1575 and 1227 MHz. A substrate with low dielectric constant is used to achieve higher bandwidth.

A dual-polarized dual-band stacked aperture coupled antenna with two apertures and two feed lines is reported [25]. High isolation of two-polarization port is obtained around 40.5 dB by T-shape feed line and H- shape perpendicular slots.

In this thesis, mainly, multi band and wideband aperture coupled stacked microstrip patch antennas are investigated. Parametrical analysis of aperture coupled microstrip patch antennas and aperture coupled stacked microstrip patch antennas are provided to guide the antenna designer to design various aperture-coupled stacked patch antennas. In addition, circular and dual polarization application of aperture coupled patch antennas and coupling between aperture coupled patch antennas are analyzed.

Aperture coupled stacked microstrip patch antennas with wideband, dual band, circularly polarized, dual polarized characteristics are designed and simulated for different frequencies that are used in communication applications. Some of these antennas are produced and measured.

This thesis is organized as follows: In Chapter 2, microstrip patch antennas are briefly discussed. First, the general structure of the microstrip antenna is explained then, different feeding techniques for microstrip antennas are shown. Furthermore, common analysis methods of microstrip patch antennas and parametrical analysis of aperture coupled patch antenna are presented.

In Chapter 3, aperture coupled stacked microstrip patch antennas are investigated. Parametrical analysis of aperture coupled stacked patch antennas is given. Circularly polarized aperture coupled microstrip patch antennas are discussed. Furthermore, mutual coupling between the aperture coupled stacked patch antennas is analyzed and compared with the coupling between aperture coupled patch antennas.

In Chapter 4, designed wideband, dual band, dual polarization examples of aperture coupled stacked patch antennas for different frequencies are presented. Simulation and measurement results are compared and discussed.

Conclusions are given in Chapter 5

CHAPTER 2

MICROSTRIP ANTENNA OVERVIEW

2.1 Introduction

Microstrip patch antennas are widely used in many applications such as phased arrays in radars, satellites, base stations, mobile phone antennas in wireless communication systems. Because microstrip antennas are low profile, conformable to planar and non-planar surfaces, simple and inexpensive to manufacture, flexible to design adaptive antenna elements and suitable for antenna arrays. Contrary to these advantages, microstrip antennas have some shortcomings such as low efficiency due to the dielectric and the conductor losses, low power, high Q and narrow bandwidth. Some applications of microstrip patch antennas are listed in Table 1.

***Table 1**: Microstrip Antenna Applications*

Global Positioning Satellite	1575 MHz and 1227 MHz
Cellular Phone	824-849 MHz and 869-895 MHz
PCS	1.85-1.99 GHz and 2.18-2.20 GHz
GSM	915 MHz and 935-960 MHz
WLAN	2.40-2.48 GHz and 5.4 GHz
Cellular Video	28 GHz
Direct Broadcast Satellite	11.7-12.5 GHz
Wide Area Computer Networks	60 GHz

Researchers have been working to improve the performance of microstrip antennas. Narrow bandwidth of microstrip antenna attracts remarkable attention because several recent applications in wireless communication systems require wideband antennas. There are different approaches to increase the bandwidth of microstrip antennas. Two significant methods are to use thick and low permittivity dielectrics and to excite two/three resonances close to each other. In this thesis, both of these methods are used to obtain wideband microstrip antennas.

In Section 2.2, basics of a simple microstrip patch antenna are briefly explained. Analysis methods like cavity method, transmission line method and full wave methods are summarized in Section 2.3. Then, aperture coupled microstrip patch antenna is examined in detail.

2.2 Microstrip Antenna Structure Overview

Basic microstrip antenna structure, as shown in Figure 2.2.1, consists of a conducting patch on a grounded dielectric layer. Conducting patch may have any shape such as rectangle, square, circular and elliptic [26]. Square, rectangular, dipole and circular patch shape are most common because of easy analysis and manufacturing with good radiation characteristics (low cross-polarization). Rectangular and square shape patches are used in this thesis. The length of the patch determines the antenna operation frequency and selected approximately equal to $\lambda/2$. Other important parameters are the dielectric constant and the thickness of the dielectric layer. Dielectric constant generally selected in a range from 2.2 to 12 [26]. Thickness of the dielectric must be much smaller than the patch length, because the comparable thickness of the substrate and the patch length causes too much fringing fields that is disturbing the electric field distribution under patch. The dielectric constant and the thickness of the dielectric affect bandwidth of the antenna. Thin substrates with not very high dielectric constant are preferred to have small size and to prevent undesired strong surface wave excitation [27]. There are several feeding techniques such as microstrip line, coaxial probe, proximity coupled, and aperture coupled feeding techniques [28].

Microstrip line feeding has the advantage that the feed can be etched on the same substrate to provide a planar structure. Antenna structure for microstrip line fed antenna can be seen in Figure 2.2.1. Modeling, fabrication and impedance matching for this feeding method are easy. For the patch fed by a microstrip line, the inset of the feed line is used for input impedance matching. Microstrip line fed antenna has low bandwidth around 2-5%. Increasing dielectric thickness can improve bandwidth but increasing the dielectric substrate thickness causes increasing surface wave and

spurious feed radiation problems. In addition, cross-polarization level is high due to the feed radiation for this structure.

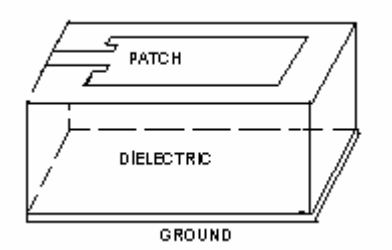

Figure 2.2.1: Microstrip line fed microstrip patch antenna structure

Coaxial line (probe) feeds are also common. Structure of the probe fed antenna can be seen from Figure 2.2.2. It is easy to manufacture and match the antenna by probe. It has low spurious radiation compared to microstrip line fed patches. Probe fed antenna also has low bandwidth that is around 2-5 % and it has relatively high cross-polarization due to asymmetric excitation. For the probe fed antenna, the position of the probe connection to the patch determines the matching of the input impedance.

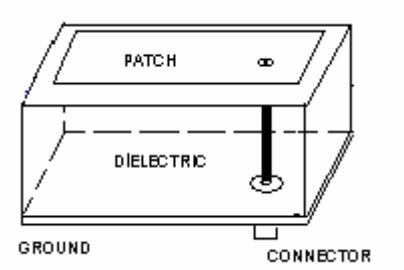

Figure 2.2.2: Coaxial-line fed microstrip patch antenna structure

Proximity coupled feed is another type of feeding technique and it has a large bandwidth (13%) compared to microstrip line fed and probe fed patches. It can be easily modeled and it has low spurious radiation. General structure of the proximity-coupled microstrip antennas can be seen from Figure 2.2.3. In proximity-coupled

feed structure, the length and the width of the feeding stub can be used for matching [29].

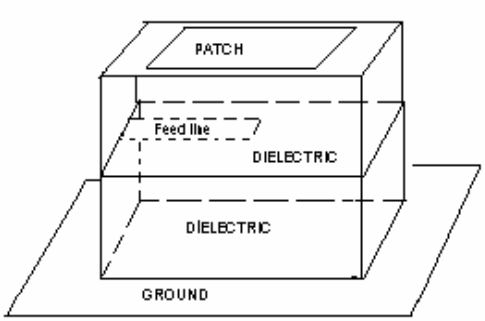

Figure 2.2.3: Proximity coupled fed microstrip patch antenna structure

Aperture coupled feed is another popular excitation technique. General structure of the aperture-coupled antenna can be seen from Figure 2.2.4. Compared to other feeding techniques, it is not easy to fabricate this antenna. It has low cross-polarization because it can prevent higher order mode generation that is originated from asymmetry. It also provides independent feed and radiation parts. The aperture coupled patch antenna feed will be analyzed in detail later. Further information about simple microstrip antenna structures can be found in [28].

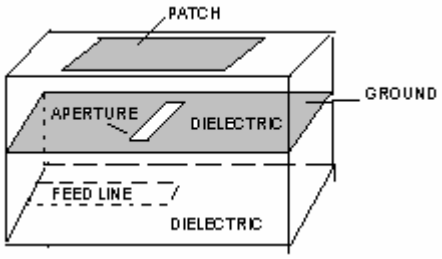

Figure 2.2.4: Aperture coupled fed microstrip patch antenna structure

2.3 Analysis Methods for Microstrip Antennas

Microstrip patch antennas can be analyzed by transmission line method, cavity method and several full wave methods. The simplest model is the transmission

line model. Transmission line model can be used to analyze simple microstrip antennas like thin patch antennas and it is useful to understand the structure and working principle of microstrip antennas.

Transmission line model is used to calculate initial design parameters. Starting from these initial parameters, final antenna design parameters can be found by iteration, using an efficient antenna analysis software.

A microstrip line fed rectangular patch antenna is suitable to be analyzed by transmission line model. Transmission line equivalent of microstrip line fed microstrip patch antenna can be seen in Figure 2.3.1. In transmission line model, two edges of the rectangular patch antenna, which are separated by length of λ/2, are taken as radiating edges for TM_{10} mode excitation. TM_{10} means electric field varies along antenna length (L) and there is no variation along antenna width (W). Electric field lines along the radiating edges are in phase for about λ/2 length of antenna. Electric fields along other two edges are out of phase and they cannot radiate. Radiating edges, fringing field distribution and phase difference can be seen in Figure 2.3.1. Two radiating edges have smooth fringing fields for thin substrate, which are perpendicular to edges and regular in the neighborhood of edges. Effective antenna length is taken electrically ΔL longer due to fringing fields. Line extension ΔL associated with the patch is given by the formula:

$$\frac{\Delta L}{h} = 0.412\left[\frac{\varepsilon_{eff} + 0.3}{\varepsilon_{eff} - 0.258}\right]\left[\frac{W/h + 0.264}{W/h + 0.813}\right] \tag{2.1}$$

ΔL= Line extension

ε_{eff} = Effective dielectric constant

W= Patch width

h= Substrate thickness

These fringing fields are approximated by regular E- field lines along two slots with WxΔL dimensions at both edges. Also due to effect of fringing fields, ε_{eff} is used in calculations instead of ε_r (permittivity of dielectric). The effective dielectric constant (ε_{eff}) due to the air dielectric boundary is given by [26]

$$\varepsilon_{eff} = \frac{\varepsilon_r + 1}{2} + \frac{\varepsilon_r - 1}{2}\left(1 + \frac{10h}{W}\right)^{-\frac{1}{2}} \tag{2.2}$$

ε_r = Dielectric constant of substrate

Operating frequency of the microstrip antenna can be found by using these parameters as follows:

$$f_r = \frac{1}{2\sqrt{\mu_0 \varepsilon_0}(L + 2\Delta L)\sqrt{\varepsilon_{eff}}} \tag{2.3}$$

μ_o = Permeability of free space

ε_o = Permittivity of free space

Input impedance of the antenna can be calculated by using transmission line model. Corresponding two slots for two radiating edges are taken as the only radiation source for the microstrip structure so that the microstrip patch antenna is represented by two slots, separated by a transmission line of length L. Each radiating slot is modeled with admittance as follows:

$$Y = G + jB \tag{2.4}$$

Two radiating slots are identical, i.e. $Y_2 = G_2 + jB_2 = Y_1 = G_1 + jB_1$. Total admittance can be found by transferring admittance of the second slot (Y_2) to the location of the first slot. Because of $\lambda/2$ distance, transferred admittance is as follows:

$$Y_{2T} = G_2 - jB_2 = G_1 - jB_1 \tag{2.5}$$

Total admittance is

$$Y_{in} = Y_1 + Y_{2T} = 2G_1 \quad , \quad G_1 = \frac{2P_{rad}}{|V_0|^2} \tag{2.6}$$

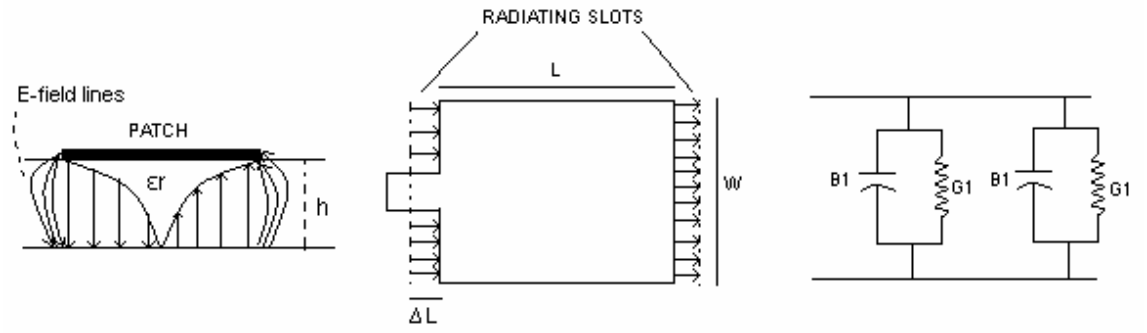

(a) Side view (b) Top view (c) Transmission Line Equivalent Circuit

Figure 2.3.1: Transmission line model of microstrip line fed microstrip patch antenna

As it is mentioned, patch antenna becomes a radiator for about λ/2 antenna length. There is a more precise approximation for the width and the length of the antenna. Based on the substrate parameter, the width and the length of the microstrip patch can be estimated. Rough approximation for patch length can be given by following formula:

$$L = 0.48\lambda_g \sim 0.49\lambda_g \tag{2.7}$$

$$\lambda_g = \frac{c}{f_r\sqrt{\varepsilon_r}}$$

The width (W) is usually chosen to be in the range of L < W < 2L for good radiation characteristics, large W can cause excitation of the higher order modes in the operation frequency band. A microstrip patch antenna is generally designed as a broadside radiator and it has large beam width and low gain characteristics. The formulas for the E-plane and the H-plane radiation patterns are given by [26]

E-plane $$F(\theta) = \frac{\sin\left(\frac{k_0 h}{2}\cos\theta\right)}{\frac{k_0 h}{2}\cos\theta}\cos\left(\frac{k_0 L}{2}\cos\theta\right) \tag{2.8}$$

H-plane $$F(\phi) = \frac{\sin\left(\frac{k_0 W}{h}\cos\phi\right)\sin\phi}{\frac{k_0 W}{2}\cos\phi} \qquad (2.9)$$

$k_o = 2\pi/\lambda_o$ (free space wavenumber)

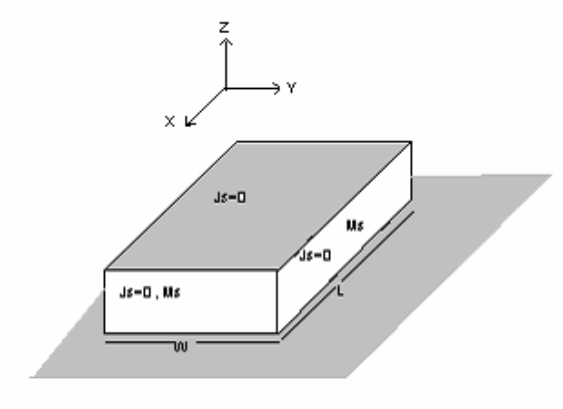

Figure 2.3.2: Equivalent current densities on the microstrip patch antenna for cavity model

Second analysis method is cavity model. In this approach microstrip patch antenna is modeled as a cavity, which is bounded by electric conductors (upper patch and ground plane) and four magnetic walls that enclose the patch. Basis for the cavity modeling is originated from observation of patch on thin substrates ($h << \lambda$). First observation is that interior field does not vary much in z- direction because of thin substrate. Second observation is that the electric field is z- directed only, and H_x and H_y magnetic fields just exist in the region enclosed by the patch and the ground plane. Then fields are solved by boundary conditions. These boundary conditions are: tangential E-fields on the ground plane and on the patch are zero and transverse magnetic fields inside cavity are zero (H_x and H_y for TM^z mode). Calculated E- and H- fields of cavity can be used to approximate the input impedance and the resonance frequency. Microstrip antenna can be represented by equivalent current densities on each side of patch with Huygen`s principle: J_t and J_b are current on the top and bottom surfaces of the patch. Four side slots are represented by equivalent

electric current density J_s and equivalent magnetic current density M_s. J_t is negligible and it is taken as zero for thin substrates. Tangential magnetic fields along patch edges are small and taken as zero so corresponding electric current density J_s are set to zero. There are only non-zero magnetic currents along the periphery of the patch (Figure 2.3.2). Radiation due to magnetic current on non-radiating edges is zero due to equal and opposite current distribution on the slots. Thus, the radiation pattern can be calculated by only magnetic currents on radiating edges.

Cavity model is easier to understand and explains radiation mechanism but less accurate than full-wave methods. The full-wave analysis methods obtain the current distribution on the antenna structure and find the related E-, H- fields from these current distributions but full-wave models takes too much time and effort. Some of the commercial antenna design softwares use full wave methods, such as Finite Element Method (FEM), Finite Difference Method (FD), Finite Difference Time Domain Method (FDTD) and Method of Moments method (MoM). In this thesis, software called Ensemble by Ansoft based on MoM method is used. Ensemble is effective for 2-Dimensional layered antenna problems. It assumes that the ground plane and dielectric layer are infinite extent. Thus, the effects of finite ground plane and truncated dielectric can not be observed. For three-dimensional analysis of antennas, software called HFSS by Ansoft based on FEM or IE3D by Zeland based on moment method can be used.

2.4 Analysis of Aperture Coupled Microstrip Patch Antennas

Microstrip line fed and probe fed microstrip patch antennas have some disadvantages that can be disregarded by aperture coupled structure. An aperture coupled fed antenna structure provides features like independent selection of the antenna and the feed substrates, larger space for antenna elements and the feed network, easy array construction, flexible design with different patch and aperture shapes. Ground layer of aperture coupled patch antenna separates feed network and antenna side. Especially antenna arrays of circularly polarized, dual polarized and dual band antenna elements that require extra feed network space are easily built with aperture coupled antenna elements [24], [30]. Also, separation of the feed

network and the antenna side provides less spurious feed radiation and surface waves. In addition, 10-15% bandwidth for single layer and 30-50% bandwidth for stacked structure is mentioned in literature for aperture-coupled antennas [15].

2.4.1 Structure of Aperture Coupled Microstrip Patch Antennas

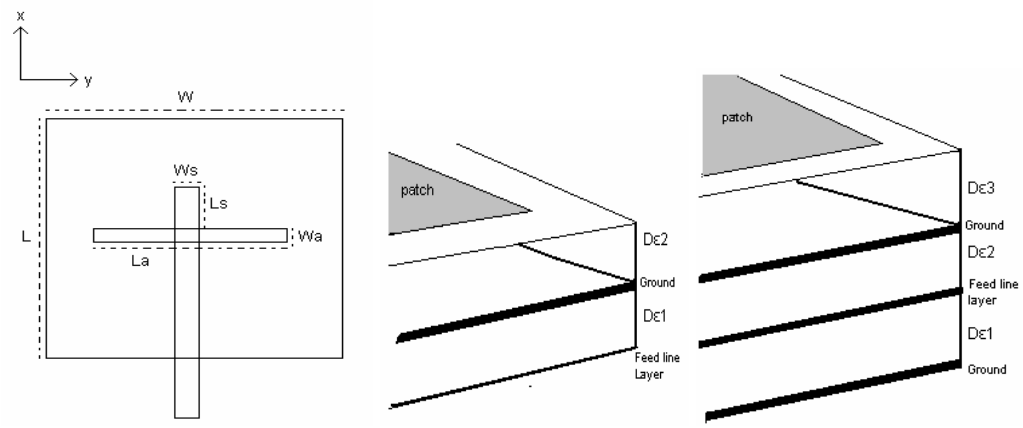

(a) Top view (b) Side view (c) Side view with base ground

Figure 2.4.1: Aperture coupled microstrip patch antenna structure

Structure of an aperture coupled microstrip patch antenna can be seen in Figure 2.4.1. Aperture coupled microstrip patch antenna consists of radiating patch at the top, dielectric layer between patch and ground plane, aperture on ground plane, dielectric layer between ground plane and feed line. As seen from Figure 2.4.1 (c), to prevent back radiation from aperture and transmission line, another ground layer can be located at the bottom. Radiation mechanism of aperture coupled microstrip patch antenna can be explained as follows. Antenna is excited by microstrip feed line. Fields created by feed line couple to patch through the aperture on ground plane.

Transmission line model of an aperture-coupled microstrip patch antenna is given in [31]. Transmission line equivalent of an aperture-coupled microstrip patch antenna can be seen in Figure 2.4.2 and Figure 2.4.3.

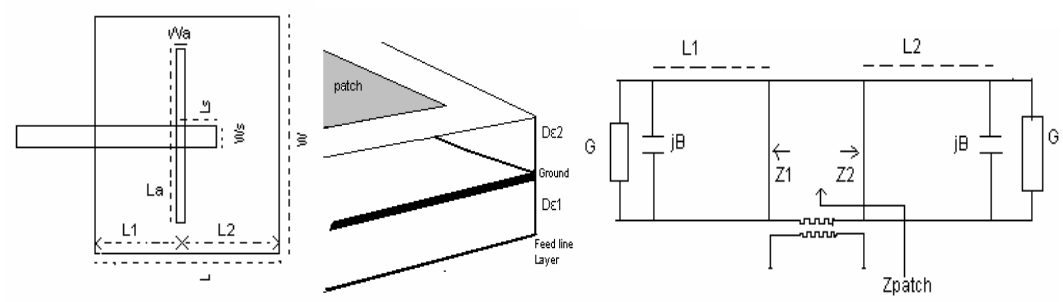

(a) Top view (b) Side view (c) Transmission line equivalent circuit

Figure 2.4.2: Aperture coupled microstrip patch antenna transmission line model for patch side

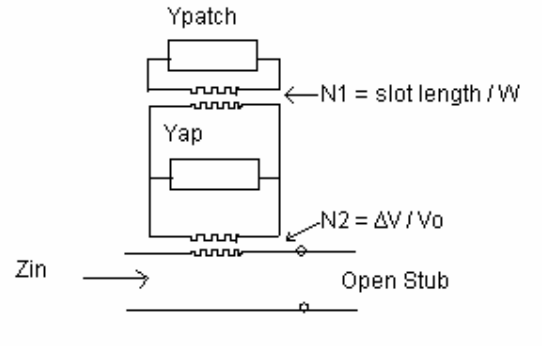

Figure 2.4.3: Aperture coupled microstrip patch antenna transmission line model for aperture side

Two radiating edges due to fringing fields are represented by a conductance and susceptance G + jB as seen in Figure 2.4.2 (c). These two impedances are transferred to a feed point by transmission line theory (L1 and L2 distances between feed point and edges). Transferred impedances are Z_1 and Z_2. Patch impedance can be found as:

$$Z_{patch} = Z_1 + Z_2 \tag{3.1}$$

Then Y_{patch} and Y_{ap} are used to achieve Z_{in} as:

$$Z_{in} = \frac{N_2^{\,2}}{N_1.Y_{patch} + Y_{ap}} - jZ_c.\cot(k_1.L_s) \tag{3.2}$$

$N_1 = L_a/W$, coupling ratio between patch and aperture

$N_2 = \Delta V/V_{0,}$ coupling ratio between aperture and feed line

ΔV= Discontinuity in modal voltage of feeding microstrip line

V_0= Aperture voltage

L_a = The aperture length

W= Patch width

L_s= Feed line length

k_1= Wavenumber of dielectric

Z_C= Characteristic impedance

For small aperture lengths, $\left(n_1^2 Y_{patch} + Y_{ap}\right)$ term of Z_{in} becomes dominant and defines the resonant frequency. Total susceptance should be zero for resonance frequency

$B_{total}=B_{patch}+B_{ap}$ so $B_{patch} \cong \frac{4}{Z_{ca} k_a L_a^3}$ (3.3)

where Z_{ca} is the characteristic impedance for aperture line used to find Y_{ap}, k_a is the wavenumber for aperture used to find Y_{ap}.

According to (3.3), antenna resonance changes with aperture length L_a. Increasing L_a cause decrease in the resonance frequency and vice versa. Furthermore, L_a has an effect on the coupling. Larger aperture causes more coupling, i.e input impedance loop on smith chart gets bigger with stronger coupling. Another approximation is about coupling ratio of aperture and feed line

$$N_2 = \frac{L_a}{\sqrt{D.D_{\varepsilon 1}}} \quad (3.4)$$

D is effective width of feed line

$D_{\varepsilon 1}$ is the thickness of the dielectric of the feed line

As it can be seen from (3.4), increase in the width of the feed line and the thickness of dielectric under the feed line causes decrease in input impedance. Parameters such as aperture size and shape, substrate thickness and dielectric constants can be chosen to improve the bandwidth and to optimize radiation characteristics.

2.4.2 Parametrical Study of Aperture Coupled Microstrip Patch Antennas

In this section, effects of different design parameters to the performance of the aperture coupled microstrip antenna are investigated. An aperture coupled microstrip antenna, as shown in Figure 2.4.1 (a), (b), with parameters given in Table 2 is designed to operate at 2.4 GHz.

***Table 2**: Parameters of the antenna designed for parametrical analysis of aperture coupled microstrip patch antennas*

W	L	L_s	W_s	L_a	W_a	ε_2	ε_1	$D_{\varepsilon 2}$	$D_{\varepsilon 1}$
60mm	50mm	13mm	2.5mm	50mm	0.5mm	1	9.2	6.8mm	4mm

Some important design parameters are changed to observe their effects on input impedance, resonance frequency and bandwidth. Input return loss of the designed microstrip patch antenna with mentioned parameters can be seen from Figure 2.4.4.

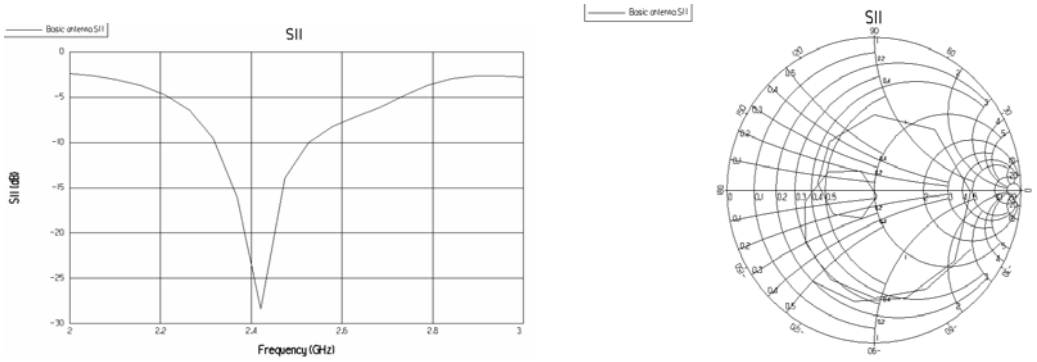

(a) (b)

Figure 2.4.4: Input return loss graph of the simulated aperture coupled microstrip patch antenna with parameters given in Table 2, (a) linear plot (b) smith chart plot

Patch Length (L):

Length of the patch determines the antenna resonance frequency. Patch length is selected approximately equal to half of a guided wavelength $\lambda_g/2$, where $\lambda_g = \lambda_0/$

$(\varepsilon_r)^{1/2}$. As it can be seen from Figure 2.4.5, increase in the patch length causes decrease in the resonance frequency and vice versa, such as 4% decrease of the patch length causes about 5% increase of the resonance frequency. Thus, the antenna operating frequency can be mainly adjusted by the antenna length.

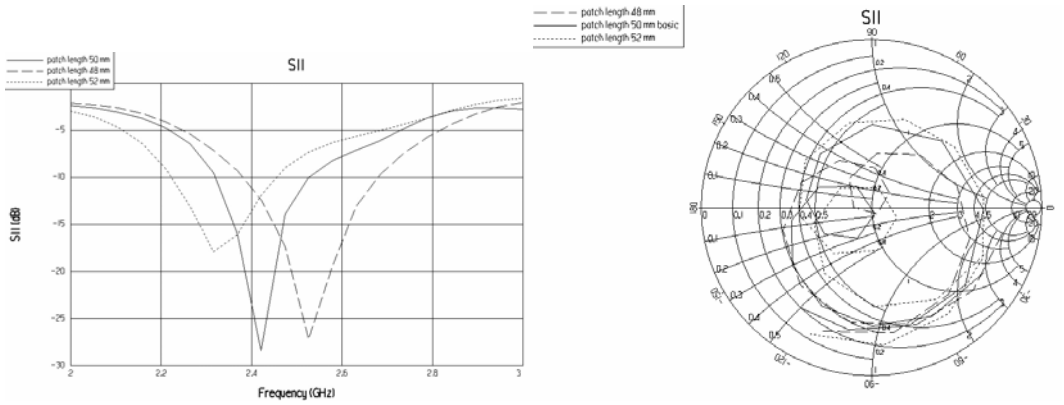

(a) (b)

Figure 2.4.5: Change of input return loss with the change in the patch length of the simulated aperture coupled microstrip patch antenna with parameters given in Table 2, (a) linear plot, (b) smith chart plot

Patch width (W):

The patch width has an effect on the radiation resistance and the bandwidth of the antenna. Wider patch results in lower resistance, i.e. increased radiated power, increased bandwidth and increased radiation efficiency. Patch width also affects the cross polarization level. Square patch causes more cross-polarization compared to rectangular patch antenna because other edge with the same length will cause cross-polar components. Change of patch width does not have a significant effect on the resonance frequency, as can be seen from Figure 2.4.6. Increasing patch width causes an increase of coupling so impedance loop gets smaller and close to the center. However, these changes are very small.

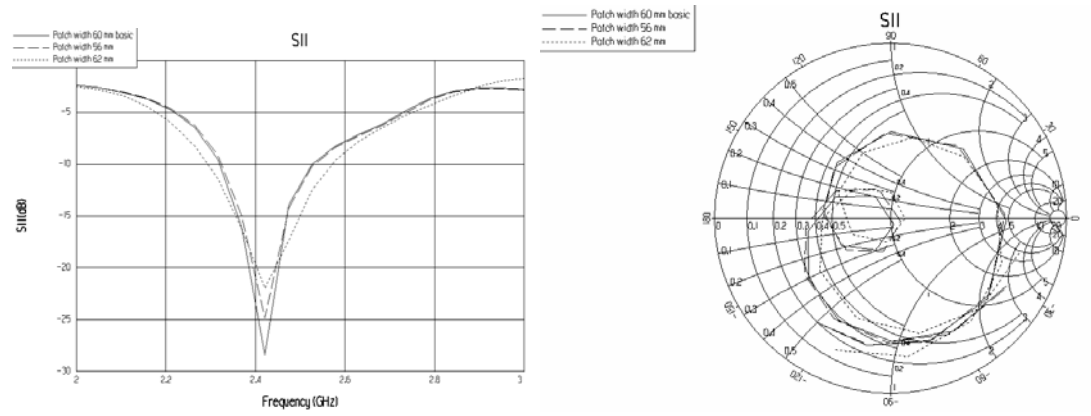

(a) (b)

Figure 2.4.6: Change of input return loss with the change in the patch width of the simulated aperture coupled microstrip patch antenna with parameters given in Table 2, (a) linear plot, (b) smith chart plot

Stub Length (L_s):

Stub length can be changed to tune the reactance of the antenna. Stub length is generally less than $\lambda_g/4$. Input return loss graphs of the antenna for different stub lengths are plotted on Figure 2.4.7. It is observed that input impedance loop shifts around the smith chart center with changing stub length. Increase of the stub length causes impedance loop to shift in clock-wise direction and to get slightly wider; decrease of the stub length causes impedance loop to shift in counter clock-wise direction and to get slightly narrower. Because longer stub length increases coupling to the aperture and affects the reactance. In addition, center frequency is slightly affected due to the change in the stub length.

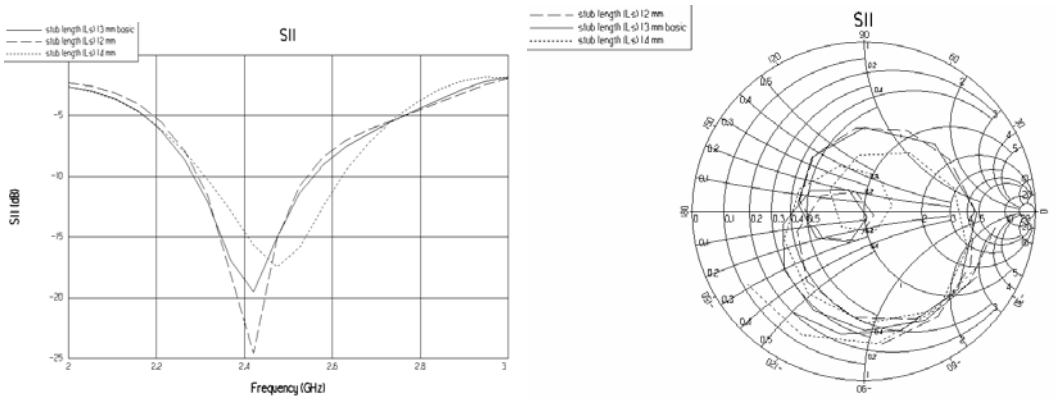

(a) (b)

Figure 2.4.7: Change of input return loss with the change in the stub length (L_s) of the simulated aperture coupled microstrip patch antenna with parameters given in Table 2, (a) linear plot, (b) smith chart plot

Aperture length (L_a):

For aperture coupled microstrip patch antennas, coupling of the feed and the radiating patch depends on the aperture length. Longer aperture causes more coupling but longer aperture also causes high back radiation. Input return losses of the antenna for different aperture lengths are plotted on Figure 2.4.8. It is observed that increase of aperture length slightly shifts the impedance loop in the clockwise direction and shifts the loop toward the center of the smith chart. This effect is due to the increase of coupling between the aperture and the patch. Decrease of the aperture length slightly shifts the impedance loop in the counter clockwise direction and increases the distance to the center of the smith chart.

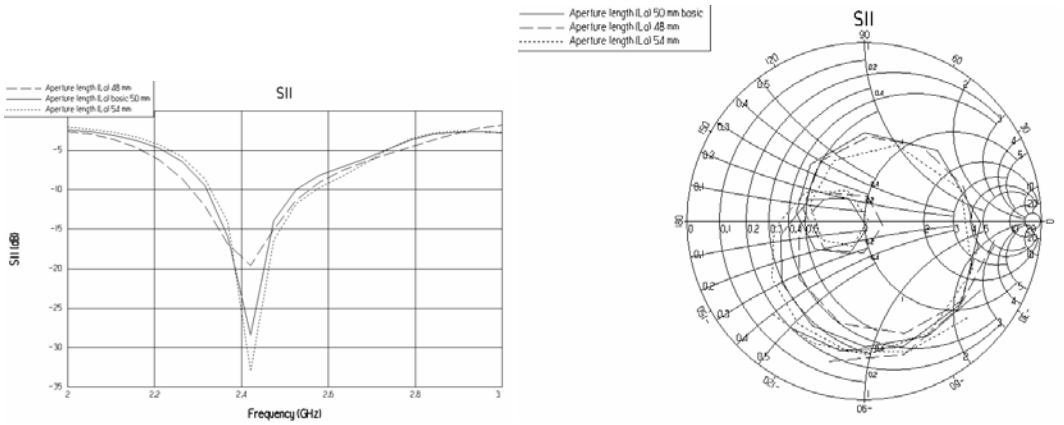

(a) (b)

Figure 2.4.8: Change of input return loss with the change in the aperture length (L_a) of the simulated aperture coupled microstrip patch antenna with parameters given in Table 2, (a) linear plot, (b) smith chart plot

Aperture width (W_a):

Aperture width has also effect on the coupling of the fields through aperture but not as much as the effect of the aperture length. Typically 1/10 width to length ratio is good. As it can be seen from Figure 2.4.9, increase of the aperture width causes increase of coupling to the patch through aperture so that impedance loop gets bigger and closer to the smith chart center.

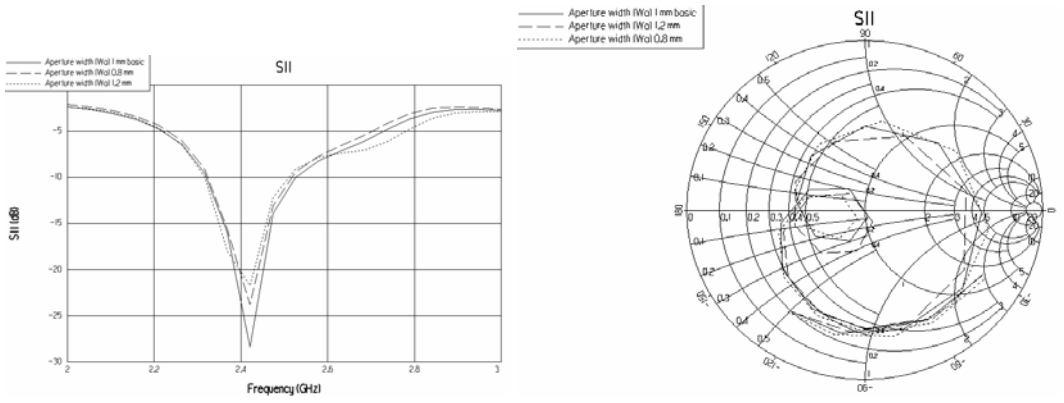

(a) (b)

Figure 2.4.9: Change of input return loss with the change in the aperture width (W_a) of the simulated aperture coupled microstrip patch antenna with parameters given in Table 2, (a) linear plot, (b) smith chart plot

Aperture Offset from the antenna center (in y- direction):

Coupling of the aperture and the patch is in maximum level, when the aperture is centered with respect to the patch. Symmetrical interaction of the feed line and aperture provides better coupling. When aperture has an offset from the center, coupling level decreases, impedance loop gets smaller, and finally it disappears. Figure 2.4.10 shows these changes on input return loss graphs.

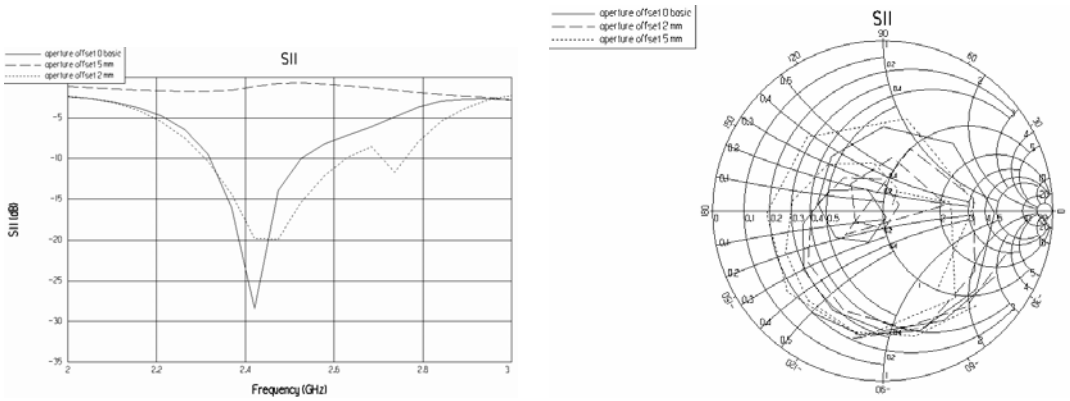

(a) (b)

Figure 2.4.10: Change of input return loss with the change in the aperture offset of the simulated aperture coupled microstrip patch antenna with parameters given in Table 2, (a) linear plot, (b) smith chart plot

Thickness of dielectric substrate of feed line ($D_{\varepsilon 1}$):

The substrate thickness for the feed line should be thin to confine field lines between the microstrip line and the ground plane. Otherwise, there will be spurious radiation from the feed line. As it can be seen from Figure 2.4.11, increase in the dielectric thickness shifts impedance loop in counter clock-wise direction and impedance loop gets smaller. Because increasing the thickness of the substrate of the feed line decreases coupling of the feed line to the patch.

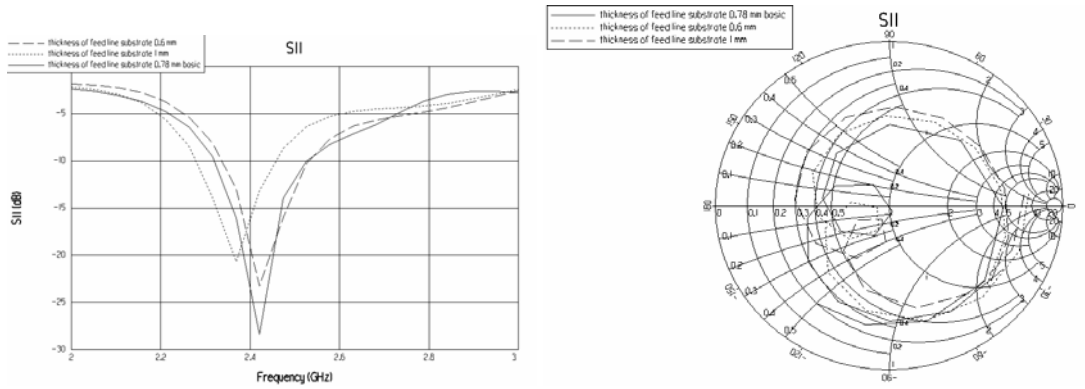

(a) (b)

Figure 2.4.11: Change of input return loss with the change in the substrate thickness of dielectric under feed line of the simulated aperture coupled microstrip patch antenna with parameters given in Table 2, (a) linear plot, (b) smith chart plot

Thickness of dielectric under patch ($D_{\varepsilon 2}$):

This parameter has an effect on bandwidth, efficiency and coupling from feed to patch. Higher thickness of the dielectric causes wider bandwidth but less coupling to the patch through the aperture. Also high thickness causes more spurious radiation, strong excitation of surface waves and it decreases antenna efficiency. As it can be seen from Figure 2.4.12, increase of the dielectric thickness ($D_{\varepsilon 2}$) causes shift in the impedance loop in the counter clockwise direction and the impedance loop disappears.

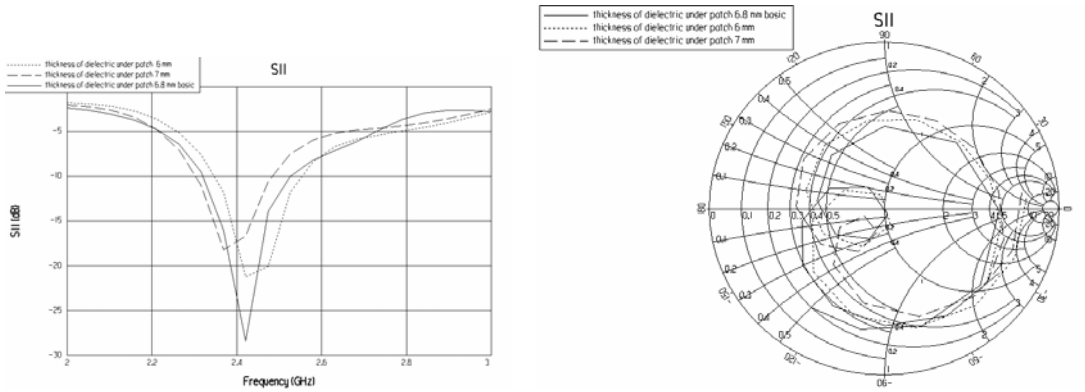

(a) (b)

Figure 2.4.12: Change of input return loss with the change in the thickness of dielectric under the patch of the simulated aperture coupled microstrip patch antenna with parameters given in Table 2, (a) linear plot, (b) smith chart plot

Dielectric constant of substrate under patch (ε_2):

This parameter has an effect on bandwidth and radiation efficiency of the antenna. Antenna bandwidth and antenna efficiency are inversely proportional to the dielectric constant. Lower permittivity dielectric causes higher bandwidth and higher antenna efficiency. This parameter also affects the size of the antenna. Higher dielectric constant requires lower dimension of antenna for the same operation frequency. As it can be seen from Figure 2.4.13, increasing the dielectric constant of the substrate under patch increases the coupling between the patch and the aperture so the impedance loop gets bigger. In addition, increasing the dielectric constant causes decrease in the resonance frequency because the electrical length of the patch becomes longer. It is possible to obtain higher bandwidth with low dielectric constant, when the antenna is properly matched by adjusting other parameters.

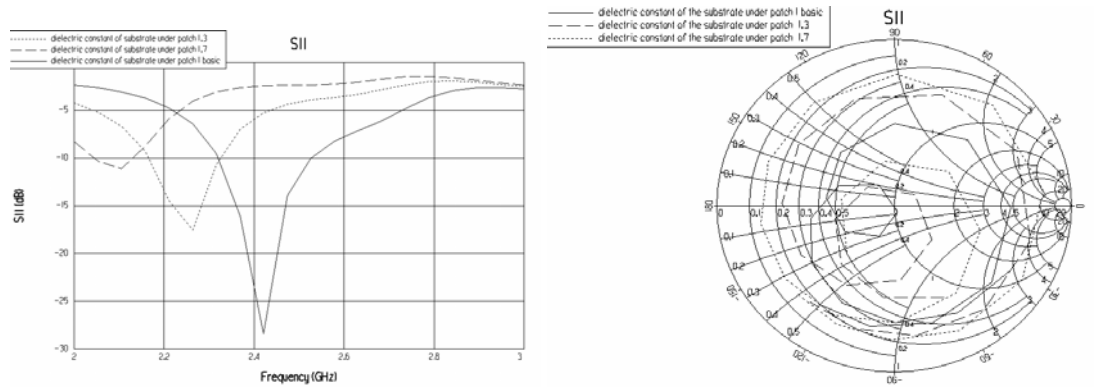

(a) (b)

Figure 2.4.13: Change of input return loss with the change in the dielectric constant of the dielectric under the patch of the simulated aperture coupled microstrip patch antenna with parameters given in Table 2, (a) linear plot, (b) smith chart plot

Dielectric constant of the substrate under feed line (ε_1):

To confine the fields beneath the feed line, a substrate with high dielectric constant is preferred. High dielectric constant substrate selection is also effective to reduce back radiation level and good for coupling to the aperture. As seen from Figure 2.4.14, increasing the dielectric constant between feed line and aperture increases the coupling to the aperture so impedance loop gets close to the smith chart center.

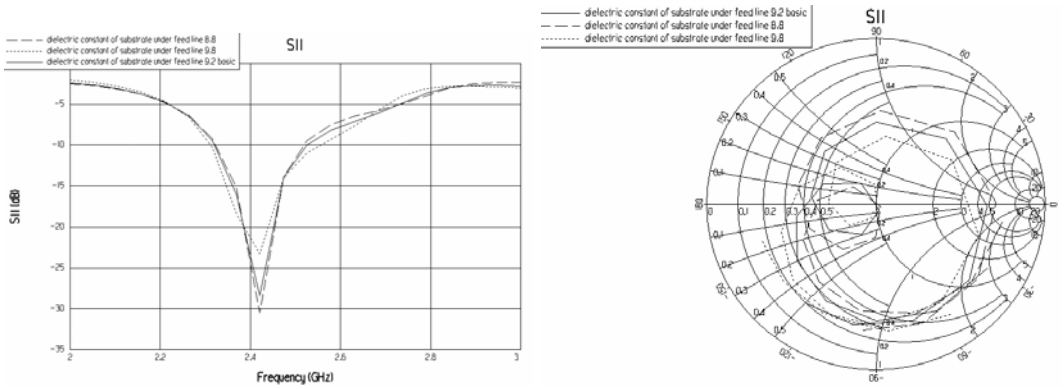

(a) (b)

Figure 2.4.14: Change of input return loss with the change in the dielectric constant of substrate under feed line of the simulated aperture coupled microstrip patch antenna with parameters given in Table 2, (a) linear plot, (b) smith chart plot

2.4.3 Circularly Polarized Aperture Coupled Microstrip Patch Antennas

In communication systems, different applications may need different polarizations. For instance, dual polarized antennas are required for polarization diversity to increase the receiver sensitivity. Circularly polarized antennas are used in satellite communications and GPS (Global Positioning System) [24].

Circular polarization can be obtained if two orthogonal modes are excited with 90^o phase difference. Different structures can be used to achieve circular polarization. Square shaped patches are preferred to obtain circular polarization by exciting two orthogonal edges with 90^o phase difference. As shown in Figure 2.4.15 (a), power dividers or 90^o hybrids can be used to obtain phase difference to feed two orthogonal modes. A nearly square shaped patch is excited from its corner for circular polarization or a thin slot can be opened on a square patch along its diagonal to get circular polarization, as shown in Figure 2.4.15 (b) and Figure 2.4.15 (c). Also, rectangular patch can be excited by a probe at a proper point on its diagonal, as shown in Figure 2.4.15 (d), to get circular polarization.

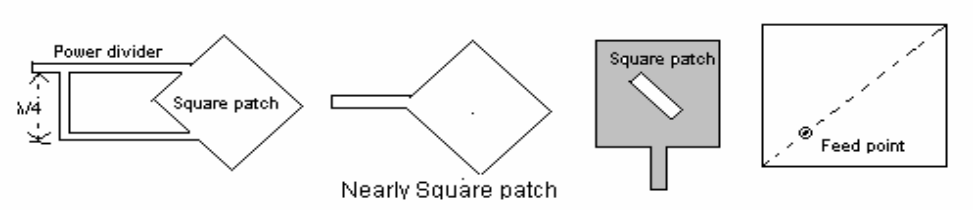

(a) (b) (c) (d)

Figure 2.4.15: Circular polarization microstrip patch antenna structures

Methods to obtain circular polarization by aperture-coupled structures are basically same with the ones used in the previous examples. Two orthogonal modes should be excited with 90^o phase difference to get circular polarization. A cross-shaped aperture can be used instead of a rectangular aperture and perpendicular legs of cross-aperture can be excited with 90^0 phase difference. For instance, a dual band circularly polarized aperture coupled stacked antenna is designed by using this method for GPS applications [24]. Although the antenna has good axial ratio values, it has a complex feed network.

Circularly polarized aperture coupled patch antenna with tilted slot

The designed circularly polarized antenna example with aperture-coupled structure is presented in this section. Tilted aperture is used to obtain circular polarization, as shown in Figure 2.4.16. Tilted slot can be considered as consisting of two apertures along H-plane and E-plane so that two orthogonal modes can be excited. For this structure, axial ratio around 2 for broadside angles are obtained but axial ratio increases rapidly for off broadside angles.

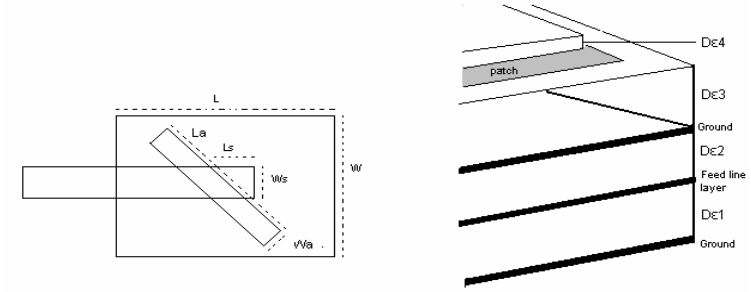

(a) Top view (b) Side view

Figure 2.4.16: Circularly Polarized Aperture Coupled Patch Antenna Geometry

The designed antenna parameters are given in Table 3. A thin dielectric layer with parameters (ε_4, $D_{\varepsilon 4}$) is placed on the patch layer for protection.

***Table 3**: Parameters of the circularly polarized aperture coupled microstrip patch antenna operating at 10.2 GHz*

W	L	L_s	W_s	L_a	W_a	$D_{\varepsilon 1}$
9.4mm	7.6 mm	2.48 mm	2 mm	10 mm	0.8mm	3mm

ε1	$D_{\varepsilon 2}$	ε2	$D_{\varepsilon 3}$	ε3	$D_{\varepsilon 4}$	ε4
1.14	0.762 mm	2.94	3mm	1.14	0.762mm	2.94

Simulated input return loss graph is shown in Figure 2.4.17. According to this figure, bandwidth of the antenna is 10.7% at 10.2 GHZ for the criterion S11< -15 dB. Axial ratios of the antenna for different frequencies can be seen in Figure 2.4.18. As seen from figures, it can be concluded that this antenna has circular polarization characteristic over its bandwidth. Although axial ratio increases to 5 for 80^o at 10.68 GHz which is the end of band, axial ratio level is about 2 over the majority of bandwidth.

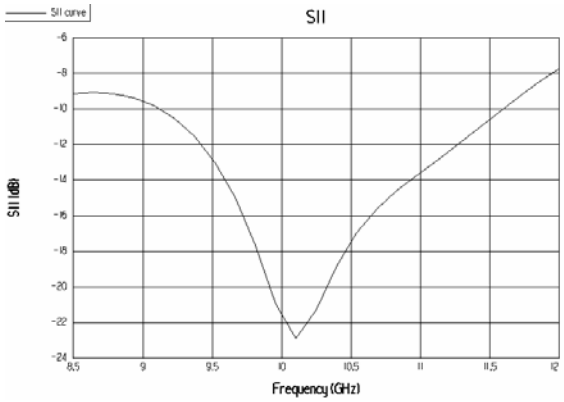

Figure 2.4.17: Input return loss versus frequency plot of the simulated circularly polarized aperture coupled microstrip patch antenna with tilted slot

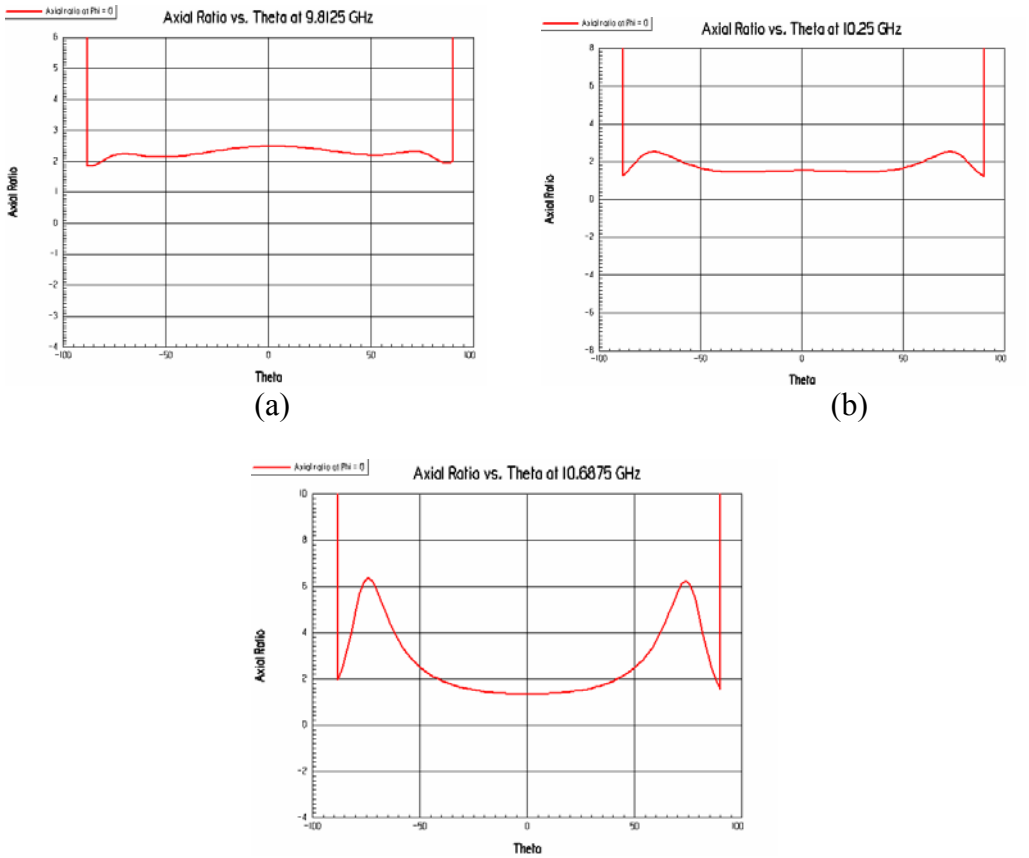

Figure 2.4.18: Axial ratio graphs of the simulated circular polarized aperture coupled microstrip patch antenna with inclined aperture operating at 10.2 GHz, (a) at 9.8 GHz, (b) at 10.25 GHz, (c) at 10.68 GHz

CHAPTER 3

APERTURE COUPLED STACKED MICROSTRIP PATCH ANTENNAS

3.1 Introduction

Using different resonant modes to get broadband microstrip patch antenna is a successful approach. Typical application of this idea is to use two or more resonant elements with slightly different resonant frequencies. These elements are parasitically coupled to each other to get wideband operation. Stacked antenna structure is a common implementation of this idea. Basically, two patches are put together with a dielectric layer between them. Bottom patch can be excited by a probe or by a microstrip line. An upper patch is proximity coupled to the bottom patch. Two kinds of feeding are commonly used for wideband operation in literature. One of these structures is the probe fed stacked structure, which has 10%-29% bandwidth [19]. Other structure is aperture coupled stacked structure which has up to 70% bandwidth (for VSWR<2) [17]. Also aperture coupled stacked patch antennas have low and symmetrical cross polarization patterns compared to probe fed stacked antennas.

Geometry of a typical aperture coupled stacked microstrip patch antenna is shown in Figure 3.1.1. There are two patches; upper and bottom patches. There is a dielectric layer between patches. Bottom patch is excited by coupling through an aperture. Upper patch is proximity coupled to the bottom patch.

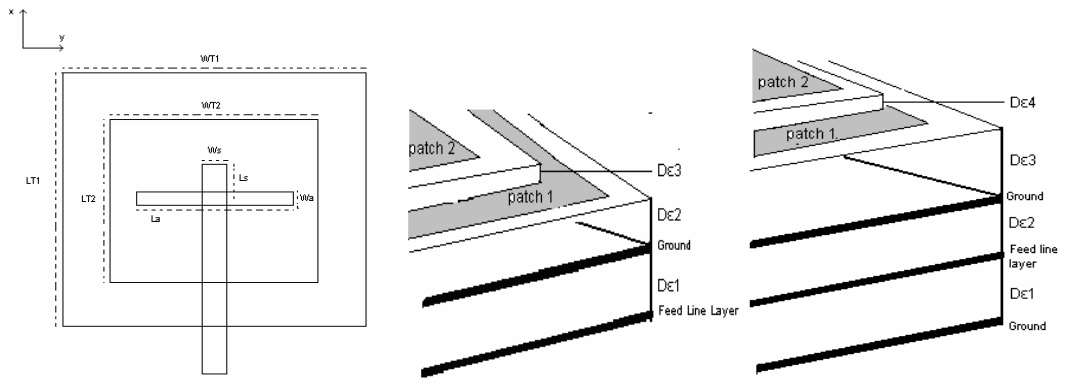

(a) Top view (b) Side view (c) Side view of antenna with ground layer

Figure 3.1.1: Aperture coupled stacked microstrip patch antenna structure

More than two patches can be used to get wider bandwidth but additional patches do not provide significant increase in the bandwidth of the antenna. The reason can be explained by examining the current distributions on patches. Currents on the bottom and upper patches are in phase at a lower frequency, as shown in Figure 3.1.2 (a), which is called the even mode; whereas currents on patches are out of phase at higher frequencies, as shown in Figure 3.1.2 (b), which is called odd mode. Since this mode is not suitable for radiation, this odd mode frequency is a limit for the stacked antenna bandwidth and it will not change with addition of more patches.

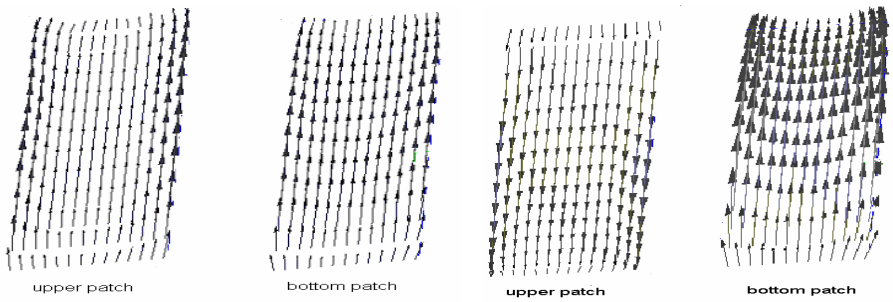

(a) Even Mode (b) Odd Mode

Figure 3.1.2: Current distributions obtained from Ensemble simulation of the aperture coupled stacked patch antenna with parameters given in Table 8, (a) Even Mode, current distributions of patches at 8 GHz, (b) Odd Mode, current distributions of patches at 9.7 GHz

Analysis of aperture coupled stacked microstrip patch antennas is complicated, because the coupling mechanism between patches and aperture is complex. There are too many design parameters in this structure.

There are three resonators in the aperture coupled stacked microstrip patch antenna structure. Namely, two patches and one aperture have their own resonances. Various design parameters (patch size, dielectric thickness etc.) of aperture coupled stacked patch antenna can be tuned to make the corresponding impedance loops close to each other and to the center of the smith chart for wideband operation. In general, two impedance loops corresponding to coupling between two patches and coupling between aperture and bottom patch are seen on the smith chart plots. These two impedance loops should be shifted inside VSWR = 2 circle positioned at the center of smith chart. The size and the position of the input impedance loops change with design parameters. For example, an impedance circle on smith chart gets bigger if coupling between patch and aperture increases. This situation can be realized by decreasing dielectric thickness between the patch and the aperture or by increasing size of the patch and the length of aperture. Almost all antenna parameters, which can be seen in Figure 3.1.1, have effects on the characteristics of the antenna but some of them are significant. These parameters are the aperture length, the upper patch size, the bottom patch size, the substrate thickness between bottom patch and ground and substrate thickness between patches. Typically, these parameters have effect on the coupling between patches and coupling of each patch with aperture. Furthermore, size of the patch and dielectric constants determine the operation frequency. Following section is dedicated to analyze design parameters of aperture coupled stacked microstrip patch antennas.

3.2 Parametrical Study of Stacked Aperture Coupled Microstrip Patch Antenna

The effects of some design parameters of aperture coupled stacked patch antennas are analyzed in this part. Namely, stub length (L_s), dielectric constant and thickness of substrate of feed line, dielectric constant and thickness of substrate under patches, patch offset, aperture offset, aperture length, aperture width, bottom

patch length, upper patch length parameters are examined. For analysis purpose, a stacked aperture coupled microstrip patch antenna is designed to operate at 8 GHz. Structure of the aperture coupled stacked microstrip patch antenna can be seen in Figure 3.1.1 (a), (b) and the antenna parameters are listed in Table 4.

***Table 4**: Parameters of the antenna designed for parametrical analysis of the stacked aperture coupled microstrip patch antennas*

L_{t2}	L_{t1}	L_s	W_s	L_a	W_a
11.3mm	10.4mm	3.2mm	4,75mm	11mm	0.5mm

ε_3	ε_2	ε_1	$D_{\varepsilon 1}$	$D_{\varepsilon 2}$	$D_{\varepsilon 3}$
1.07	2.2	2.33	1.6mm	3.33mm	3.9mm

Effects of the parameters of the antenna are observed by parametric analysis. Input return loss versus frequency plots are given for different cases to observe the effects of antenna parameters on the resonance frequency and the bandwidth.

Dielectric constant of substrate of feed line (ε_1)

As it can be seen from Figure 3.2.1, increasing dielectric constant of the substrate between the feed line and the aperture shifts impedance loop in counter-clockwise direction. Coupling to the bottom patch increases due to higher dielectric constant so that the corresponding impedance loop gets bigger. This change also shifts resonance frequency. High dielectric constant of the substrate is better to confine the fields under the feed line to prevent radiation from the feed line.

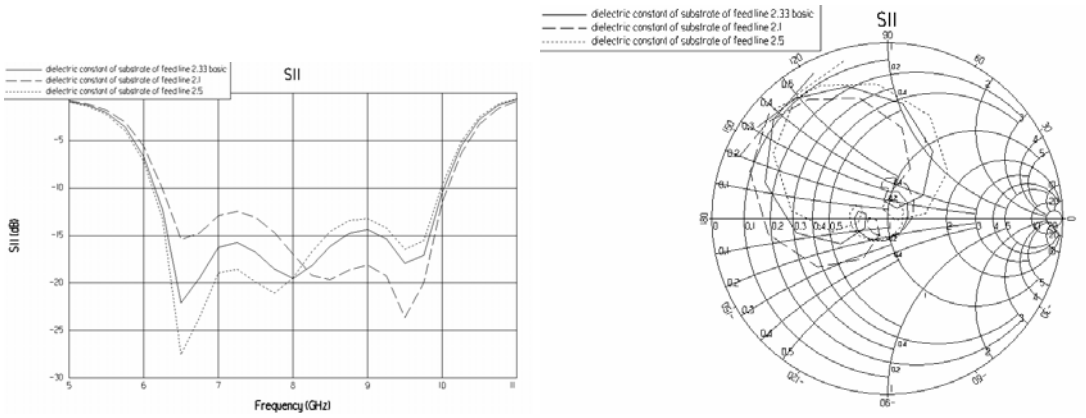

(a) (b)

Figure 3.2.1: Change of input return loss with the change in the dielectric constant of feed line substrate of the simulated aperture coupled stacked microstrip patch antenna with parameters given in Table 4, (a) linear plot, (b) smith chart plot

Thickness of dielectric under feed line ($D_{\varepsilon 1}$)

Increasing the thickness of dielectric between the feed line and the aperture causes a decrease in the coupling of the feed and patches so that impedance loop gets far from smith chart center, as seen in Figure 3.2.2. For good performance, substrate thickness can be selected between 0.01λ-0.02λ to prevent radiation from feed line.

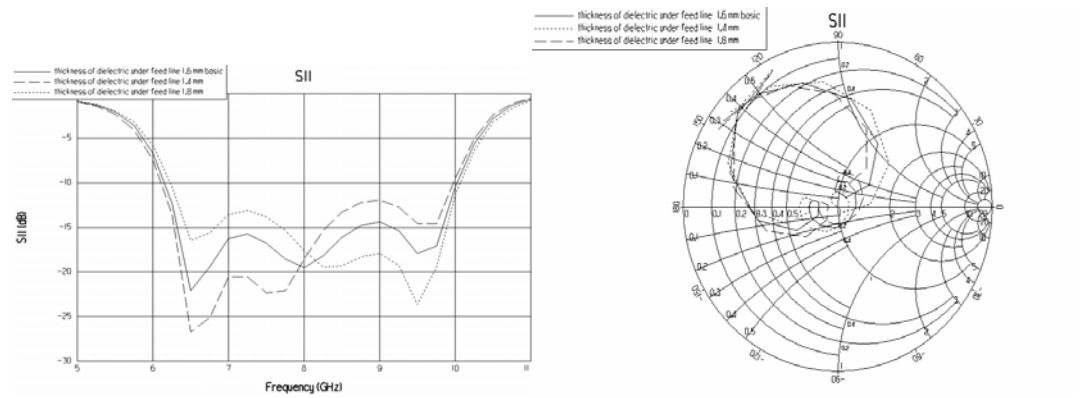

(a) (b)

Figure 3.2.2: Change of input return loss with the change in the thickness of dielectric under feed line of the simulated aperture coupled stacked microstrip patch antenna with parameters given in Table 4, (a) linear plot, (b) smith chart plot

Dielectric constant of substrate under bottom patch (ε_2)

As it can be seen from Figure 3.2.3, increasing the dielectric constant of the substrate under bottom patch decreases the resonance frequency. Increase in dielectric constant increases the coupling to the bottom patch, but decreases the coupling to the upper patch. It is observed from Figure 3.2.3 (b) that one of the impedance loops becomes smaller while the other one becomes larger when dielectric constant is decreased. These roles are interchanged when dielectric constant is increased. Thus, the optimum value should be found for good excitation of both patches.

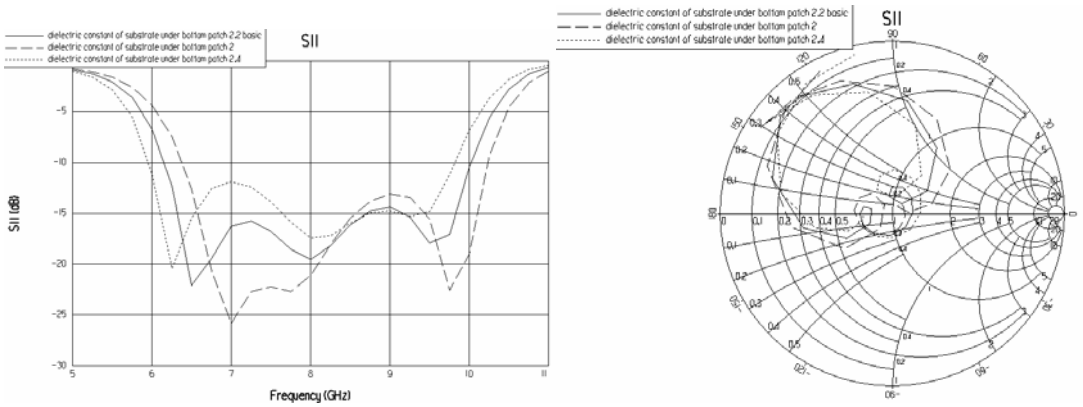

(a) (b)

Figure 3.2.3: Change of input return loss with the change in the dielectric constant of substrate under bottom patch of the simulated aperture coupled stacked microstrip patch antenna with parameters given in Table 4, (a) linear plot, (b) smith chart plot

Thickness of dielectric layer under bottom patch ($D_{\varepsilon 2}$)

Decreasing the thickness of dielectric between the aperture and the bottom patch affects coupling of both patches but the coupling of the bottom patch increases more. Impedance loop corresponding to the bottom patch gets bigger with the decrease in substrate thickness, as seen from Figure 3.2.4. Very thick substrates are not recommended because of strong excitation of surface waves, which reduces the radiation efficiency and perturbs radiation pattern. On the other hand, thin substrates result in narrow bandwidth.

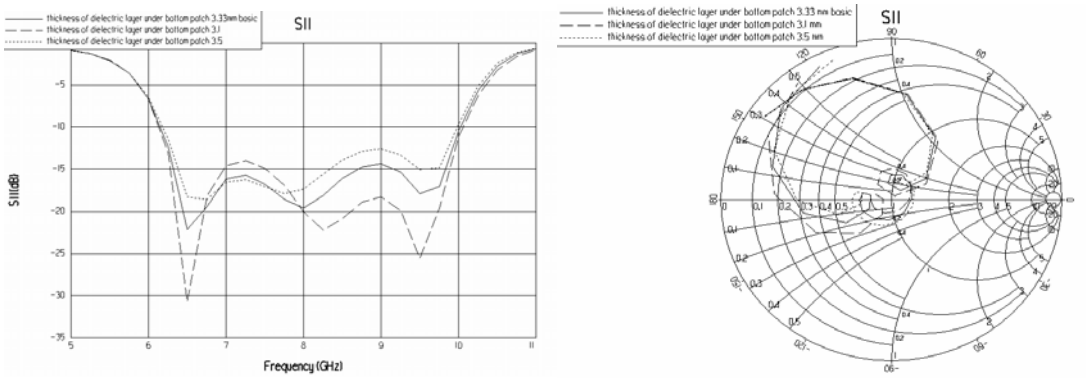

(a) (b)

Figure 3.2.4: Change of input return loss with the change in the thickness of dielectric layer under bottom patch of the simulated aperture coupled stacked microstrip patch antenna with parameters given in Table 4, (a) linear plot, (b) smith chart plot

Dielectric constant of substrate under upper patch (ε_3)

As it can be seen from Figure 3.2.5, increasing dielectric constant between bottom and upper patches increases the coupling of upper patch so corresponding resonance loop gets bigger. Further increase of the dielectric constant has bad effect on bottom patch radiation. Structure tends to behave like an antenna with only upper patch. Higher dielectric constant results in better coupling but it decreases the bandwidth.

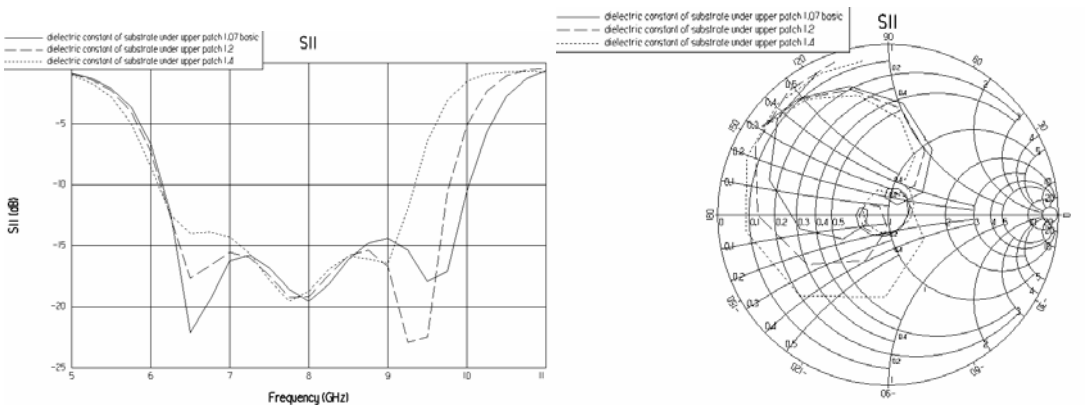

(a) (b)

Figure 3.2.5: Change of input return loss with the change in the dielectric constant of substrate under the upper patch of the simulated aperture coupled stacked microstrip patch antenna with parameters given in Table 4, (a) linear plot, (b) smith chart plot

Thickness of dielectric under upper patch ($D_{\varepsilon 3}$)

Decreasing the thickness of the dielectric between upper and bottom patches increases the coupling of upper patch so the corresponding impedance loop gets bigger. Increasing the thickness decreases the coupling. Effect of this parameter can be seen from input return loss plots given in Figure 3.2.6. It seems that closer upper patch disturbs bottom patch radiation.

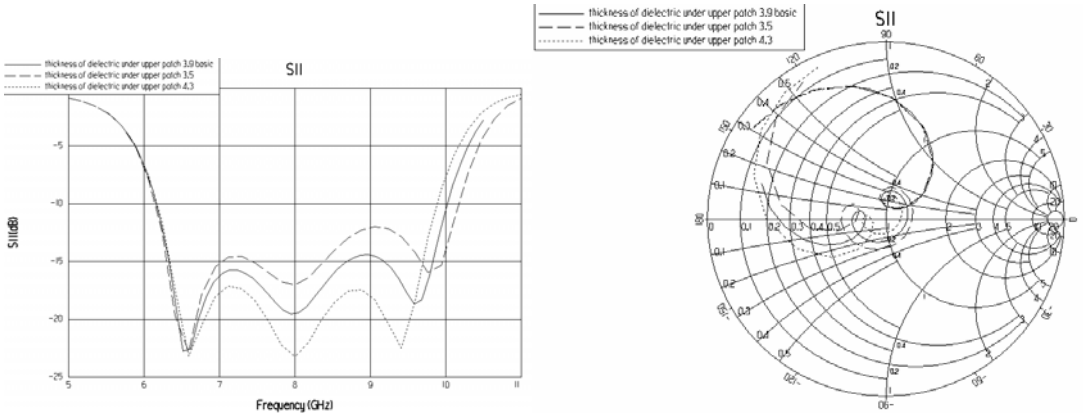

Figure 3.2.6: Change of input return loss with the change in the thickness of dielectric under the upper patch of the simulated aperture coupled stacked microstrip patch antenna with parameters given in Table 4, (a) linear plot, (b) smith chart plot

Stub length (L_s)

Increasing stub length shifts impedance loop in clockwise direction and vice versa, as seen from Figure 3.2.7 (b). Also increasing stub length decreases the S11 values for higher part of the band and increases S11 values for lower part of the band and decreasing the stub length causes an opposite effect. Stub length is important for the coupling of feed line to patches.

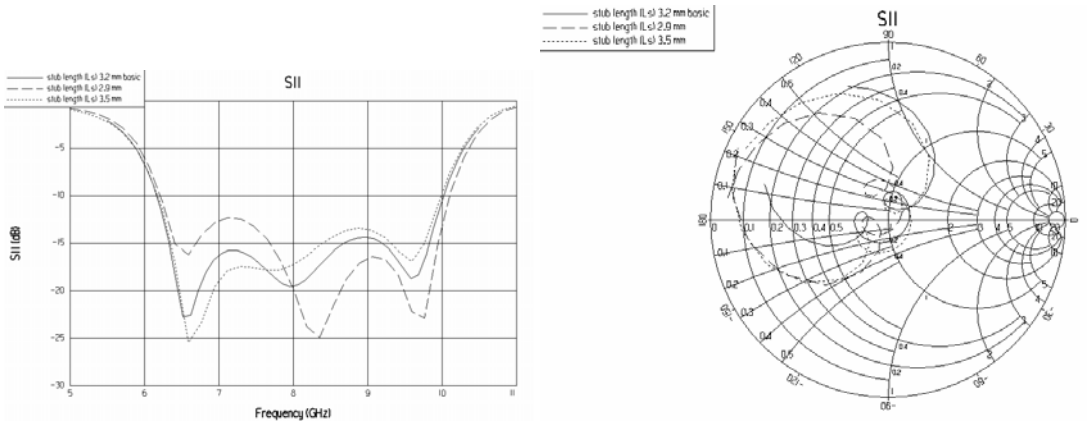

(a) (b)

Figure 3.2.7: Change of input return loss with the change in the stub length (L_s) of the simulated aperture coupled stacked microstrip patch antenna with parameters given in Table 4, (a) linear plot, (b) smith chart plot

Upper patch offset from antenna center (in x- direction)

As it can be seen from Figure 3.2.8, patch offset in –x direction has no significant effect for small offset. Large offset can cause decrease of coupling level.

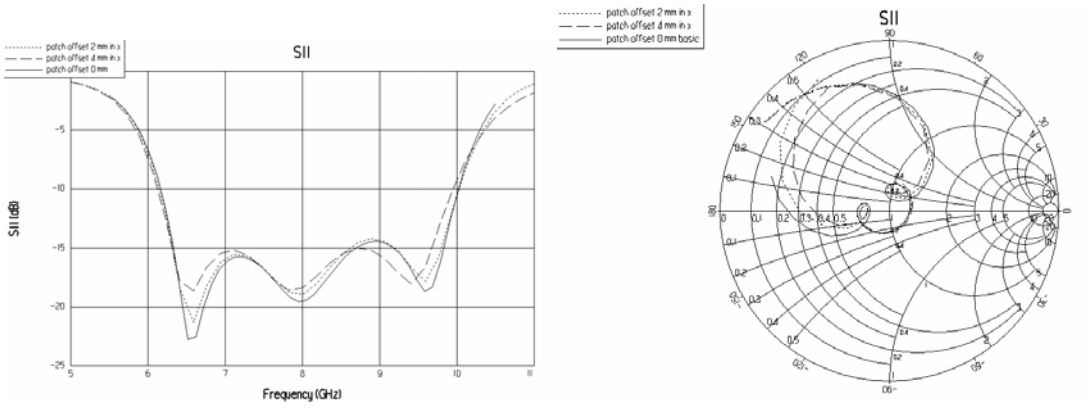

(a) (b)

Figure 3.2.8: Change of input return loss with the change in the upper patch offset (in x- direction) of the simulated aperture coupled stacked microstrip patch antenna with parameters given in Table 4, (a) linear plot, (b) smith chart plot

Bottom patch length (L_{t1})

Decrease in length of bottom patch (L_{t1}) causes increase in the resonance frequency, as seen from Figure 3.2.9. Relative sizes of patches are important for coupling. Bigger bottom patch has more coupling through the aperture so that the size of the corresponding loop is larger. On the other hand, bigger bottom patch reduces the coupling to upper patch.

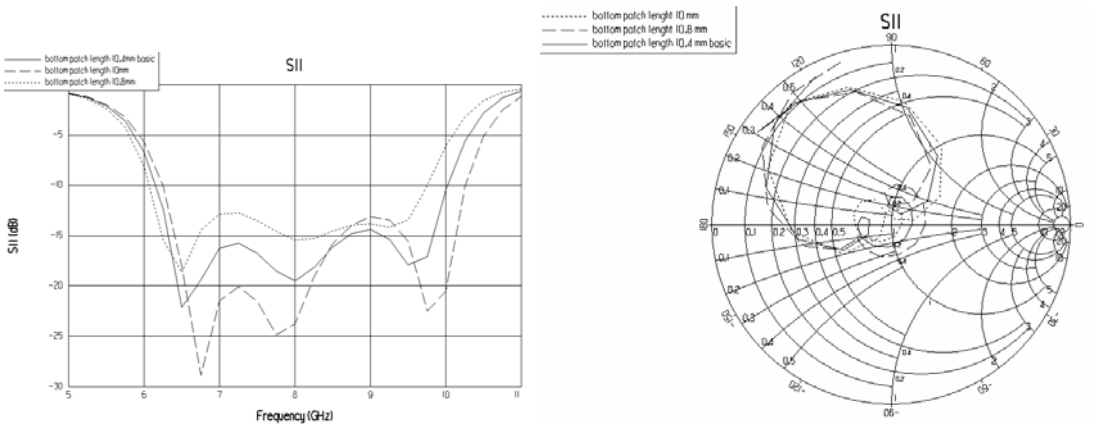

(a) (b)

Figure 3.2.9: Change of input return loss with the change in the bottom patch length of the simulated aperture coupled stacked microstrip patch antenna with parameters given in Table 4, (a) linear plot, (b) smith chart plot

Upper patch length (L_{t2})

As it can be seen from Figure 3.2.10, decrease of the upper patch length (L_{t2}) causes increase in the resonance frequency. Patch dimensions are important for coupling between two patches. Increasing the size of upper patch causes more coupling between the bottom patch and the upper patch so that loop size corresponding to the upper patch gets bigger. Decreasing the size of the upper patch makes this loop narrower.

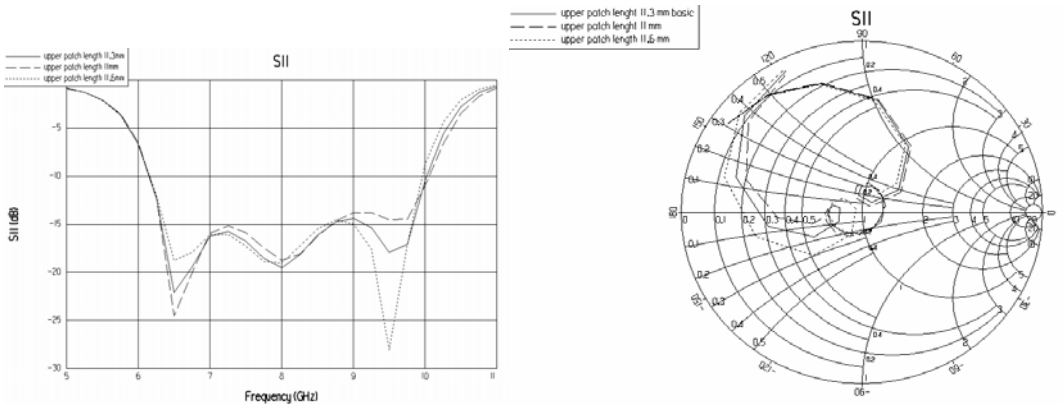

(a) (b)

Figure 3.2.10: Change of input return loss with the change in the upper patch length of the simulated aperture coupled stacked microstrip patch antenna with parameters given in Table 4, (a) linear plot, (b) smith chart plot

Aperture length (L_a)

As it can be seen from Figure 3.2.11, increasing the aperture length increases coupling of the aperture and the bottom patch. This brings impedance loops closer to the center of the smith chart so that impedance loop corresponding to the bottom patch gets bigger and both loops get closer to the smith chart center. Decreasing the aperture length reduces the size of loop and both loops get far from the smith chart center.

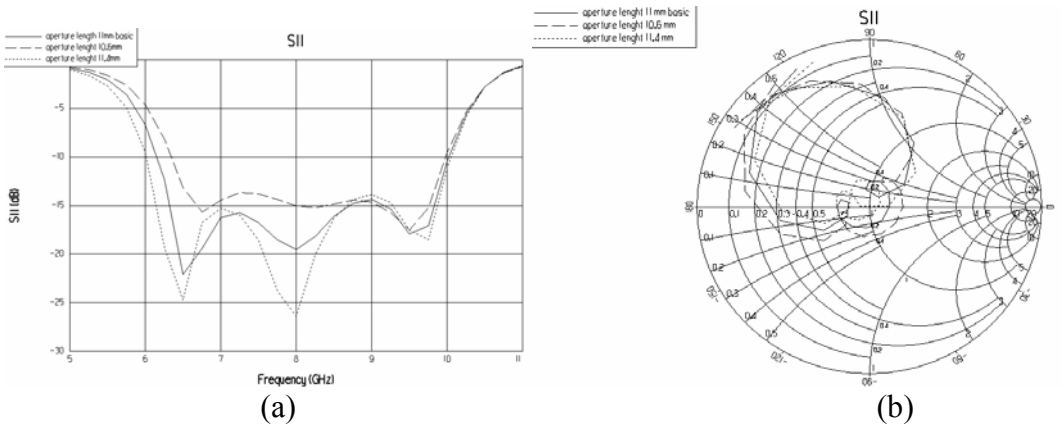

(a) (b)

Figure 3.2.11: Change of input return loss with the change in the aperture length of the simulated aperture coupled stacked microstrip patch antenna with parameters given in Table 4, (a) linear plot, (b) smith chart plot

Aperture width (W_a)

It is observed from Figure 3.2.12 that small changes of aperture width does not have a significant effect but it may affect coupling between the aperture and patches for significant changes. Generally, length to width ratio is selected about 10:1.

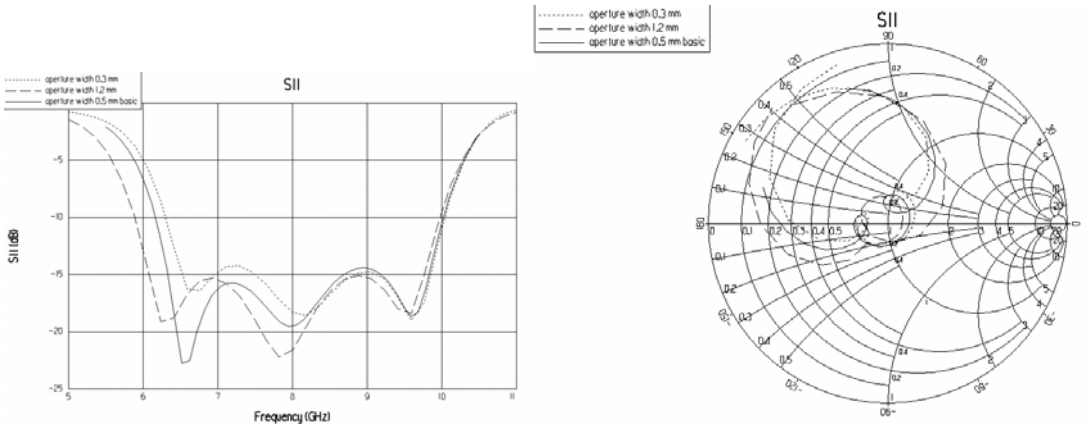

(a) (b)

Figure 3.2.12: Change of input return loss with the change in the aperture width of the simulated aperture coupled stacked microstrip patch antenna with parameters given in Table 4, (a) linear plot, (b) smith chart plot

Aperture offset (in y- direction)

As it can be seen from Figure 3.2.13, aperture offset shifts impedance loop far from the smith chart center because maximum coupling occurs with centered aperture. By the given shift, the coupling decreases so impedance loop gets far from the smith chart center.

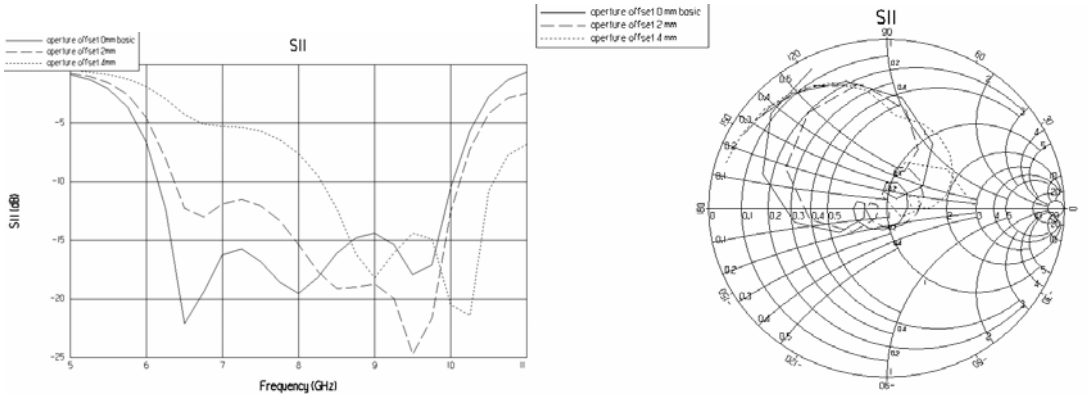

(a) (b)

Figure 3.2.13: Change of input return loss with the change in the aperture offset of the simulated aperture coupled stacked microstrip patch antenna with parameters given in Table 4, (a) linear plot, (b) smith chart plot

As a summary of the parametrical analysis, coupling of upper patch is sensitive to the change of bottom patch dimension. Frequency of the antenna can be adjusted mainly by patch dimensions. Also increasing aperture length increases coupling between the bottom patch and the aperture so that the size of the impedance loop also increases. Size of the other loop corresponding to upper patch changes depending on coupling between two patches. Increasing the dielectric constant between two patches increases the coupling between patches so impedance loop gets bigger. Increasing thickness of the dielectric between patches decreases the coupling so that size of loop decreases.

Different examples of wideband aperture coupled stacked patch antennas can be found in literature [15]. 67 % bandwidth is computed and 69 % bandwidth (S11< -9.54 dB) is measured for the design given in [17]. Front to back ratio of 8-14 dB is achieved which is better than other aperture coupled single patch antennas. It can be decreased further by using a ground plane under the feed line.

3.3 Dual Polarized Aperture Coupled Stacked Microstrip Patch Antennas

Dual polarization antennas have been investigated in the literature. Some of these antennas use aperture coupled stacked microstrip patch antenna structure. Two

different dual polarization examples of aperture coupled stacked patch antenna structures are examined in this thesis. In principle, dual polarization can be obtained by excitation of two orthogonal modes and different methods can be used to excite two orthogonal modes. One of these methods is used to design a wideband dual polarization antenna with aperture coupled stacked structure. Two perpendicular separate apertures on the same ground plane and corresponding two feed lines are used to excite two orthogonal modes, as shown in Figure 3.3.1. H-shaped aperture and T-shaped feed line can be used to improve isolation [25]. A dual polarized broadband aperture coupled antenna is designed by using this structure. This antenna operates at 9.2 GHz with 20.7% and 19.1% bandwidth (for VSWR<2) for each polarization [25].

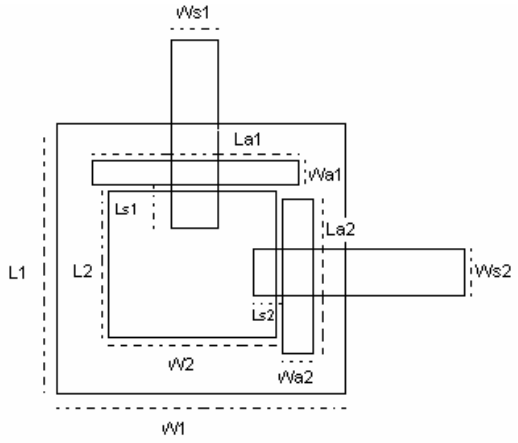

Figure 3.3.1: Antenna structure and parameters for dual polarized stacked aperture coupled microstrip patch antenna with two apertures

Another kind of antenna uses a different structure to excite the orthogonal modes. This structure has cross shape aperture instead of a rectangular aperture and two perpendicular feed lines for orthogonal excitation. These two feed lines are placed on different layers. One feed line is placed under the aperture on ground so that it provides aperture coupled feeding. Other feed line is placed just under the bottom patch so that it provides proximity-coupled feeding. Excitation of first port provides first polarization of the antenna and excitation of second port provides the

second polarization, which is perpendicular to the first polarization. Antenna structure and its parameters can be seen from Figure 3.3.2. There is a wideband antenna example of this structure with 52% bandwidth for 10 dB return loss and 39 dB isolation of excitation [30]. Triple band example of this structure is also included in Chapter 4.

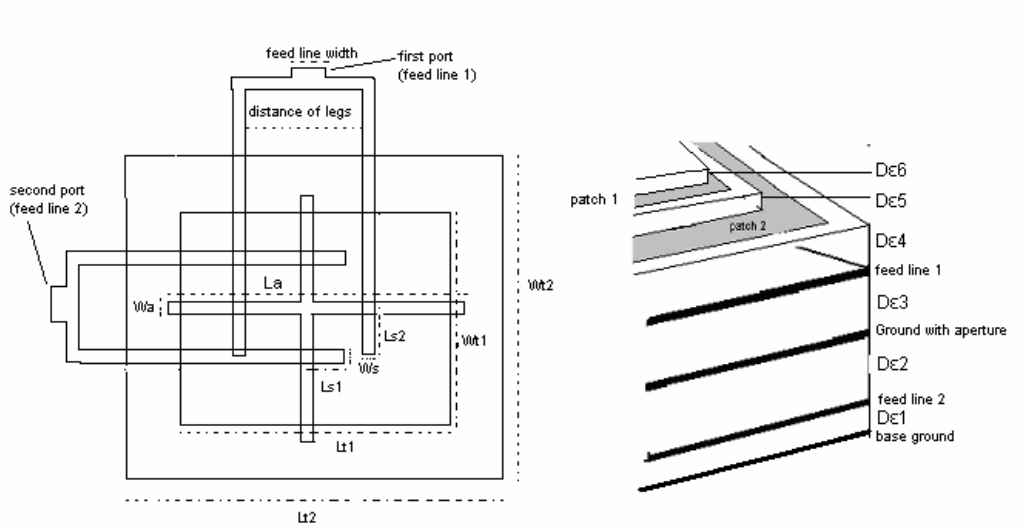

(a) Top view (b) Side view

Figure 3.3.2: Antenna Structure and parameters for dual polarized stacked aperture coupled microstrip patch antenna with cross-shaped aperture

3.4 Mutual Coupling Analysis of Two Aperture Coupled Microstrip Patch Antennas

In antenna arrays, antenna elements are located close to each other. Coupling between antennas disturbs the current distribution and affects the input impedance of the array elements. Hence, in the antenna array design, it is important to know the mutual coupling between array elements.

Mutual coupling between microstrip antennas are originated from the fields in air and the dielectric. These fields are space waves, surface waves, leaky waves and higher order waves [26]. Although space waves (with $1/\rho$ radial variation) and

higher order waves (with $1/\rho^2$ radial variation) are dominant for small antenna elements spacing, surface waves (with $1/\rho^{1/2}$ radial variation) are dominant for large element spacing for E- plane alignment as shown in Figure 3.4.1. For the alignment of antennas shown in Figure 3.4.2, TM_{10} surface wave component decays faster and the mutual coupling is mainly due to space waves.

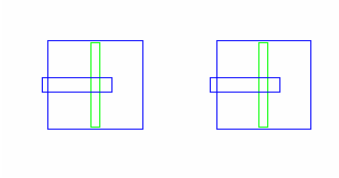

Figure 3.4.1: E-plane alignment

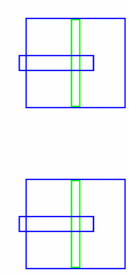

Figure 3.4.2: H-plane alignment

In this section; first, mutual coupling between two aperture coupled patch antennas is examined for different separations between elements. Then, mutual coupling between two aperture coupled stacked patch antennas is obtained and the results are compared.

The structure of aperture coupled microstrip patch antenna can be seen in Figure 2.4.1 (a), (b). An aperture coupled microstrip patch antenna is designed to operate at 9.7 GHz with antenna parameters given in Table 5.

Table 5: *Parameters of the aperture coupled microstrip patch antenna used for mutual coupling analysis*

W	L	L_S	W_S	L_a	W_a	$D_{\varepsilon 1}$	$\varepsilon 1$	$D_{\varepsilon 2}$	$\varepsilon 2$
10.4 mm	10.4 mm	1.7 mm	0.9 mm	6.6 mm	1 mm	0.762 mm	2.94	2 mm	1.14

In Figure 3.4.3, mutual coupling versus separation between antennas are plotted for aperture coupled microstrip patch antennas. It is observed that coupling level for $\lambda_0/2$

separation of aperture coupled microstrip patch antennas is under -15 dB for H-plane but coupling level for $\lambda_0/2$ separation is over -15 dB for E-plane. Coupling between antennas is decreasing with increasing separation for both planes. Coupling level for H-plane is always lower than E-plane coupling, as expected.

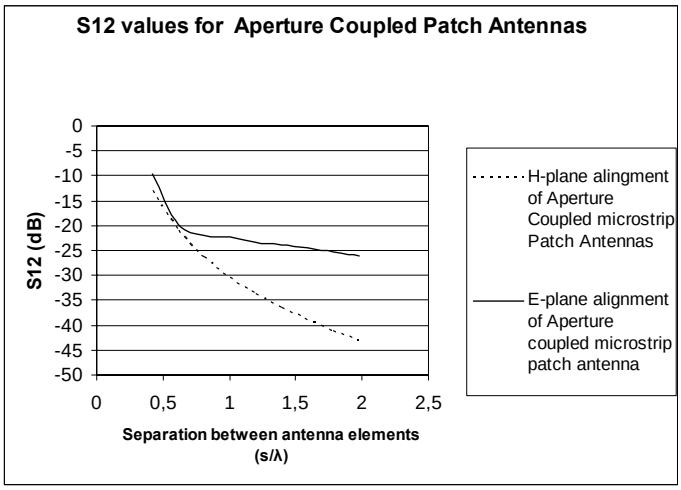

Figure 3.4.3: Mutual coupling versus antenna separation graph obtained by Ensemble simulations for two aperture coupled microstrip patch antennas

The structure shown in Figure 3.1.1 (a), (b) is used in the design of aperture coupled stacked microstrip patch antenna. Parameters of the designed antenna are given in Table 6.

Table 6: *Parameters of the aperture coupled stacked microstrip patch antenna used for mutual coupling analysis*

W_{t2}	L_{t2}	W_{t1}	L_{t1}	L_s	W_s	L_a
11.3 mm	11.3 mm	10.4 mm	10.4 mm	3.17 mm	4,75 mm	11 mm

W_a	$D_{\varepsilon 3}$	$\varepsilon 3$	$D_{\varepsilon 2}$	$\varepsilon 2$	$D_{\varepsilon 1}$	$\varepsilon 1$
0.5	3.9mm	1.07	3.33mm	2.2	1.6mm	2.33

In the Figure 3.4.4, coupling between two aperture coupled stacked patch antennas is plotted as a function of separation between antennas. As it can be seen from the Figure 3.4.4, coupling level for $\lambda_0/2$ separation is lower than -27 dB for H-plane but higher than -15 dB for E-plane. Coupling of antennas for both planes is decreasing with increasing separation. If we compare the coupling of aperture coupled patch antennas and aperture coupled stacked patch antennas, stacked patch antenna has lower coupling in H-plane for smaller separation. Coupling of aperture coupled patch antenna decreases faster than coupling of stacked patch antennas for larger separation. It is interesting to observe that when spacing between antennas is around half a wavelength, mutual coupling between stacked patch antennas is small compared to mutual coupling between aperture coupled patch antennas.

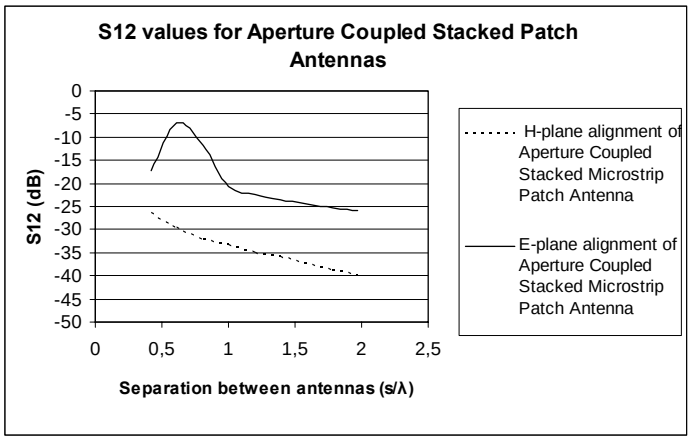

Figure 3.4.4: Mutual coupling versus antenna separation obtained by Ensemble simulations for two aperture coupled stacked microstrip patch antennas

CHAPTER 4

DESIGNED APERTURE COUPLED MICROSTRIP PATCH ANTENNAS

4.1 Wideband Aperture Coupled Microstrip Patch Antenna Designs

This section involves wideband and dual band antennas designed in this study. Majority of the wideband antenna examples are aperture coupled stacked patch type. In addition to stacking of patches, other techniques such as using low dielectric constant, thick substrate are also applied to increase the bandwidth. For different wireless communication applications, five antennas are designed. Input return loss and radiation pattern graphs are given for the designed antennas. Three of these antennas are manufactured and measured. Simulation and measurement results are given and compared.

Antenna 1

The first wideband antenna example is an aperture coupled microstrip patch antenna. Thick dielectric substrate with low dielectric constant is used to get wide bandwidth. Resonances of the patch and the aperture are selected close to each other to achieve wideband operation. Aperture is selected large to achieve wide bandwidth but large aperture size causes back radiation problem. A ground layer is placed at the bottom of the antenna to prevent back radiation.

Antenna structure shown in Figure 2.4.1 (a), (c) is used in this design. Parameters of the designed antenna are given in Table 7. A thin dielectric layer with parameters ($\varepsilon 4$, $D_{\varepsilon 4}$) is placed on top of patch layer for protection. Input return loss and radiation patterns are given in Figure 4.1.1 and 4.1.2 respectively. As it can be observed the 21% bandwidth at 9.2 GHz for S11<-15 dB is obtained.

***Table 7**: Parameters of the wideband aperture coupled microstrip patch antenna operating at 9.2 GHz*

W	L	L_s	W_s	L_a	W_a	$D_{\varepsilon 1}$
12 mm	9.6 mm	1.8 mm	1.8 mm	9mm	1mm	3mm

ε1	$D_{\varepsilon 2}$	ε2	$D_{\varepsilon 3}$	ε3	$D_{\varepsilon 4}$	ε4
1.14	0.762 mm	2.94	3mm	1.14	0.762 mm	2.94

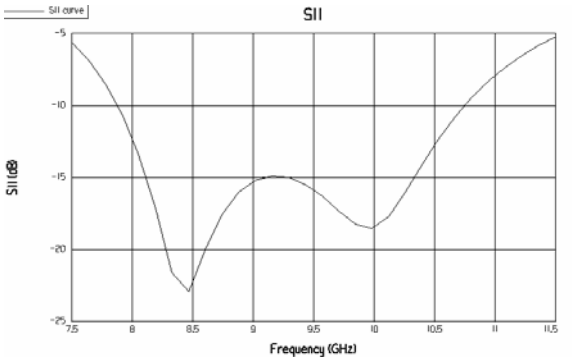

Figure 4.1.1: Input return loss vs. frequency graph of the simulated wideband aperture coupled microstrip patch antenna operating at 9.2 GHz

Radiation pattern shown in Figure 4.1.2 reveals that cross-polarization level of antenna is around -30 dB and there is no back radiation due to base ground layer. In addition, radiation pattern does not change significantly over the whole band. HPBW of the antenna is 75^o at 8.2 GHz and 66^o at 10.25 GHz.

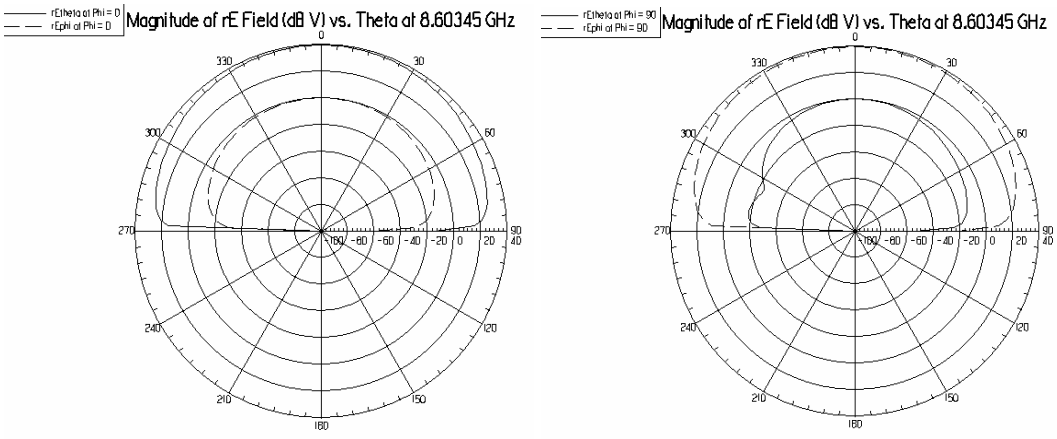

(a) (b)

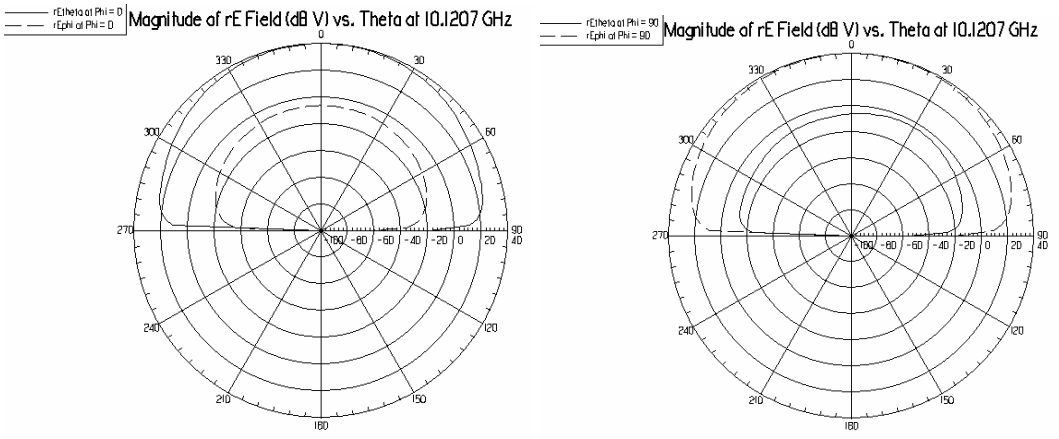

(c) (d)

Figure 4.1.2: Radiation patterns of the simulated wideband aperture coupled microstrip patch antenna operating at 9.2 GHz, (a) E-plane pattern at 8.6 GHz, (b) H-plane pattern at 8.6 GHz, (c) E-plane pattern at 10.1 GHz, (d) H-plane pattern at 10.1 GHz

Antenna 2

As a second example, a wideband aperture coupled stacked microstrip patch antenna is designed to operate at 8 GHz. The geometry of the antenna is given in Figure 3.1.1 (a), (b). Parameters of the designed antenna are tabulated in Table 8.

***Table 8**: Parameters of the wideband aperture coupled stacked microstrip patch antenna operating at 8 GHz*

W_{t2}	L_{t2}	W_{t1}	L_{t1}	L_s	W_s	L_a
11.3mm	11.3 mm	10.4 mm	10.4 mm	3.17 mm	4,75mm	11 mm

W_a	$D_{\varepsilon 3}$	$\varepsilon 3$	$D_{\varepsilon 2}$	$\varepsilon 2$	$D_{\varepsilon 1}$	$\varepsilon 1$
0.5	4.1 mm	1.07	3.14 mm	2.2	1.57 mm	2.2

Resonant frequencies of two patches are tuned to intersect so that wideband characteristic is obtained. This antenna is manufactured and measured.

To manufacture the antenna, antenna layout models are created in AutoCAD format for each metal layer of the antenna. AutoCAD models of patches are inputted to LPKF Protomat 93s tool to carve metals over dielectrics. Each metal layer is etched over a dielectric and then those layers are combined to form the antenna. Layers are put together by using screws or two-sided adhesive band.

Vector network analyzer 8720D is used to measure the return loss of the antenna. Antenna is connected to network analyzer by N-type connector. Network analyzer is calibrated for operating frequency range of the antenna. After measurements of S11, simulation and measurement results are plotted in Figure 4.1.3. Antenna has 43% simulated bandwidth at 8 GHz and 40% measured bandwidth at 7.8 GHz for S11<-15 dB. As it can be seen from this figure, measured values and simulation results are in agreement with each other. However, there is slight difference between measurements and simulation. One reason is that the thickness of the manufactured antennas 9.1 mm ($0.25\lambda_0$) is not same with the thickness of simulated one 8.9 ($0.24\lambda_0$) mm, since two sided adhesive bands are used in the production of antenna. As it can be seen from Figure 3.2.6, increase of the thickness of dielectric layer under upper patch ($D_{\varepsilon 3}$) causes slight shift to lower frequency range.

Simulation and measurement results for radiation patterns of E-plane and H-plane of the antenna are presented in Figure 4.1.4 - 4.1.9 for three different frequencies in the band. Back radiation level is more than the simulation results. Produced antenna has truncated dielectric and finite ground plane. However, in simulations it is assumed that both ground plane and the dielectric are infinite. This situation can be a reason for the difference of measured and simulated radiation patterns. When radiation patterns for three frequencies are compared, decrease of back radiation and increase of cross-polarization can be observed regarding to increasing frequency. Manufactured antenna is fed by a long and wide microstrip line. It seems that this microstrip line also contributes to the back radiation.

According to simulation results cross-polarization level is 50 dB less than co-polarization level, however measured cross-polarization level is 20 dB less than co-

polarization level. One reason for this disagreement can be the small size of dielectric and ground plane compared to the thickness of the antenna. The distance from the patch edge to the edge of the antenna is about $0.1\lambda_0$ whereas; thickness of antennas is $0.2\lambda_0$. Probably, this small size of dielectric caused more fringing fields so that cross-polar components appear stronger. This situation is effective over the band but cross-polarization problems becomes more critical for higher frequencies. Because upper patch of the antenna is responsible for the higher frequency operation, so that electrical thickness of the antenna is larger for high frequency. Keeping in mind the measurement conditions, 20 dB cross-polarization level can be accepted as low cross-polarization level.

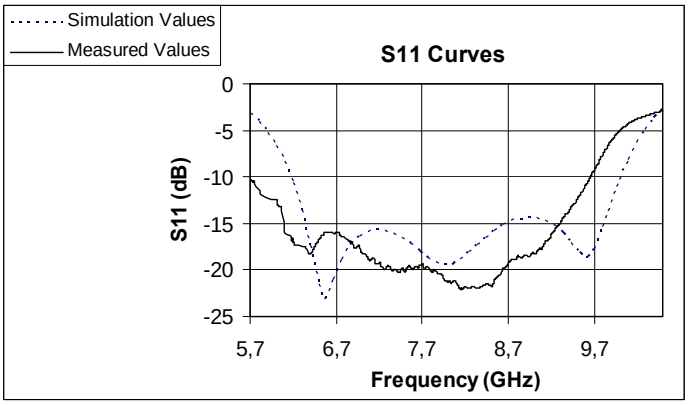

Figure 4.1.3: Comparison of simulated and measured input return loss vs. frequency for the wideband aperture coupled stacked microstrip patch antenna operating at 8 GHz

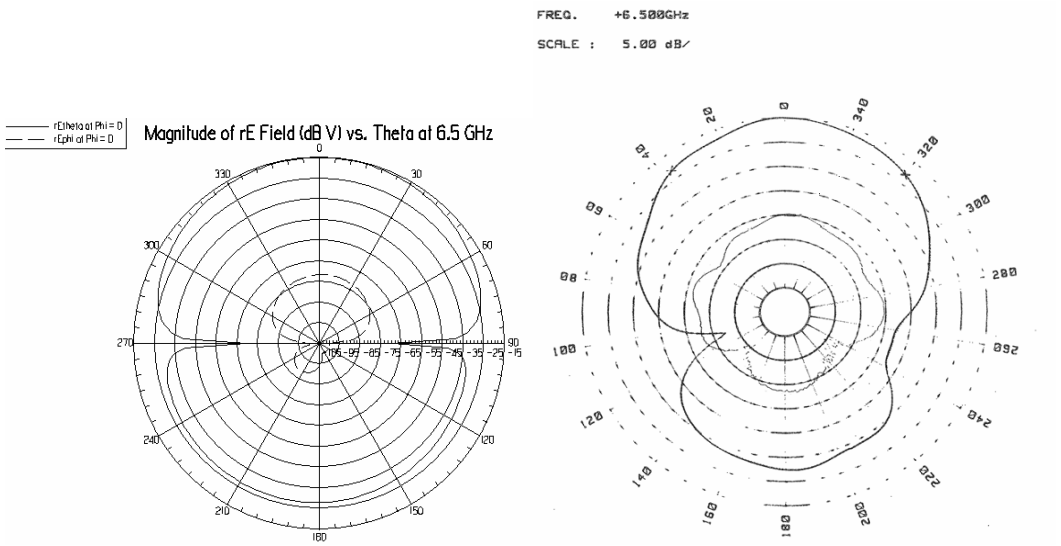

(a) Simulation result (b) Measurement result

Figure 4.1.4: Simulation and measured radiation patterns of the wideband aperture coupled stacked microstrip patch antenna at 6.5 GHz for E-plane

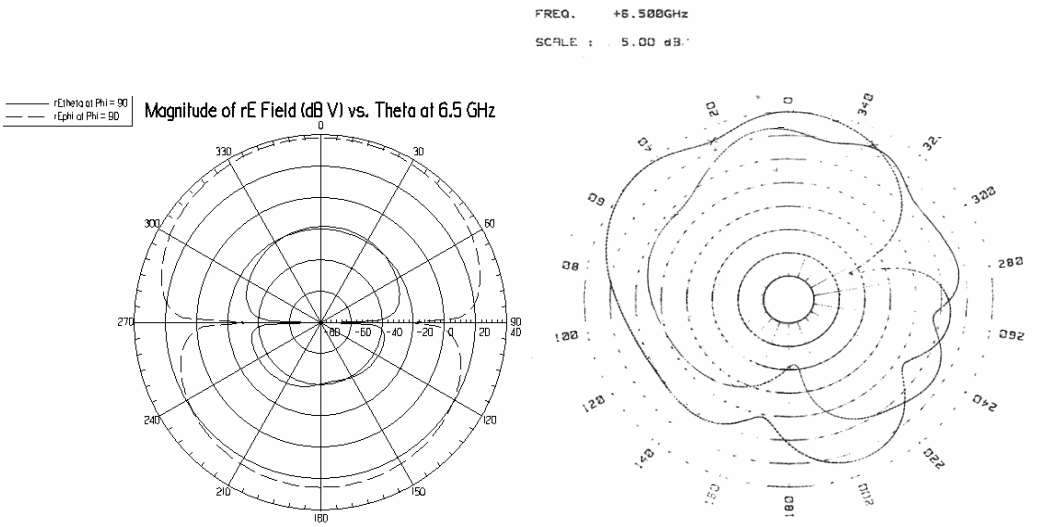

(a) Simulation result (b) Measurement result

Figure 4.1.5: Simulation and measured radiation patterns of the wideband aperture coupled stacked microstrip patch antenna at 6.5 GHz for H-plane

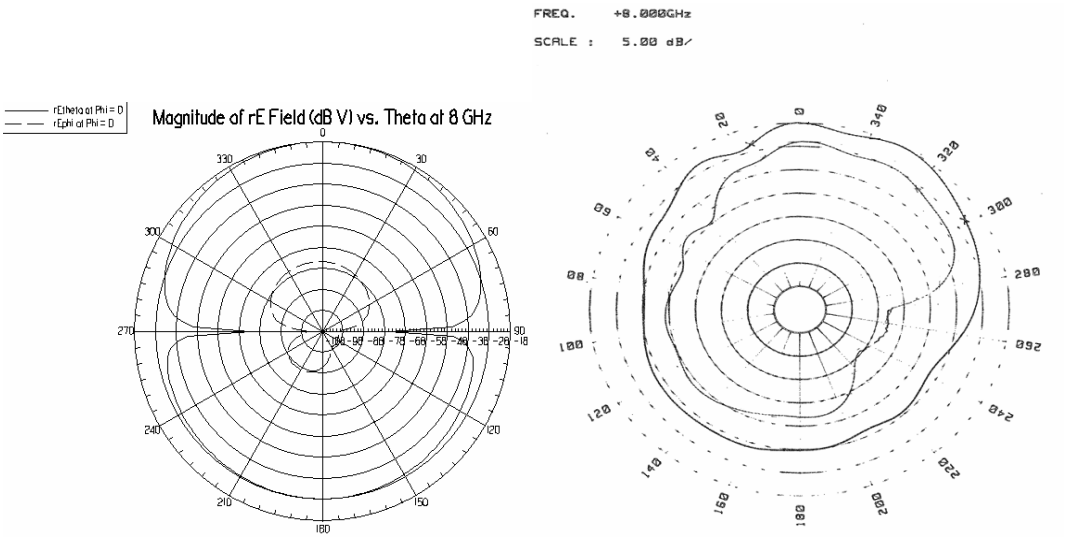

(a) Simulation result (b) Measurement result

Figure 4.1.6: Simulation and measured radiation patterns of the wideband aperture coupled stacked microstrip patch antenna at 8 GHz for E-plane

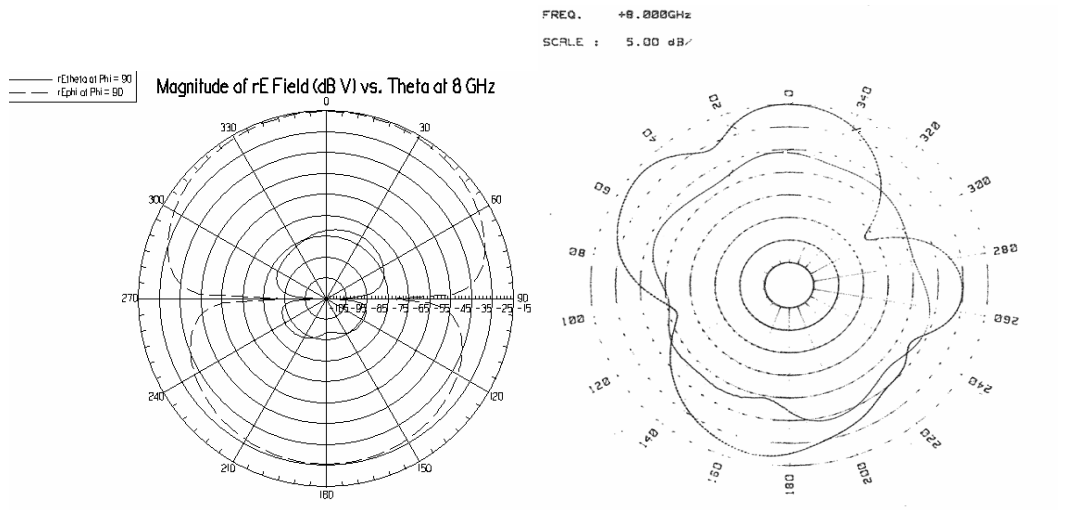

(a) Simulation result (b) Measurement result

Figure 4.1.7: Simulation and measured radiation patterns of the wideband aperture coupled stacked microstrip patch antenna at 8 GHz for H-plane

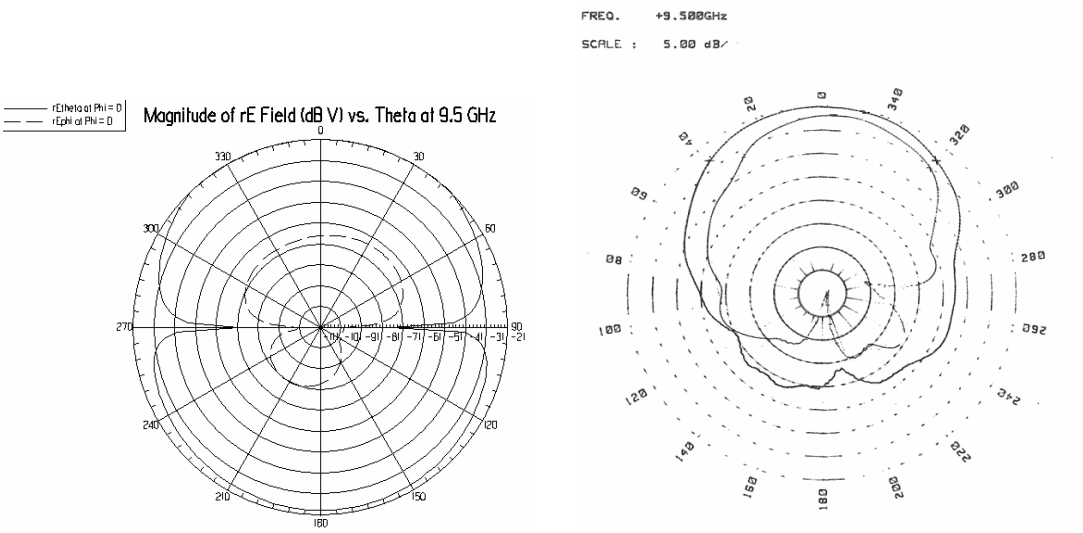

(a) Simulation result (b) Measurement result

Figure 4.1.8: Simulation and measured radiation patterns of the wideband aperture coupled stacked microstrip patch antenna at 9.5 GHz for E-plane

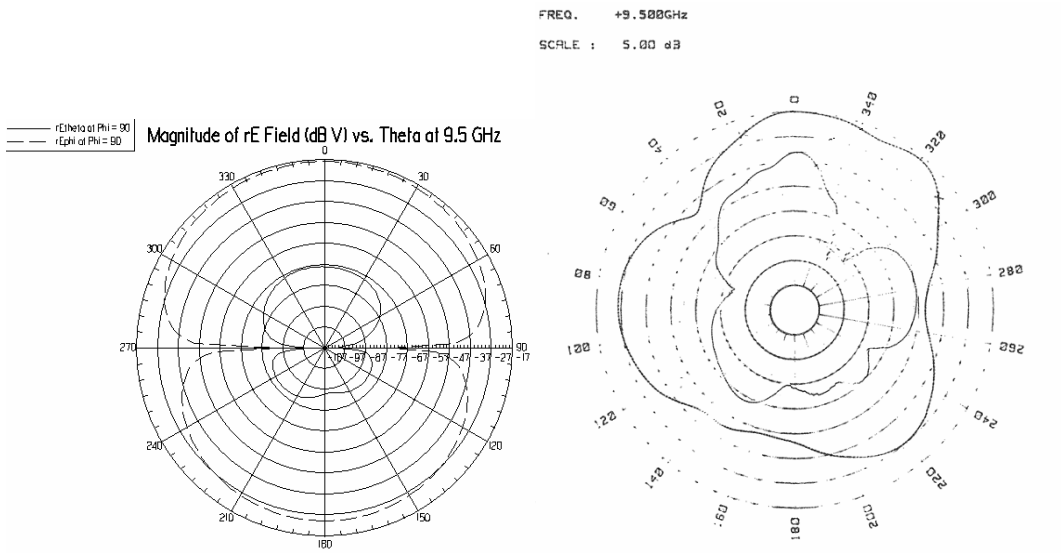

(a) Simulation result (b) Measurement result

Figure 4.1.9: Simulation and measured radiation patterns of the wideband aperture coupled stacked microstrip patch antenna at 9.5 GHz for H-plane

This antenna can be used for IEEE 802.15.3a (UWB) standard for ultra wideband personal area Network (PAN). System operation frequency in North America is 3.1-10.6 GHz frequency range with 528 MHz or grater bandwidth [32].

Antenna 3

The third example has a ground layer under the feed line to prevent back radiation. Two stacked patches are used to achieve wideband characteristic. Wideband aperture coupled stacked microstrip patch antenna is designed around 8 GHz with structure shown in Figure 3.1.1 (a), (c). Parameters of the antenna are given in Table 9.

***Table 9**: Parameters of the wideband aperture coupled stacked microstrip patch antenna with ground plane operating at 8 GHz*

W_{t2}	L_{t2}	W_{t1}	L_{t1}	L_s	W_s	L_a	W_a
11.6 mm	11.6 mm	10.8 mm	10.8 mm	6 mm	2.8 mm	14.4 mm	0.5

$D_{\varepsilon 4}$	$\varepsilon 4$	$D_{\varepsilon 3}$	$\varepsilon 3$	$D_{\varepsilon 2}$	$\varepsilon 2$	$D_{\varepsilon 1}$	$\varepsilon 1$
4.7 mm	1.07	3.65 mm	2.2	1.52 mm	4.4	4 mm	1.07

This antenna is also produced and measured. Measured and simulated antenna input return loss values are plotted in Figure 4.1.10. Up to 28% bandwidth around 8 GHz for S11< -15 is obtained. Although this structure prevents back radiation, bandwidth is remarkably decreased. Measurement and simulation results are similar but higher frequency resonance becomes deeper whereas lower frequency resonance gets closer to -10 dB limit. This situation can be originated from misalignment of layers in the production. Parametrical analysis of aperture coupled stacked antennas in Chapter 3, Section 3.2 can be useful to figure out this behavior. Figure 3.2.7, demonstrates the effect of the stub length. Slight decrease of stub length causes upper resonance to dominate. Another point is about thickness of layers. As mentioned before, two sided adhesive bands may cause slight increase in layer thicknesses. Calculated thickness of designed antenna is about 13.9 mm ($0.34\lambda_0$) whereas measured thickness of produced antenna is around 15 mm ($0.4\lambda_0$). As it can be seen from Figure 3.2.2, slight increase of the thickness of dielectric layer under feed line ($D_{\varepsilon 1}$) causes shift of resonance to higher frequencies. In addition, as shown in Figure 3.2.4, slight increase of the thickness of dielectric under bottom patch causes increase in S11 level, since structure of the produced antenna slightly differs

from the simulated one. Thus, there are small differences between measurement and simulation results.

Radiation patterns obtained by simulation and measurements are plotted in Figure 4.1.11 - 4.1.14 for E-plane and H-plane. Measured and simulated patterns have some differences. Although a base ground is used to prevent back radiation in this structure, there is still high back radiation. Because ground plane of the manufactured antenna has finite size whereas it is taken as infinite in simulations. Surface waves are diffracted from truncated dielectric and finite ground plane, hence the radiation patterns perturbed and back radiation is observed. Just like the previous manufactured stacked aperture coupled antenna, this antenna shows high cross-polarization levels in measurements. The difference between cross-polarization and co-polar components for simulation is about 50 dB but measurement shows just about 13 dB difference. High thickness of antenna compared to its size can be the reason behind this problem. Antenna thickness is $0.4\lambda_0$ and the distance from patch edge to the border of the structure is about $0.1\lambda_0$. Small size of dielectric can cause more fringing fields that causes higher cross-polarization.

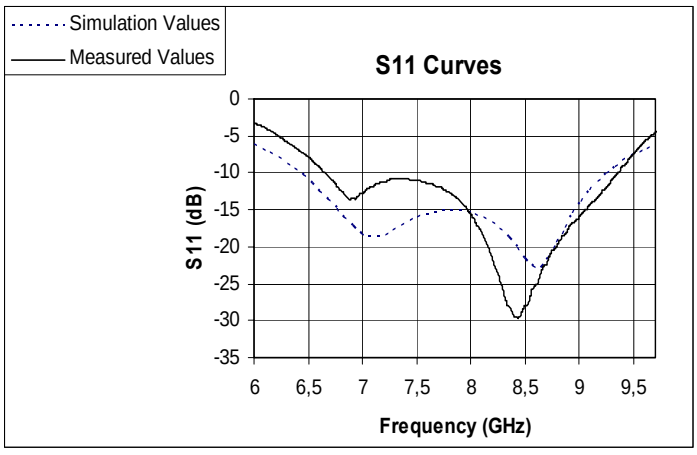

Figure 4.1.10: Comparison of simulated and measured input return loss vs. frequency for the wideband aperture coupled stacked microstrip patch antenna with base ground operating at 8 GHz

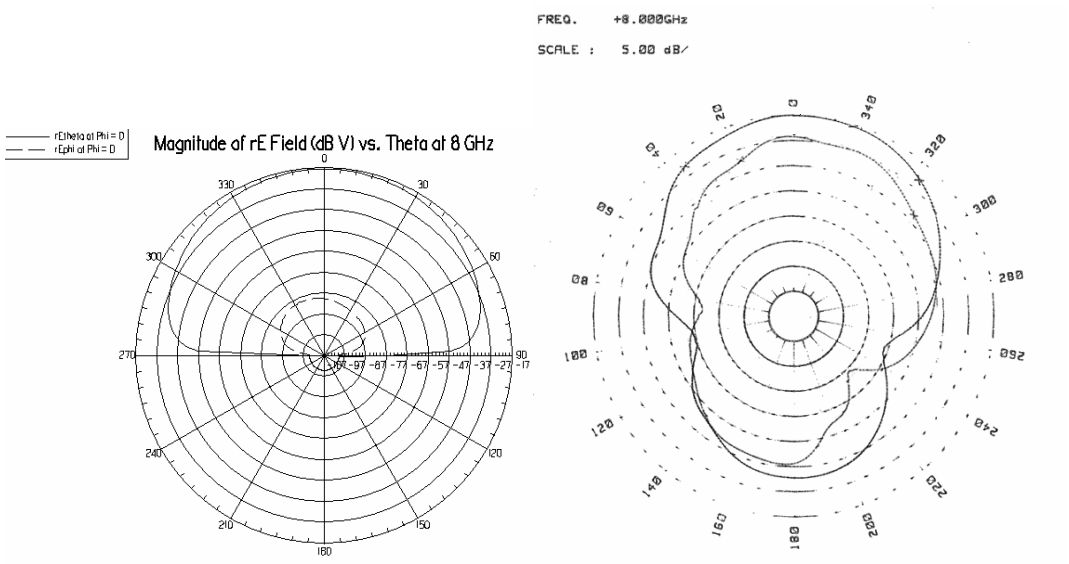

(a) Simulation result (b) Measurement result

Figure 4.1.11: Simulation and measured radiation patterns of the wideband aperture coupled stacked microstrip patch antenna with base ground at 8 GHz for E-plane

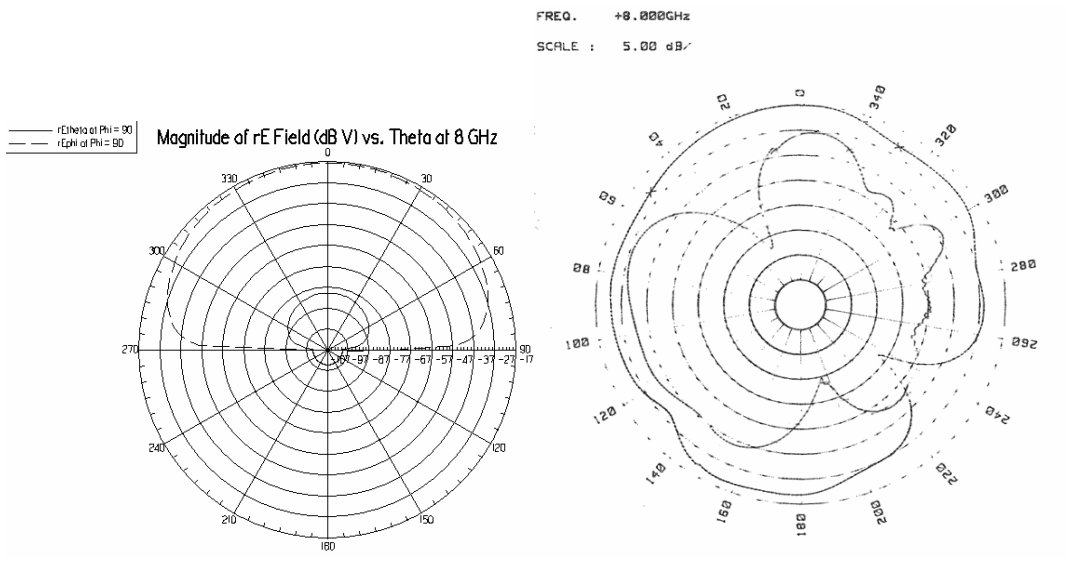

(a) Simulation result (b) Measurement result

Figure 4.1.12: Simulation and measured radiation patterns of the wideband aperture coupled stacked microstrip patch antenna with base ground at 8 GHz for H-plane

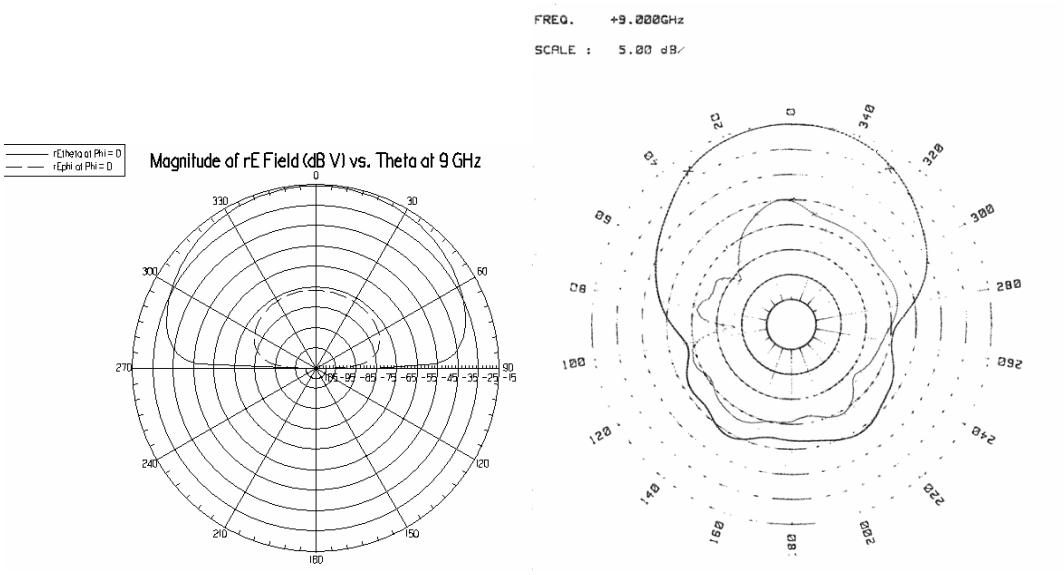

(a) Simulation result (b) Measurement result

Figure 4.1.13: Simulation and measured radiation patterns of the wideband aperture coupled stacked microstrip patch antenna with base ground at 9 GHz for E-plane

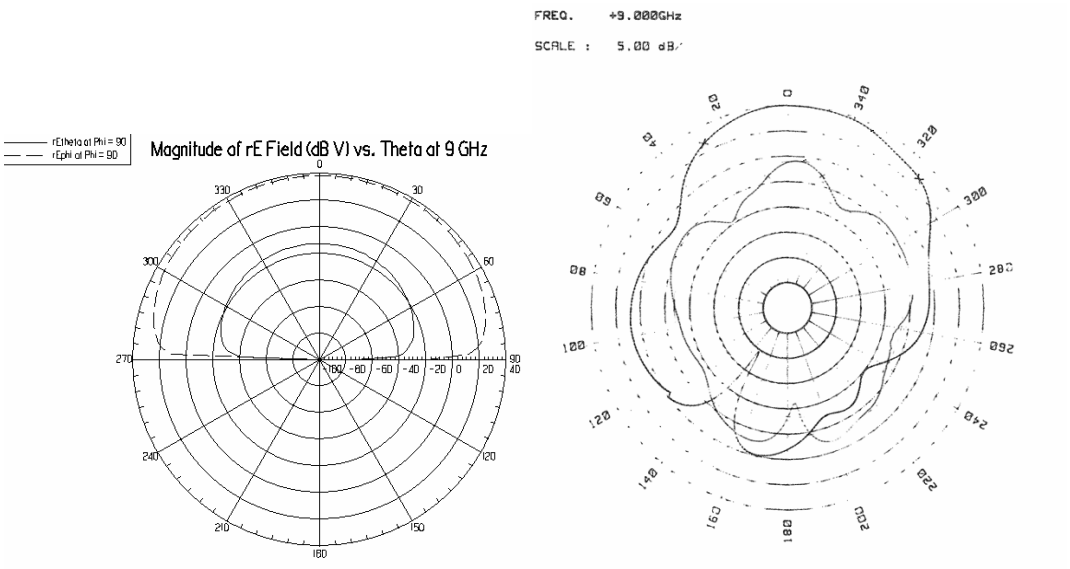

(a) Simulation result (b) Measurement result

Figure 4.1.14: Simulation and measured radiation patterns of the wideband aperture coupled stacked microstrip patch antenna with base ground at 9 GHz for H-plane

Antenna 4

In this example, a wideband aperture coupled stacked microstrip antenna with three patches is designed. Parameters of the designed antenna are given in Table 10. Input return loss and radiation pattern plots, obtained by simulations, are shown in Figure 4.1.15 and Figure 4.1.16. As it can be seen from input return loss graph, an antenna with 51 % bandwidth at 6.1 GHz for S11< -15 dB is obtained.

Table 10: *Parameters of the wideband aperture coupled stacked microstrip antenna of three patches*

W_{t3}	L_{t3}	W_{t2}	L_{t2}	W_{t1}	L_{t1}	L_s	W_s	L_a
11.6mm	11.6mm	13.6mm	13.6mm	13.8mm	13.8mm	4.1mm	2.35mm	14.4mm

W_a	$D_{\varepsilon 4}$	$\varepsilon 4$	$D_{\varepsilon 3}$	$\varepsilon 3$	$D_{\varepsilon 2}$	$\varepsilon 2$	$D_{\varepsilon 1}$	$\varepsilon 1$
0.5mm	2mm	2.2	4.3 mm	1.07	3.9mm	2.2	1.6 mm	2.33

It is observed from radiation patterns obtained at different frequencies shown in Figure 4.1.16 that radiation patterns have similar characteristics, but the beam width of the antenna decreases at the end of the frequency band. Antenna has 90^o HPBW at 4.6 GHz, 90^0 HPBW at 6 GHz and 72^o at 7.7 GHz. As explained in Section 3.1, use of the third patch does not increase the bandwidth significantly.

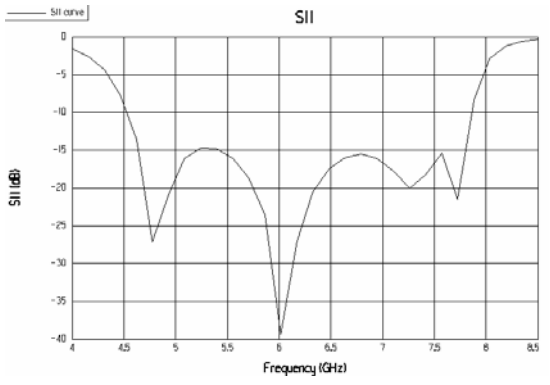

Figure 4.1.15: Input return loss vs. frequency graph for the simulated wideband aperture coupled stacked microstrip antenna with three patches operating at 6.1 GHz

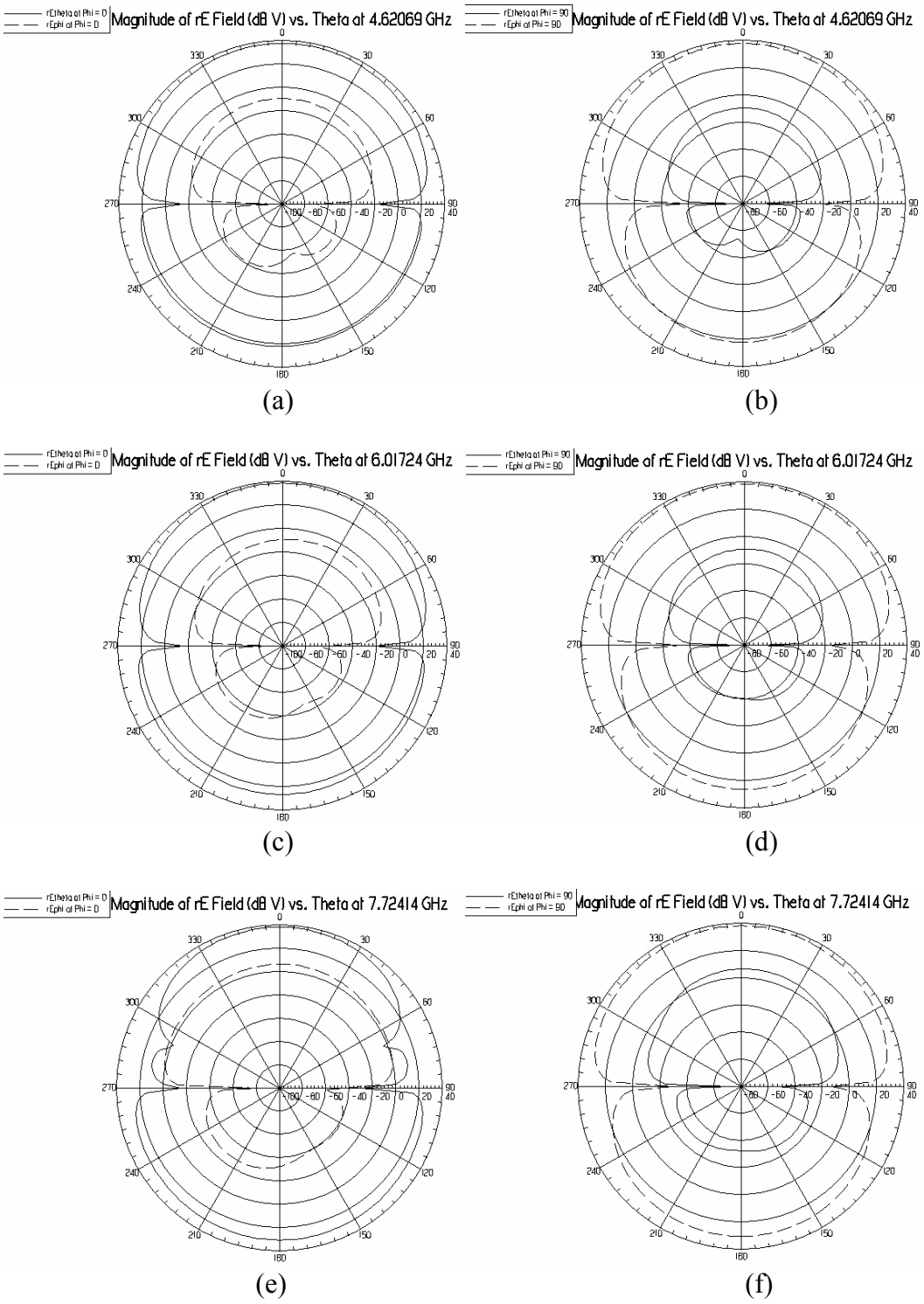

Figure 4.1.16: Radiation patterns of the simulated wideband aperture coupled stacked microstrip antenna with three patches, (a) E-plane pattern at 4.6 GHz, (b) H-plane pattern at 4.6 GHz, (c) E-plane pattern at 6 GHz, (d) H-plane pattern at 6 GHz, (e) E-plane pattern at 7.72 GHz, (f) H-plane pattern at 7.72 GHz

This antenna can be used for IEEE 802.11 a/h/j WLAN standards. WLAN models complying this standard operates at following frequencies [32]

a/h/j: (with 20 MHz bandwidth)

4.9-5 GHz (japan), 5.03-5.091 GHz (japan)

5.15-5.35 GHz (UNII)

5.47-5.725 GHz (Europe)

5.725-5.825 GHz (ISM, UNII)

Antenna 5

This antenna is designed to provide an antenna operating over personal communication systems (PCS) frequency band. Antenna structure shown in Figure 3.1.1 (a), (b) is used in this design. Thick foam substrates with low dielectric constant are used in this design to improve antenna bandwidth. These foam substrates are covered with thin and high dielectric constant substrate for easy production so there are two more dielectric layers with parameters ($\varepsilon 5$, $D_{\varepsilon 5}$) and ($\varepsilon 3$, $D_{\varepsilon 3}$) than shown in Figure 3.1.1 (b). Parameters of the designed antenna are tabulated in Table 11.

***Table 11**: Parameters of the wideband aperture coupled stacked microstrip patch antenna operating at PCS frequencies*

W_{t2}	L_{t2}	W_{t1}	L_{t1}	L_s	W_s	L_a	W_a
58.4 mm	58.4 mm	59.4 mm	59.4 mm	21.4mm	2.35mm	46 mm	1mm

$D_{\varepsilon 5}$	$\varepsilon 5$	$D_{\varepsilon 4}$	$\varepsilon 4$	$D_{\varepsilon 3}$	$\varepsilon 3$	$D_{\varepsilon 2}$	$\varepsilon 2$	$D_{\varepsilon 1}$	$\varepsilon 1$
0.79mm	2.2	6.8 m	1.07	0.79mm	2.2	6.8mm	1.07	4 mm	9.8

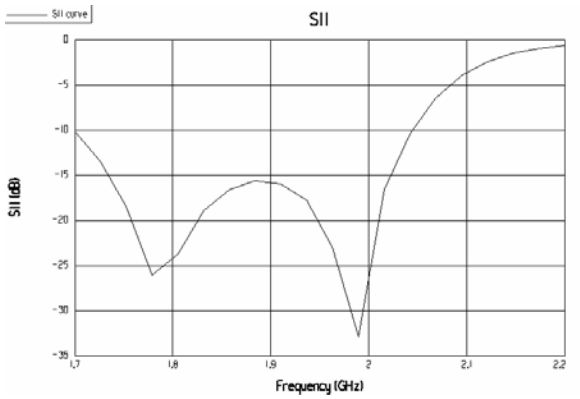

Figure 4.1.17: Input return loss vs. frequency graph for the simulated wideband aperture coupled stacked patch antenna operating at PCS frequencies

Input return loss graph obtained by Ensemble simulation is shown in Figure 4.1.17. As seen from the figure, the bandwidth of the antenna is 15.6 % around 1.85 GHz for S11< -15 dB.

This antenna can be used

for EDGE

PCS 1900 band systems [UL 1850-1910 MHz, DL 1930-1990 MHz],

DCS 1800 band [UL 1710-1785, DL 1805-1880 MHz];

for W-CDMA

PCS 1900 band [UE 1850-1910 MHz, BS 1930-1990 MHz],

DCS 1800 band [UL 1710-1785 MHz, DL 1805-1880 MHz];

for HSPDA

PCS 1900 band [UE 1850-1910 MHz, BS 1930-1990 MHz],

DCS 1800 band [UL 1710-1785 MHz, DL 1805-1880 MHz];

for TD-SCDMA

3GPP [UL 1900-1920, DL 2010-2015]

Simulated radiation patterns of the antenna for different frequencies are given in Figure 4.1.18. It is observed that radiation patterns over the operation band have

similar characteristics. Antenna has 70^{o} HPBW at 1.72 GHz and 60^{o} HPBW at 2.04 GHz.

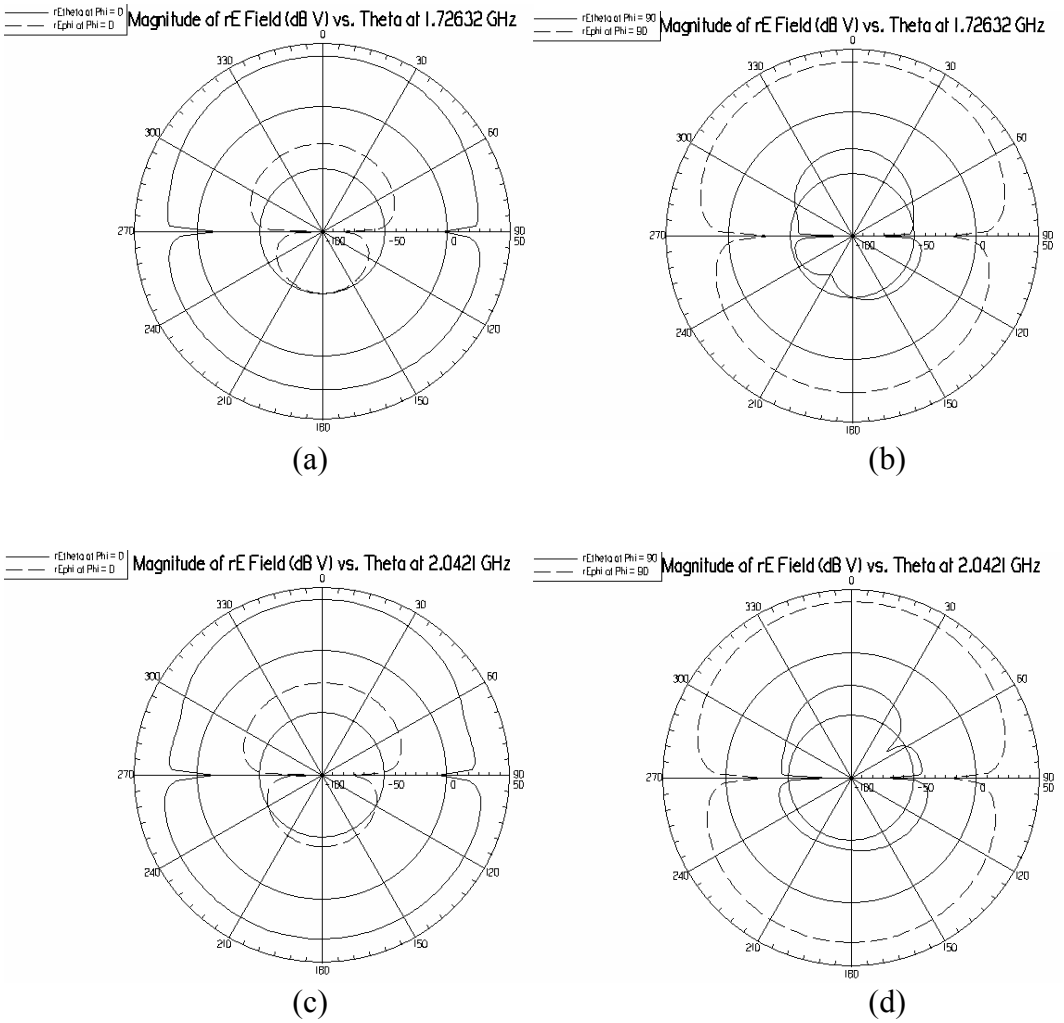

Figure 4.1.18: Radiation patterns of the simulated wideband aperture coupled stacked microstrip patch antenna operating at PCS frequencies, (a) E-plane pattern at 1.72 GHz, (b) H-plane pattern at 1.72 GHz, (c) E-plane pattern at 2 GHz, (d) H-plane pattern at 2 GHz

4.2 Dual-Band Aperture Coupled Microstrip Patch Antenna Designs

Same methods to obtain wideband antenna can be used to get dual band microstrip antennas. There are different dual band patch antenna examples in literature, which are obtained by using orthogonal mode, multi-patch and reactive

loading methods. There are still extensive researches on multi band and dual band microstrip patch antenna structures because of different wireless applications. Among various methods, this thesis focuses on stacking method. For stacked antenna structure, dual band operation is originated from two-coupled stacked patches. Each frequency corresponds to one patch. Resonance frequency values can be controlled by patch dimensions. Patch dimensions can be calculated based on the desired frequency but in fact, the operation frequency depends on both patches, because two patches have strong coupling in between. There are several design parameters to tune antenna frequencies. These parameters are analyzed in Section 3.2.

4.2.1 Dual-Band Aperture Coupled Stacked Microstrip Patch Antennas

In the light of the study on stacked aperture coupled patch antennas, following dual band microstrip patch antennas are designed. Some of these designs are modified versions of wideband antenna designs.

Antenna 1

A wideband aperture coupled stacked microstrip patch antenna is modified to achieve dual frequency characteristics. Antenna structure shown in Figure 3.1.1 (a), (b) is used in the design. A thin dielectric layer with parameters (ε_4, $D_{\varepsilon 4}$) is placed on the upper patch for protection. Antenna parameters can be seen from Table 12.

Table 12: *Parameters of the dual-band aperture coupled stacked microstrip patch antenna operating at 7.66 GHz & 9.66 GHz*

W_{t2}	L_{t2}	W_{t1}	L_{t1}	L_s	W_s	L_a	W_a
11.6 mm	11.6 mm	10.4 mm	10.4 mm	3.5 mm	4.75mm	11.8 mm	0.5mm

$D_{\varepsilon 4}$	$\varepsilon 4$	$D_{\varepsilon 3}$	$\varepsilon 3$	$D_{\varepsilon 2}$	$\varepsilon 2$	$D_{\varepsilon 1}$	$\varepsilon 1$
0.127 mm	2.2	3.65mm	1.07	3.3 mm	2.33	1.6 mm	2.33

Input return loss pattern obtained by simulations is plotted in Figure 4.2.1. According to this figure, a dual band aperture coupled stacked antenna with 19% bandwidth at 7.66 GHz and 10.4% bandwidth at 9.66 GHz for S11<-15 dB is obtained. Radiation patterns for each band are plotted in Figure 4.2.2. According to these figures, radiation patterns for both bands are similar. Antenna has 88^o HPBW at 7.66 GHz and 76^o HPBW at 9.66 GHZ. Small frequency ratio 9.66/7.66 = 1.26 should be noted.

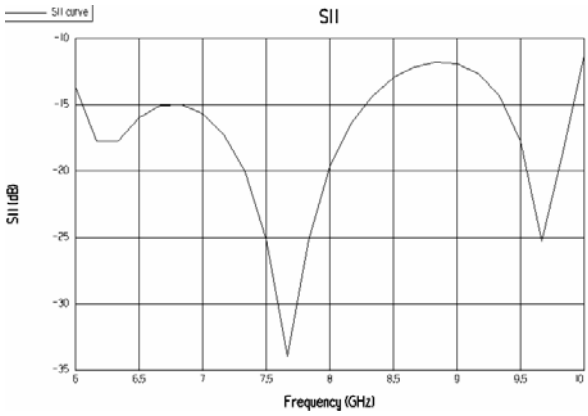

Figure 4.2.1: Input return loss vs. frequency graph of the simulated dual band aperture coupled stacked microstrip patch antenna operating at 7.66 & 9.66 GHz

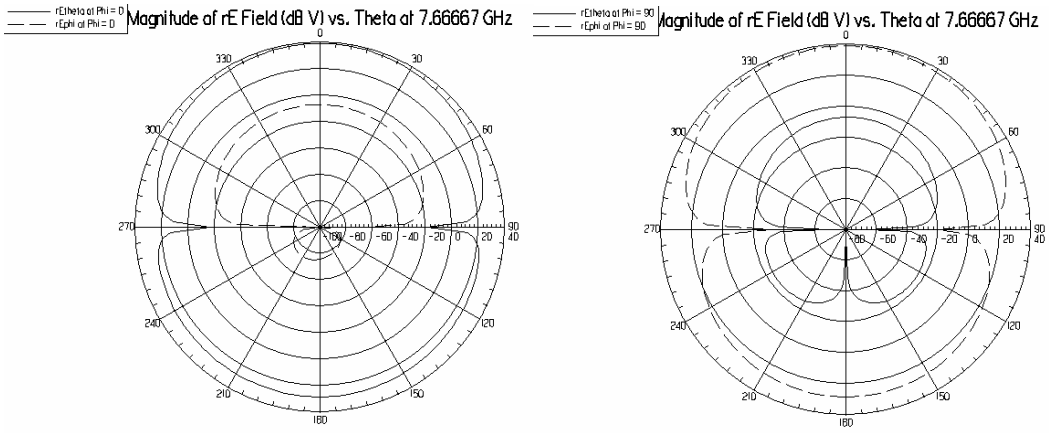

(a) (b)

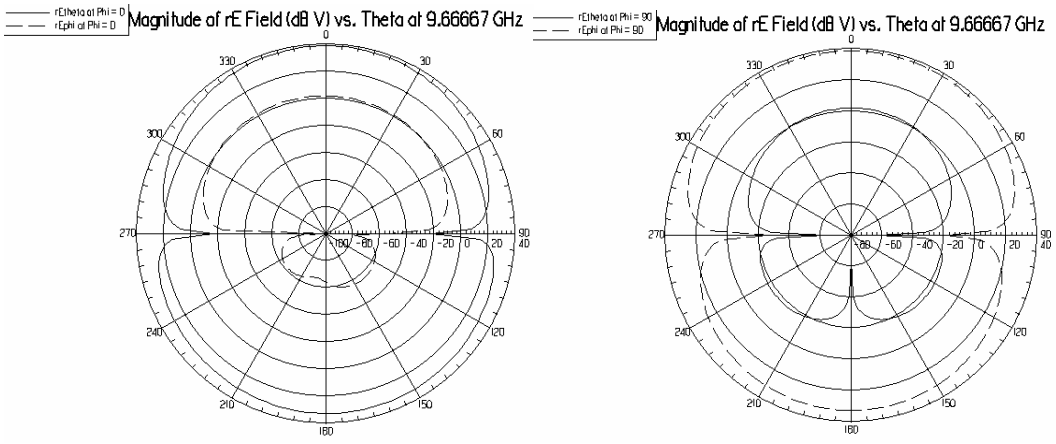

(c) (d)

Figure 4.2.2: Simulated radiation patterns of the dual-band aperture coupled stacked microstrip patch antenna operating at 7.66 GHz&9.66 GHz, (a) E-plane pattern at 7.66 GHz, (b) H-plane pattern at 7.66 GHz, (c) E-plane pattern at 9.66 GHz, (d) H-plane pattern at 9.66 GHz

Antenna 2

A ground plane is added to the previous dual band antenna structure to prevent high back radiation. Antenna structure shown in Figure 3.1.1 (a), (c) is used in this design. A thin dielectric layer with parameters ($\varepsilon 5$, $D_{\varepsilon 5}$) is placed on the upper patch for protection. Antenna parameters can be seen in Table 13.

Table 13: *Parameters of the dual-band aperture coupled stacked microstrip patch antenna operating at 6.9 GHz& 9.3 GHz*

W_{t2}	L_{t2}	W_{t1}	L_{t1}	L_s	W_s	L_a	W_a	$D_{\varepsilon 5}$
11.4mm	11.4mm	10.8mm	10.8mm	6 mm	2.8mm	13.8mm	0.5mm	0.127mm

$\varepsilon 5$	$D_{\varepsilon 4}$	$\varepsilon 4$	$D_{\varepsilon 3}$	$\varepsilon 3$	$D_{\varepsilon 2}$	$\varepsilon 2$	$D_{\varepsilon 1}$	$\varepsilon 1$
2.2	3.3 mm	1.07	3.6 mm	2.2	1.6 mm	4.2	4 mm	1.07

Input return loss values obtained by simulations are plotted in Figure 4.2.3. A dual band aperture coupled stacked patch antenna is obtained with 10% bandwidth at 6.9 GHz and 6.4% bandwidth at 9.3 GHz for S11< -15 dB. Antenna bandwidth is

reduced compared to previous example but there is no back radiation. Radiation patterns for both frequencies are plotted in Figure 4.2.4. They seem to have same directivities and 3 dB beamwidths. This antenna can be used for incoming new wireless applications. For example, WiMax mobile communication system has frequency license range of 2-11 GHz and 11-66 GHz.

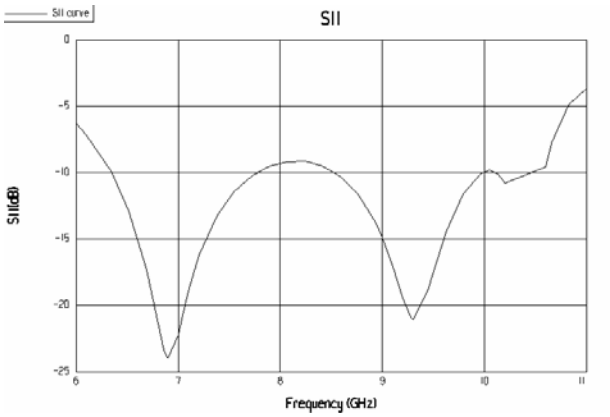

Figure 4.2.3: Input return loss vs. frequency graph of the simulated dual-band aperture coupled stacked microstrip patch antenna with ground plane operating at 6.9 GHz & 9.3 GHz

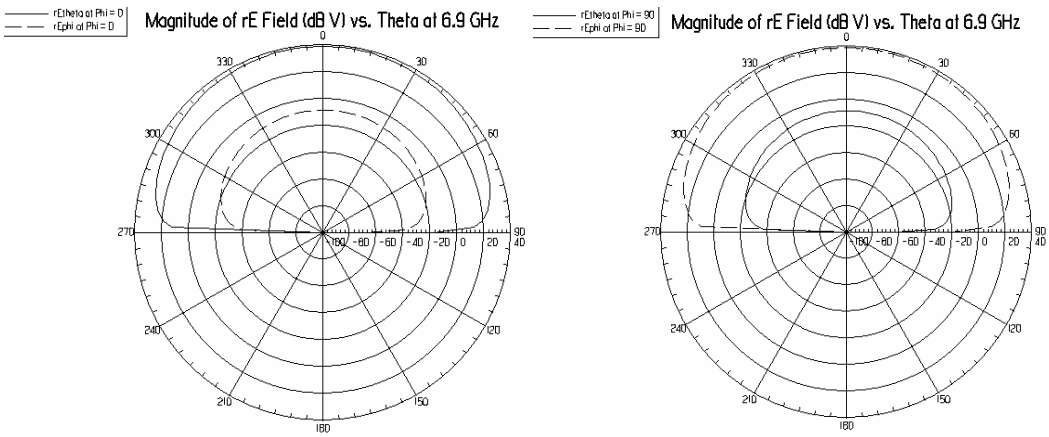

(a) (b)

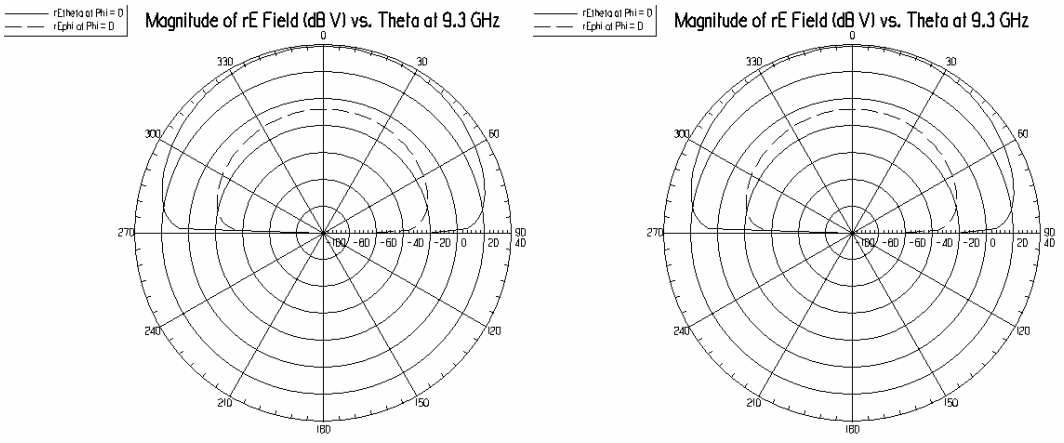

(c) (d)

Figure 4.2.4: Radiation patterns of the simulated dual-band aperture coupled stacked microstrip patch antenna operating at 6.9 GHz&9.3 GHz, (a) E-plane pattern at 6.9 GHz, (b) H-plane pattern at 6.9 GHz, (c) E-plane pattern at 9.3 GHz, (d) H-plane pattern at 9.3 GHz

4.2.2 Dual Band and Triple Band Aperture Coupled Stacked Microstrip Patch Antenna Designs for GSM and WLAN applications

New stacked antennas are designed to operate at common GSM and WLAN application bands. GSM system requires antennas at 800-900 MHz and 1800-1900 MHz and Bluetooth or WLAN requires 2.4 GHz frequency [32].

Antenna 1

This antenna is designed to support GSM 850 and WLAN IEEE 802.11 b/g application bands [32]. Antenna structure shown in Figure 3.1.1 (a), (c) is used in the design. A ground plane is placed under the feed line to prevent back radiation and a thin dielectric layer with parameters (ε_5, $D_{\varepsilon 5}$) is placed on the upper patch for protection. Antenna parameters are listed in Table 14.

***Table 14**: Parameters of the dual-band aperture coupled stacked microstrip patch antenna operating at GSM 850 and WLAN IEEE 802.11 b/g bands*

W_{t2}	L_{t2}	W_{t1}	L_{t1}	L_s	W_s	L_a	W_a	$D_{\varepsilon 5}$
94 mm	94 mm	60 mm	60 mm	22 mm,	2mm	84 mm	1.6mm	0.127 mm

Table 14 (continued)

ε5	$D_{\varepsilon 4}$	ε4	$D_{\varepsilon 3}$	ε3	$D_{\varepsilon 2}$	ε2	$D_{\varepsilon 1}$	ε1
2.2	5 mm	1.07	9 mm	2.2	1.3 mm	4.2	4 mm	1.07

Input return loss graph is shown in Figure 4.2.5. According to this figure, a dual band aperture coupled stacked patch antenna is designed with 4.7% bandwidth at 850 MHz and 7% bandwidth at 2.4 GHz for S11<-15 dB.

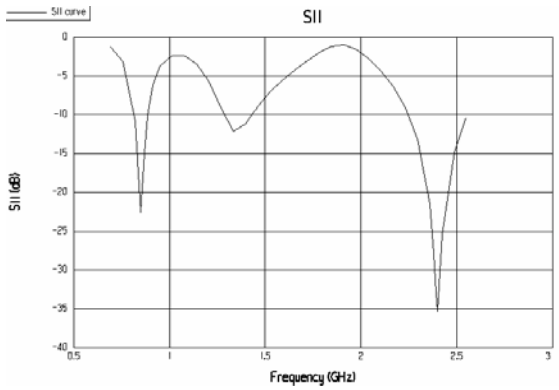

Figure 4.2.5: Input return loss vs. frequency graph of the simulated dual-band aperture coupled stacked microstrip patch antenna operating at GSM 850 and WLAN IEEE 802.11 b/g bands

Simulated radiation patterns of both frequency bands are plotted in Figure 4.2.6. Radiation pattern of lower frequency has better beamwidth and directivity than the one for higher frequency. It seems that radiation patterns have different characteristics at 850 MHz and 2.4 GHz. Compared to the first example of this section, frequency ratio f1/f2 = 2.6 is higher in this antenna. To obtain wide radiation bandwidth is a challenge with stacked patch structures, for such a high frequency ratio.

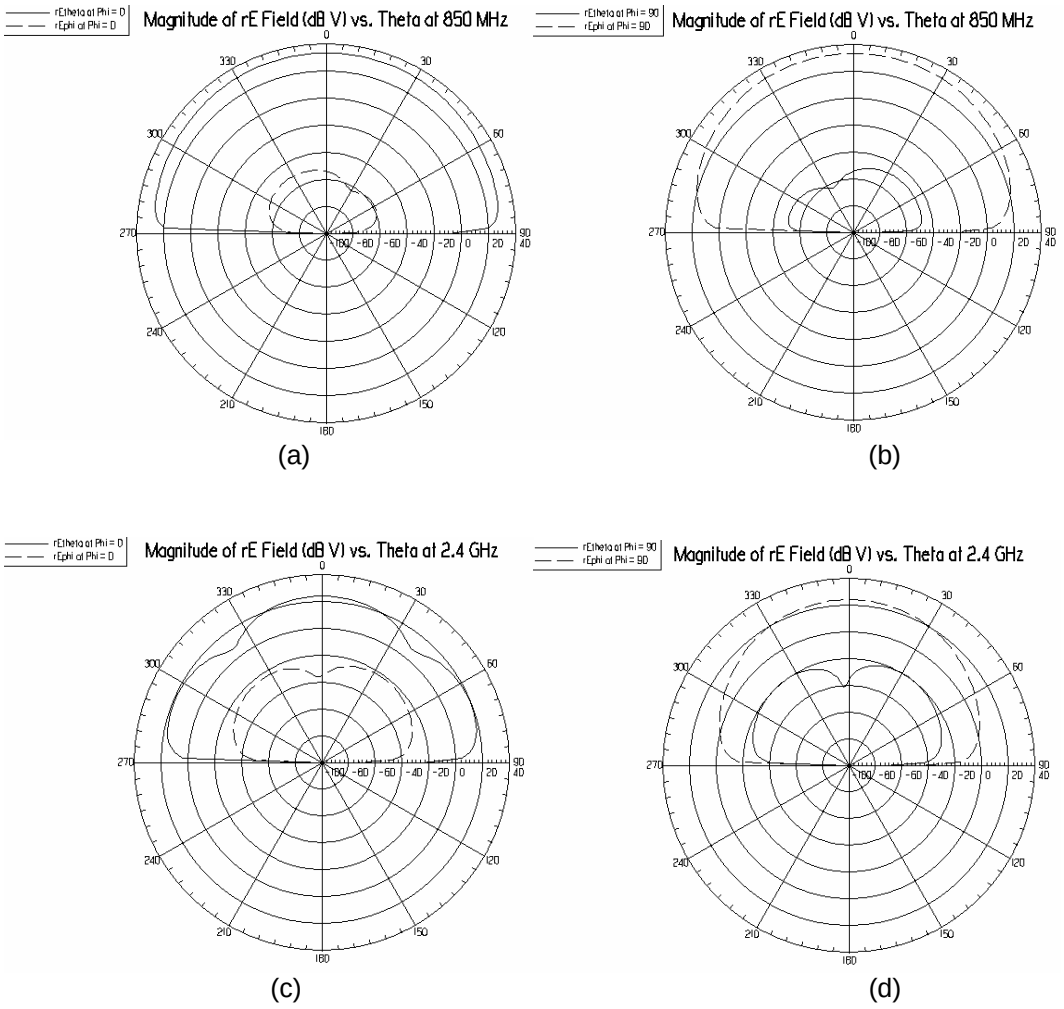

Figure 4.2.6: Radiation patterns of the simulated dual-band aperture coupled stacked microstrip patch antenna operating at GSM 850 and WLAN 802.11 b/g bands, (a) E-plane pattern at 850 MHz, (b) H-plane pattern at 850 MHz, (c) E-plane pattern at 2.4 GHz, (d) H-plane pattern at 2.4 GHz

Antenna 2

Another dual-band aperture coupled stacked microstrip patch antenna is designed to operate at GSM 850 and PCS 1900 frequencies [32]. Antenna structure shown in Figure 3.1.1 (a), (c) is used in design. A ground plane is placed under the feed line to prevent back radiation and a thin dielectric layer with parameters ($\varepsilon 5$, $D_{\varepsilon 5}$) is placed on the upper patch for protection. Antenna parameters are listed in Table 15.

***Table 15**: Parameters of the dual band aperture coupled stacked microstrip patch antenna operating at GSM 850 and PCS 1900 bands*

W_{t2}	L_{t2}	W_{t1}	L_{t1}	L_s	W_s	L_a	W_a	$D_{\varepsilon 5}$
74 mm	74 mm	60 mm	60 mm	24 mm	2mm	84 mm	1.6mm	0.127 mm

ε5	$D_{\varepsilon 4}$	ε4	$D_{\varepsilon 3}$	ε3	$D_{\varepsilon 2}$	ε2	$D_{\varepsilon 1}$	ε1
2.2	5 mm	1.07	6.8 mm	2.2	1.3 mm	4.2	4 mm	1.07

Input return loss of the antenna is given in Figure 4.2.7. According to this figure, a dual band aperture coupled stacked microstrip patch antenna is designed with 4.76% bandwidth at 840 MHz and 9.2% bandwidth at 1.88 GHz for S11<-15 dB.

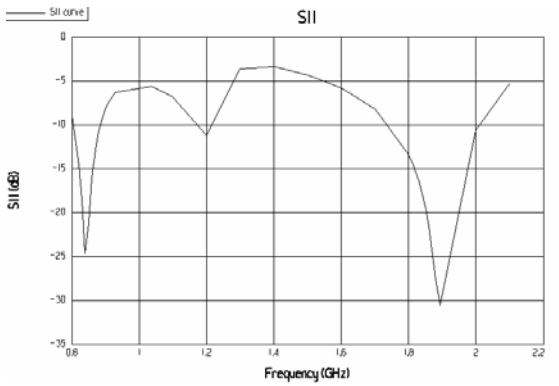

Figure 4.2.7: Input return loss vs. frequency graph of the simulated dual band aperture coupled stacked microstrip patch antenna operating at GSM 850 and PCS 1900 bands

Radiation patterns at each band are plotted in Figure 4.2.8. It is observed that radiation patterns of these two bands are again not similar. Antenna has 92^o HPBW at 840 MHz but 44^0 HPBW at 1.88 GHz. Probably, high ratio of f2/f1 = 1880/840 =2.23 causes this problem. It seems that aperture coupled stacked patch antennas are not suitable for high frequency ratios of dual band operation.

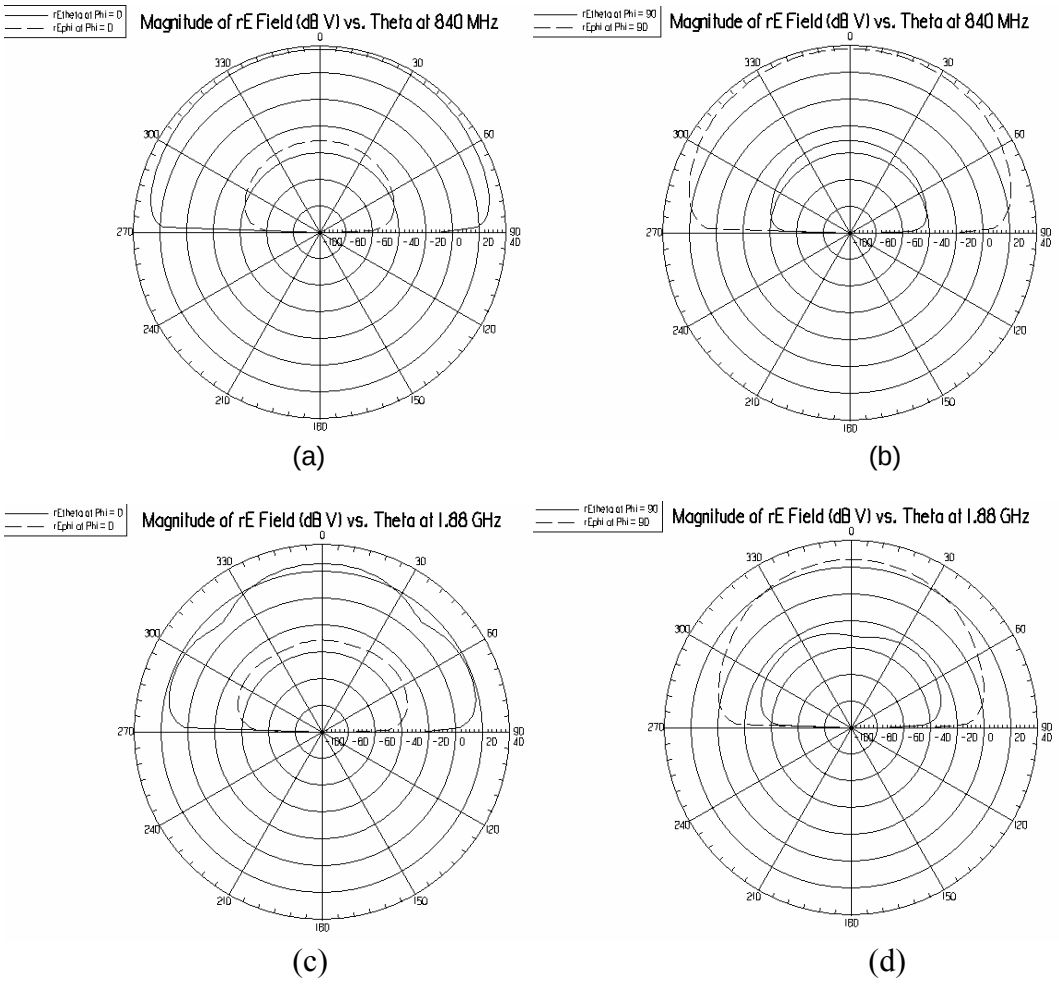

Figure 4.2.8: Radiation Pattern of the simulated dual-band aperture coupled stacked microstrip patch antenna operating at GSM 850 & PCS 1900 bands, (a) E-plane pattern at 840 MHz, (b) H-plane pattern at 840 MHz, (c) E-plane pattern at 1.88 GHz, (d) H-plane pattern at 1.88 GHz

Antenna 3

A triple band aperture coupled stacked microstrip patch antenna is designed to support GSM 850, DCS 1800 bands of GSM systems and WLAN IEEE 802.11 b/g application band [32]. Antenna structure shown in Figure 3.1.1 (a), (c) is used in design. A ground plane is placed under the feed line to prevent back radiation and a thin dielectric layer with parameters ($\varepsilon 5$, $D_{\varepsilon 5}$) is placed on the upper patch for protection. Antenna parameters are listed in Table 16.

***Table 16**: Parameters of the triple band aperture coupled stacked microstrip patch antenna operating at GSM 850, DCS 1800 and WLAN IEEE 802.11 b/g bands*

W_{t2}	L_{t2}	W_{t1}	L_{t1}	L_s	W_s	L_a	W_a	$D_{\varepsilon 5}$
73 mm	73 mm	60 mm	60 mm	24 mm,	2mm	84 mm	1.6mm	0.127mm

ε5	$D_{\varepsilon 4}$	ε4	$D_{\varepsilon 3}$	ε3	$D_{\varepsilon 2}$	ε2	$D_{\varepsilon 1}$	ε1
2.2	3.5 mm	1.07	8.6 mm	2.2	1.3 mm	4.2	4 mm	1.07

Input return loss vs. frequency graph obtained by Ensemble simulations is given in Figure 4.2.9. According to this figure, a triple band antenna aperture coupled stacked microstrip patch antenna is obtained with 4.6% bandwidth at 870 MHz, 6.3% bandwidth at 1.8 GHz and 5.6% bandwidth at 2.4 GHz for S11<-15 dB.

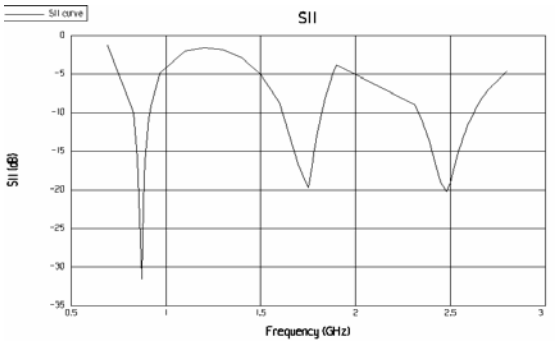

Figure 4.2.9: Input return loss vs. frequency graph of the simulated triple band aperture coupled stacked patch antenna operating at GSM 850, DCS 1800 and WLAN IEEE 802.11 b/g bands

Simulated radiation patterns at three frequencies are given in Figure 4.2.10. It is observed that radiation pattern for these three bands are not similar. This antenna has 150^o HPBW at 870 MHz, 66^o HPBW at 1.75 GHz and 44^o HPBW at 2.45 GHz. The frequency ratio f2/f1=1800/900=2 is again too large to be realized by stacked patch structure, in terms of radiation pattern characteristics.

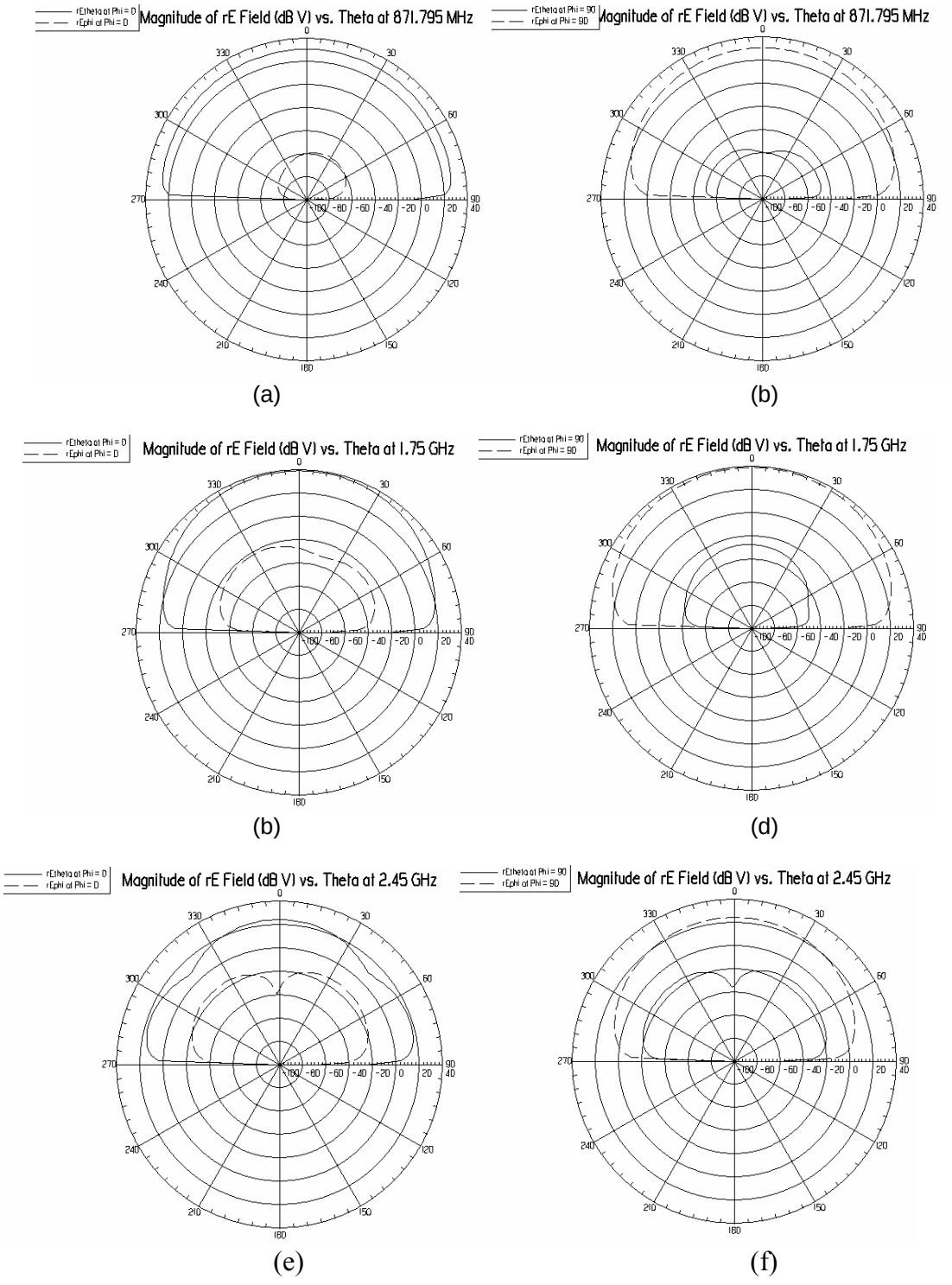

Figure 4.2.10: Radiation patterns of the simulated triple band aperture coupled stacked microstrip patch antenna operating at GSM 850, DCS 1800 and WLAN IEEE 802.11 b/g bands, (a) E-plane pattern at 871 MHz, (b) H-plane pattern at 871 MHz, (c) E-plane pattern at 1.75 GHz, (d) H-plane pattern at 1.75 GHz, (e) E-plane pattern at 2.45 GHz, (f) H-plane pattern at 2.45 GHz

Antenna 4

A dual band aperture coupled stacked patch antenna operating at DCS 1800 and WLAN IEEE 802.11 b/g bands is designed, manufactured and measured [32]. Frequency ratio f2/f1 = 1.33 is small compared to previous examples. A ground plane is placed under the feed line to prevent back radiation. Antenna structure shown in Figure 3.1.1 (a), (c) is used in this design. Thick foam substrates with low dielectric constant are used in the design to improve antenna bandwidth. These foam substrates are covered with thin and high dielectric constant substrate for easy production so there are two more dielectric layers with parameters ($\varepsilon 6$, $D_{\varepsilon 6}$) and ($\varepsilon 4$, $D_{\varepsilon 4}$) than the layers shown in Figure 3.1.1 (c). Antenna parameters are shown in Table 17.

Table 17: *Parameters of the dual band aperture coupled stacked microstrip patch antenna operating at DCS 1800 & WLAN IEEE 802.11 b/g bands*

W_{t2}	L_{t2}	W_{t1}	L_{t1}	L_s	W_s	L_a	W_a	$D_{\varepsilon 6}$	$\varepsilon 6$
49mm	49mm	62mm	62mm	20mm	4	20mm	1	0.79mm	2.2

$D_{\varepsilon 5}$	$\varepsilon 5$	$D_{\varepsilon 4}$	$\varepsilon 4$	$D_{\varepsilon 3}$	$\varepsilon 3$	$D_{\varepsilon 2}$	$\varepsilon 2$	$D_{\varepsilon 1}$	$\varepsilon 1$
6.8mm	1.06	0.79mm	2.2	6.8mm	1.06	3.81mm	9.2	8mm	1.06

Measured and simulated input return loss values are plotted in Figure 4.2.11. It is seen from the simulation results that this antenna operates at 1.8 and 2.4 GHz, however in measurements lower frequency is shifted to 1.55 GHz. One of the reasons is that the dielectric layers and ground plane are finite and the distance from patch to the antenna edge is less than the thickness of the substrates due to lack of this material with sufficient size in our laboratory.

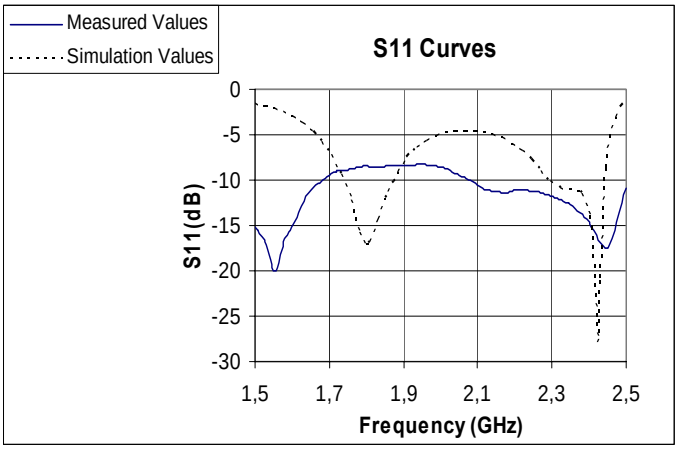

Figure 4.2.11: Comparison of simulated and measured input return loss vs. frequency for the dual-band aperture coupled stacked microstrip patch antenna

Simulated radiation patterns of both frequency bands are plotted in Figure 4.2.12. Radiation pattern for each band has similar characteristics. Antenna has 72^{o} HPBW at 1.8 GHz and 56^{o} HPBW at 2.43 GHz.

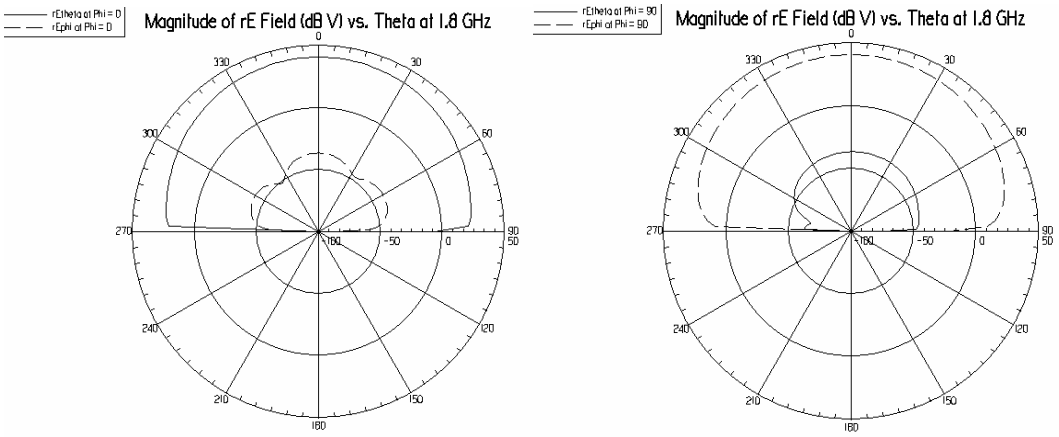

(a) (b)

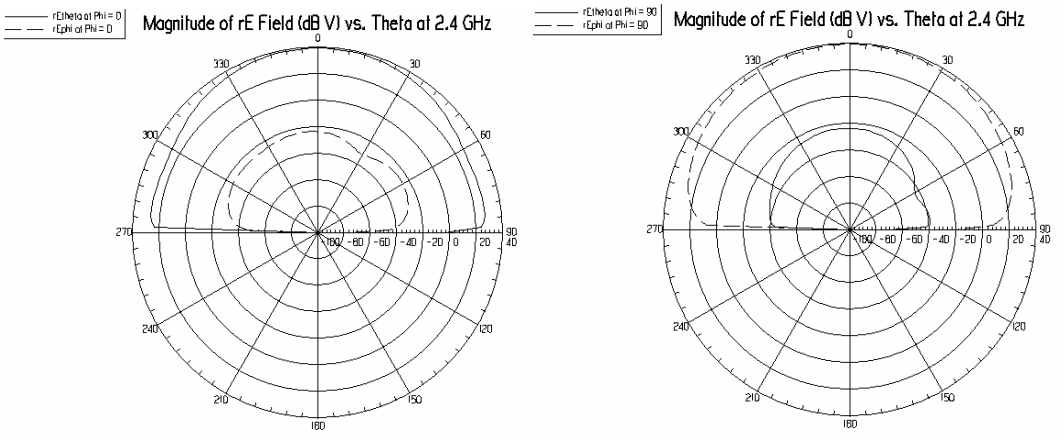

(c) d)

Figure 4.2.12: Radiation patterns of the simulated dual-band aperture coupled stacked microstrip patch antenna operating at DCS 1800 and WLAN IEEE 802.11 b/g bands, (a) E-plane pattern at 1.8 GHz, (b) H-plane pattern at 1.8 GHz, (c) E-plane pattern at 2.42 GHz, (d) H-plane pattern at 2.42 GHz.

4.3 Dual Polarized Aperture Coupled Stacked Microstrip Patch Antenna Design

This antenna is designed to demonstrate the dual polarization antenna with aperture coupled stacked patch structure. Antenna structure shown in Figure 3.3.2 is used in this design. Antenna parameters are listed in Table 18.

Table 18: *Parameters of the dual polarized triple band aperture coupled stacked microstrip patch antenna*

W_{t2}	L_{t2}	W_{t1}	L_{t1}	L_{s1}	W_s	distance of legs	L_{s2}	W_s	distance of legs	L_{a1}	W_{a1}
86 mm	86 mm	74 mm	74 mm	36 mm	2 mm	46 mm	22 mm	2 mm	46 mm	100 mm	2 mm

L_{a2}	W_{a2}	$D_{\varepsilon 6}$	ε6	$D_{\varepsilon 5}$	ε5	$D_{\varepsilon 4}$	ε4	$D_{\varepsilon 3}$	ε3	$D_{\varepsilon 2}$	ε2	$D_{\varepsilon 1}$	ε1
100 mm	2 mm	0.127 mm	2.2	5 mm	2.2	9 mm	1.07	1 mm	1.07	1.3 mm	4.2	4 mm	1.07

Antenna structure is similar to aperture coupled stacked antenna but this antenna has cross shaped aperture instead of rectangular shaped aperture, one more dielectric layer over the ground and one more perpendicular feed line on this extra dielectric layer. These two perpendicular separate feed lines are used to excite two perpendicular polarizations correspondingly.

First port excitation for the first polarization

The feed line under the bottom patch, as shown in Figure 3.3.2 (a), (b) is used to excite antenna by proximity coupling method for the first polarization. For the first polarization case, as shown Figure 4.3.1, the aperture coupled stacked triple band antenna has three resonances at 890 MHz with 7.2% bandwidth, at 1.21 GHz with 4.13% bandwidth and at 2.1 GHz with 17.6% bandwidth for S11< -15 dB.

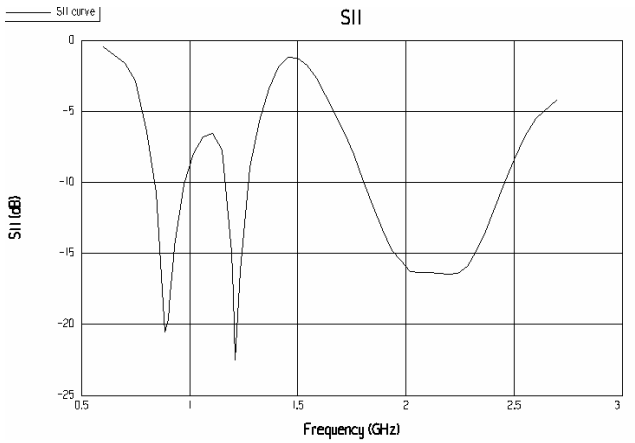

Figure 4.3.1: Input return loss vs. frequency graph of the simulated dual polarization triple band aperture coupled stacked microstrip patch antenna for the first polarization

Radiation patterns for three bands are plotted in Figure 4.3.2. This antenna has 100^{o} HPBW at 887 MHz, 70^{o} HPBW at 1.21 GHz and 33^{o} HPBW at 2.19 GHz. Although HPBW at first and second resonance frequencies are similar, it is relatively narrow at the third frequency. Again close frequencies have similar characteristics.

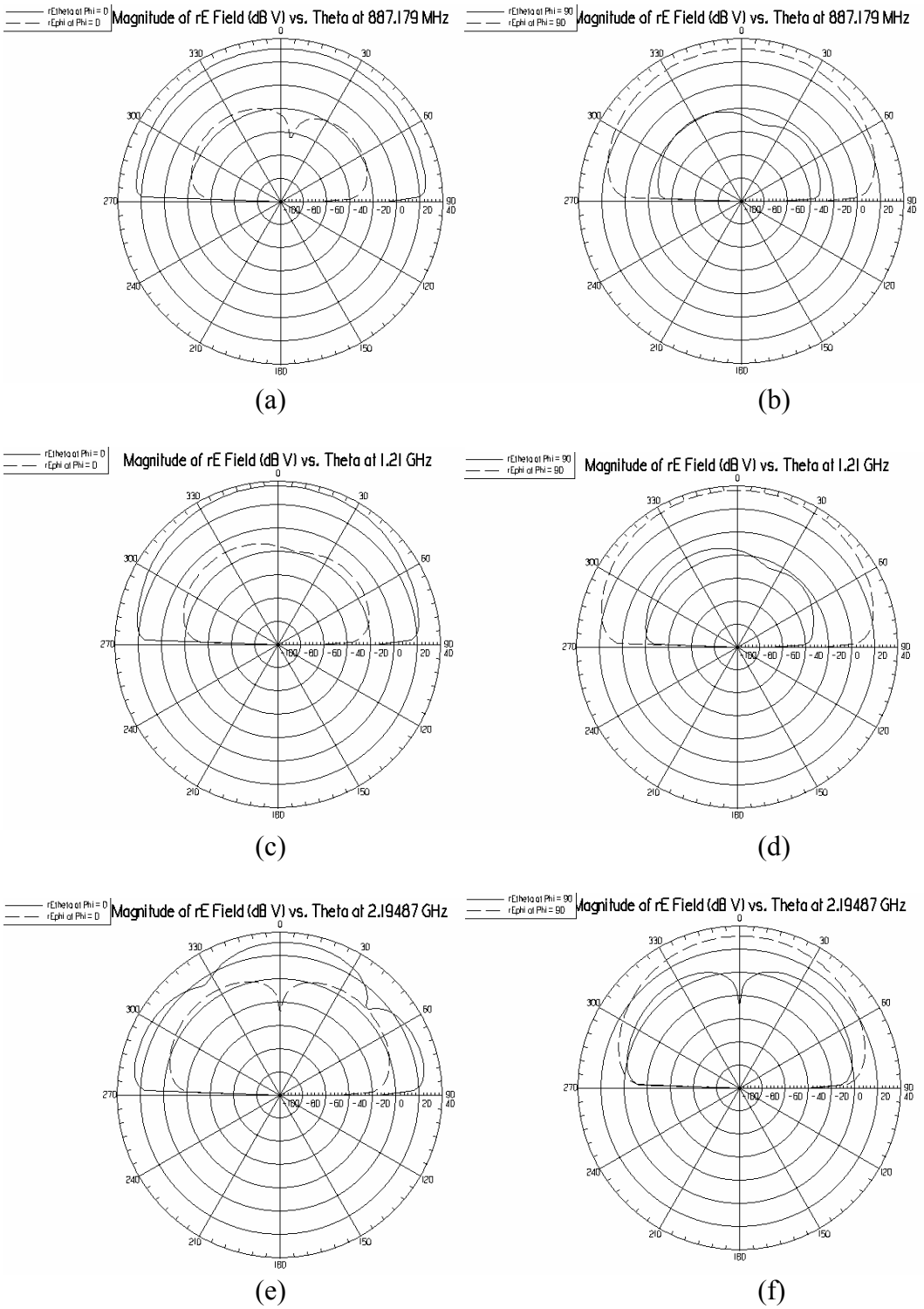

Figure 4.3.2: Radiation patterns of the simulated dual polarization triple band aperture coupled stacked microstrip patch antenna for the first polarization, (a) E-plane pattern at 887 MHz, (b) H-plane pattern at 887 MHz, (c) E-plane pattern at 1.21 GHz, (d) H-plane pattern at 1.21 GHz, (e) E-plane pattern at 2.19 GHz, (f) H-plane pattern at 2.19 GHz

Second port excitation for the second polarization

The antenna is excited from the second port by aperture coupled feeding for second polarization, as shown in Figure 3.3.2 (a), (b). Input return loss values for the second polarization are shown in Figure 4.3.3. It is observed from the figures that antenna has three resonances at 890 MHz with 5.6% bandwidth, at 1.2 GHz with 2% bandwidth and at 2.2 GHz with 23.6% bandwidth (for S11< -15 dB).

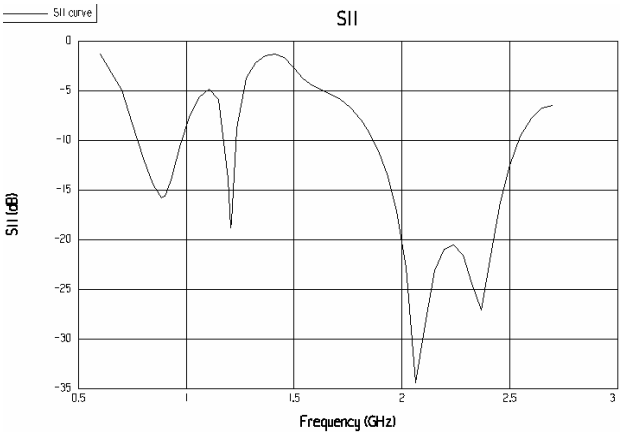

Figure 4.3.3: Input return loss vs. frequency graph of the simulated dual polarization triple band aperture coupled stacked microstrip patch antenna for the second polarization

Radiation patterns of simulated triple band antenna for the second polarization can be seen from Figure 4.3.4. It is observed from figures that the antenna has 90^o HPBW at 887 MHz, 54^o HPBW at 1.21 GHz and 36^o HPBW at 2.19 GHz. These values are very similar with ones for the first polarization. It seems that antenna shows same characteristics for both polarizations but again radiation patterns at the three resonance frequencies are different.

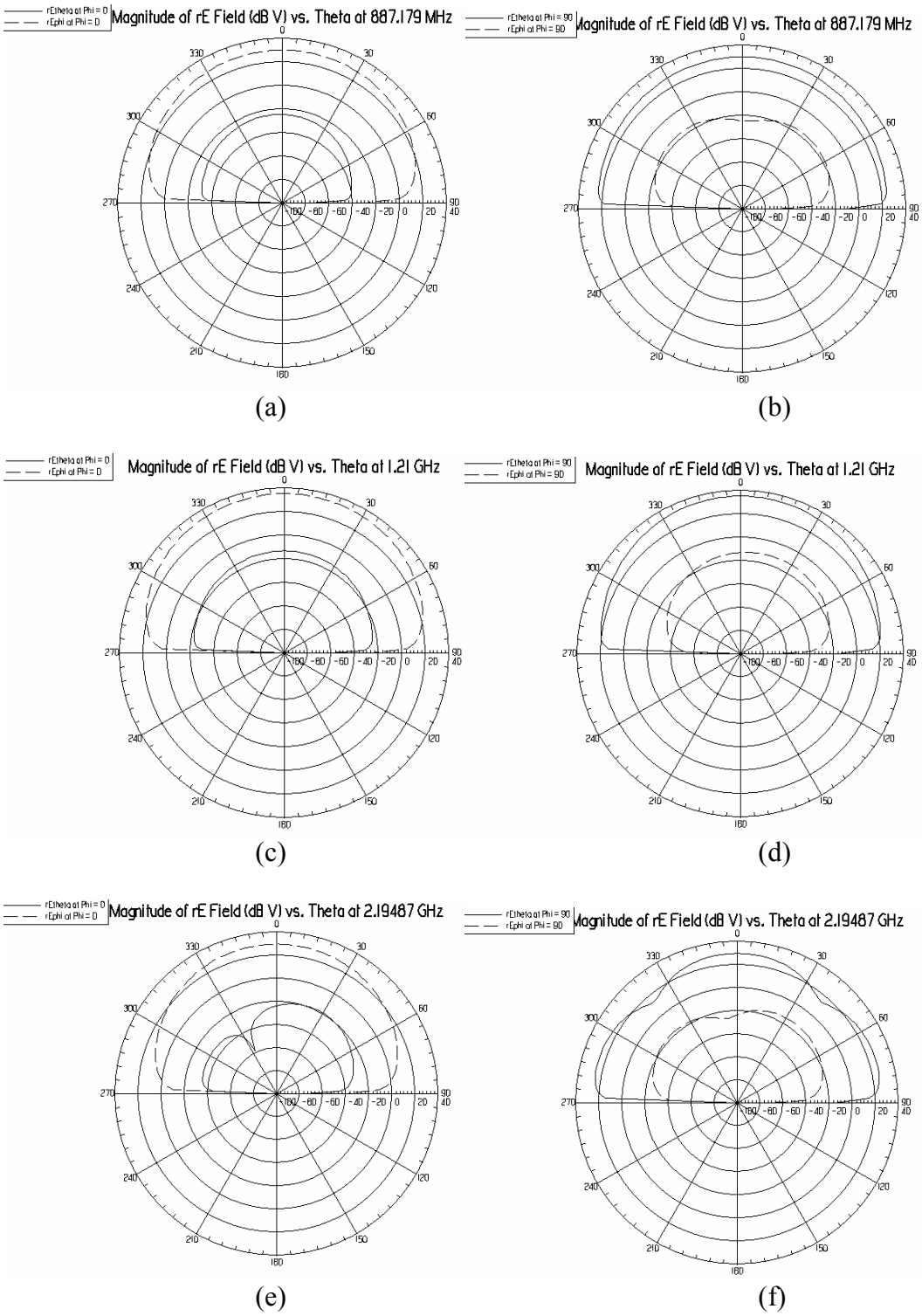

Figure 4.3.4:Radiation patterns of the simulated dual polarization triple band aperture coupled stacked microstrip patch antenna for the second polarization, (a) H-plane pattern at 887 MHz, (b) E-plane pattern at 887 MHz, (c) H-plane pattern at 1.21 GHz, (d) E-plane pattern at 1.21 GHz, (e) H-plane pattern at 2.19 GHz, (f) E-plane pattern at 2.19 GHz

CHAPTER 5

CONCLUSIONS

In this thesis, wideband and multi band characteristics of stacked microstrip patch antennas are investigated to satisfy new requirements for wideband and multi band antennas in wireless communication applications.

Basic microstrip antenna structure is discussed with different perspectives such as, antenna characteristics, feeding methods and analysis methods. Different feeding methods of microstrip antennas are compared regarding to their bandwidth characteristics and advantages. Aperture coupled feed technique preferred in this study due to its promising advantages and wide bandwidth. Aperture coupled microstrip structures are explained and parametrical analysis is performed to provide a design guideline. Different methods to obtain dual and wide band antennas are discussed. Stacking method is investigated in this thesis due to wide bandwidth characteristics. Design principles of aperture coupled stacked patch antennas are investigated and summarized to give a guidelines for wideband and dual band antenna design.

After analysis of design principles, some examples of aperture coupled stacked patch antennas are designed, manufactured and measured to achieve wideband, dual band, dual polarization and circular polarization characteristics for practical applications.

A wideband aperture coupled stacked antenna is designed with 45% bandwidth (S11<-15 dB) at frequencies of IEEE 802.15.3a standard for (UWB) ultra wideband personal area Network (PAN). Although this antenna has wide bandwidth and low cross-polarization, it has high back radiation. To solve back radiation problem, a ground plane is added. This modified antenna has 28% bandwidth at 8 GHz (for S11< -15 dB) with small back radiation. Another aperture coupled stacked patch antenna is designed with 16% bandwidth (for S11< -15 dB) at 1.85 GHz to be

used in EDGE PCS 1900 band, DCS 1800 band systems, W-CDMA PCS 1900 band, DCS 1800 band systems, HSPDA systems. Another stacked antenna with three patches is designed to increase bandwidth of antenna. A wideband aperture coupled stacked antenna is obtained with 51% bandwidth (for S11<-15 dB) at 6.1 GHz for frequencies of IEEE 802.11 a/h/j WLAN standards. However, addition of one more patch provides slight increase in the bandwidth. Addition of one more patch provides slight increase in the bandwidth.

Stacked patch antennas are designed to cover GSM 850, DCS 1800, PCS 1900 bands and WLAN IEEE 802.11 b/g band. It is observed that when the ratio of two frequencies is large, it is not easy to obtain dual band with same radiation pattern characteristics. However, for small frequency ratios (f1/f2<1.5) stacked patch antenna structure can be used to design dual band antenna with similar radiation patterns at both frequencies.

This study on stacked patch antennas shows that this structure is more suitable to obtain an antenna with wide bandwidth, by choosing slightly different patch sizes with slightly different resonant frequencies. It can also be used to design dual band antenna with frequencies close to each other, i.e. for the frequency ratio less than 2.

REFERENCES

[1] S. Maci and G. Biffi Gentili," Dual-frequency Patch Antennas", IEEE Antennas and Propagation Magazine, Vol.39, No.6, December 1997.

[2] J-S Cheng, K-L. Wong, "A Single-Layer Dual-Frequency Rectangular Microstrip Patch Antenna Using a Single Probe Feed," Microwave and Optical Technological Letters, 11, 2, 1996, pp. 38-84.

[3] Y. M. M. Antar, A. I., Ittipiboon, A. K. Bhattachatyya, "A Dual-Frequency Antenna Using a Single Patch and An Inclined Slot," Microwave and Optical Technology Letters, 8, 6, 1995, pp.309-310.

[4] M. Deepukumar, J. George, C. K Aanandan, P. Mohanan, K. G. Nair, " Broadband Dual Frequency Microstrip Antenna, " Electronic Letters, 32, 17, 15 August 1996, pp. 1531-1532.

[5] Y. Murakami, W. Chujo, I. Chiba, M. Frujise, "Dual Slot Coupled Microstrip Antenna for Dual Frequency Operation," Electronics Letters, 29, 22, 28 October 1993, pp. 1906-1907.

[6] W. F. Richards, S. E. Davidson, S. A. Long, "Dual-Band Reactively Loaded Microstrip Antennas," IEEE Transactions on Antennas and Propagation, AP-33, 5, May 1985, pp. 556-560.

[7] D. Sanchez-hernandez and I. D. Robertson "Analysis and Design of a Dual-Band Circularly Polarized Microstrip Patch Antenna," IEEE Transactions on Antennas and Propagation, AP-43, 2, February 1995, pp.201-205.

[8] S.S Zhong and Y.T. Lo, "Single Element Rectangular Microstrip Antenna for Dual-Frequency Operation," Electronics Letters, 19, 8, 1983, pp.298-300.

[9] H.F. Hammad, Y.M.M. Antar and A.P. Freundorferd, "Dual band aperture coupled antenna using spur line", Electronic Letters 4th December 1997 Vol. 33 No. 25.

[10] Dong-Jun Lee, Duk-Sun Shim , Hyung-Kyu Kim and Hyeong-Seok Kim," Dual-band Slotted Patch Antenna with Diagonally Offset Deed for GPS and WLAN" 310 KIEE International Transactions on EA, Vol. 4-C, No. 5, pp. 310~313, 2004.

[11] Stuart A. Long, Member, IEEE, and Mark D.Walton, "Dual-Frequency Stacked Circular-Disc Antenna", IEEE Transactions on Antennas and Propagation, Vol. Ap-27, NO.2, March 1979.

[12] J. Wang, R. Fralich, C. Wu and J. Litva, "Multifunctional Aperture Coupled Stack Antenna," Electronics Letters, 26, 25, December 1990, pp.2067-2068.

[13] F. Croq, D. Pozar, "Multifrequency Operation of Microstrip Antennas Using Aperture Coupled Parallel Resonators," IEEE Transactions on Antennas and Propagation, AP-40, 11, November 1992, pp.1367-1374.

[14] C. Salvador, L. Borselli, A. Falciani, S. Maci, " A Dual Frequency Planar Antenna at S and X Bands," Electronics Letters, 31, 20, October 1995, pp.1706-1707.

[15] Professor David M. Pozar, "A Review of Aperture Coupled Microstrip Antennas: History, Operation, Development, and Applications" Electrical and Computer Engineering University of Massachusetts at Amherst Amherst, MA 01003 May 1996.

[16] F. Croq and A. Papiernik, "Stacked slot-coupled printed antenna", IEEE Microwave and Guided Wave Letters,vol. 1, pp. 288-290, October 1991.

[17] S. D. Targonski, R.B Waterhouse and D.M. Pozar ," Design of Wide-Band Aperture-Stacked Patch Microstrip Antennas", IEEE Transactions On Antennas and Propagation, Vol. 46, No. 9, September 1998.

[18] A. Henderson, J.R. James, and C.M Hall, "Bandwidth Extension Techniques in Printed Conformal Antennas" Military Microwaves, MM 86, pp 329-324, 1986.

[19] R.B Waterhouse, "Broadband stacked shorted patch", Electronic Letters, Vol. 35, No.2, 21st January 1999.

[20] Jaume Anguera, Gisela Font, Carles Puente, Carmen Borja, Jordi Soler, "Multifrequency Microstrip Patch Antenna Using Multiple Stacked Elements", IEEE Microwave and Wireless Components Letters, Vol. 13, No. 3, March 2003.

[21] Jaume Anguera, *Member, IEEE*, Carles Puente, *Member, IEEE*, Carmen Borja, *Member, IEEE*, Nicolás Delbene, and Jordi Soler, *Member, IEEE,"*Dual-Frequency Broad-Band Stacked Microstrip Patch Antenna", IEEE Antennas and Wireless Propagation Letters, Vol. 2, 2003.

[22] Jashwant S. Dahele, Kai-Fhong Lee, D.P. Wong, "Dual-frequency Stacked Annular-Ring Microstrip Antenna", IEEE Transactions on Antennas and Propagation, Vol. Ap-35, No.11, November 1987.

[23] Kai-Ping Yang and Kin-Lu Wong, *Senior Member, IEEE,"*Dual-Band Circularly-Polarized Square Microstrip Antenna", IEEE Transactions on Antennas and Propagation, Vol. 49, No. 3, March 2001.

[24] David M. Pozar, *Fellow, IEEE*, and Sean M. Duffy, "A Dual-Band Circularly Polarized Aperture-Coupled Stacked Microstrip Antenna for Global Positioning Satellite", IEEE Transactions on Antennas and Propagation, Vol. 45, No. 11, November 1997.

[25] Xian-Ling Liang, Shun-Shi Zhong, and Wei Wang "Design of a Hign Isolation Dual Polarized Slot-Coupled Microstrip Antenna " Microwave and Optical Technology Letters, Vol. 47, No. 3, November 5 2005.

[26] Constantine A. Balanis, "Antenna Theory Analysis and Design,", John Wiley & Sons. Inc, Second Edition.

[27] D.M Pozar, "Microstrip Antennas," Proc. IEEE, Vol. 80, No. 1, pp. 79-81, January 1992.

[28] Daniel H. Schaubert, "A Review of Some Microstrip Antenna Characteristics" Electrical and Computer Engineering University of Massachusetts Amherst, Massachusetts.

[29] D.M Pozar and B. Kauffman, "Increasing the Bandwidth of the Microstrip Antenna by Proximity Coupling," Electronic Letters, Vol. 23, pp 368-369, April 1987.

[30] K. Ghorbani and R. B. Waterhouse “Dual Polarized Wide-Band Aperture Stacked Patch Antennas “IEEE Transactions on Antennas and Propagation, Vol. 52, No. 8, August 2004.

[31] M. Himdi, J.P. Daniel, C. Terret, ”Transmission Line Analysis of Aperture-Coupled Microstrip Antenna”, Labotatoire Antennes et Microelectronique UA 8334 CNRS, University de Rennes 1 35042 Rennes Dedex, France.

[32] Agilent Technologies, “Wireless Industry”, http://www.agilent.com/find/ wireless, Last accessed on December 2005.